

**Heterocycle carbonyl pyrazolyl palladium(II) complexes: Synthesis,
ethylene oligomerisation and polymerisation catalysis**

By

Stephen Otieno Ojwach

**Submitted in partial fulfillment of the requirements for the award of
Master of Science degree**

**Department of Chemistry
Faculty of Science
University of the Western Cape
Private Bag X17
Bellville 7535**

**Supervisor: Prof. James Darkwa
Co-supervisor: Prof. Selwyn Mapolie**

November 2004

DECLARATION

I declare that the thesis, *Heterocycle carbonyl palladium(II) complexes, synthesis, ethylene oligomerisation and polymerisation catalysis*, is my original work and has never been presented for the award of any degree at any other university before and that all the information sources I have used and or quoted have been indicated and acknowledged by means of complete reference.

Name: Stephen Otieno Ojwach

Signature:

Date.....

DEDICATION

DEDICATED TO THE OJWACH FAMILY

TABLE OF CONTENTS

ABSTRACT	ix
LIST OF TABLES	xii
LIST OF FIGURES	xiii
ABBREVIATIONS	xv
ACKNOWLEDGEMENTS	xvi

CHAPTER 1

Review of late transition metal catalyzed olefin oligomerisation and polymerisation and the role of co-catalysts

1.1 General introduction	1
1.2 Ethylene oligomerisation and polymerisation	3
1.2.1 Types and properties of polyethylene	3
1.2.2 Characterisation of polyethylene	4
1.3 Principles of ethylene oligomerisation and polymerisation	6
1.3.1 Mechanistic considerations	6
1.3.2 Ethylene oligomerisation and polymerisation mechanism using late transition α -diimine catalysts	7
1.3.3 Factors controlling the performance of the catalysts in ethylene oligomerisation and polymerisation	9
1.4.1 The role of co-catalysts in metal-catalysed olefin oligomerisation and polymerisation	12

1.4.2 Aluminium alkyls as catalytic activators	13
1.4.3 Perfluoroaryl boranes as co-catalysts	15
1.5 Late transition-metal complexes as catalysts for ethylene oligomerisation	17
1.6 Late transition-metal complexes as catalysts for ethylene polymerisation	22
1.7 Objectives and rationale of this research work	30
1.8 References	31

CHAPTER 2

Synthesis and characterisation of heterocyclic carbonyl pyrazolyl palladium(II) complexes

2.1 Introduction	37
2.2. Materials and instrumentation	39
2.3 Synthesis of the ligands	40
2.3.1 Synthesis of 2-(3,5-dimethylpyrazolyl-1-carbonyl)furan (L1)	40
2.3.2 Synthesis of 2-(pyrazolyl-1-carbonyl) furan (L2)	40
2.3.3 Synthesis of 2-(3-methylpyrazolyl-1-carbonyl)furan (L3)	41
2.3.4 Synthesis of 2-(pyrazolyl-1- carbonyl)thiophene (L4)	41
2.3.5 Synthesis of 2-(3,5-di- <i>tert</i> -butylpyrazolyl-1-carbonyl)furan (L5)	42
2.3.6 Synthesis of 2-(3,5-dimethylpyrazolyl-1- carbonyl)thiophene (L6)	42
2.3.7 Synthesis of 2-(3,5-di- <i>tert</i> -butylpyrazolyl-1-carbonyl)thiophene (L7)	43
2.3.8 Synthesis of 2-(3-methylpyrazolyl-1-carbonyl)thiophene (L8)	43
2.3.9 Synthesis of 2-(3,5-diphenylpyrazolyl-1- carbonyl)furan (L9)	44

2.3.10	Synthesis of 2-(3,5-diphenylpyrazolyl-1-carbonyl)thiophene (L10)	44
2.3.11	Synthesis of (3,5-dimethylpyrazolyl-1- carbonyl)methane (L11)	45
2.3.12	Synthesis of (3,5-di- <i>tert</i> -butylpyrazolyl-1- carbonyl)methane (L12)	45
2.3.13	Synthesis of (3-di- <i>tert</i> -butylpyrazolyl-1- carbonyl)ethane (L13)	45
2.4	Synthesis of the complexes	46
2.4.1	Dichloro{bis-2-(3,5-dimethylpyrazolyl-1-carbonyl)furan}palladium(II) (1)	46
2.4.2	Dichloro{bis-2-(3,5-dimethylpyrazolyl-1-carbonyl)thiophene}palladium(II) (2)	46
2.4.3	Dichloro{bis-2-(3,5-di- <i>tert</i> -butylpyrazolyl-1-carbonyl)furan}palladium(II) (3)	47
2.4.4	Dichloro{bis-2-(3,5-di- <i>tert</i> -butylpyrazolyl-1-carbonyl)thiophene}palladium(II) (4)	47
2.4.5	Dichloro{bis-2-(3-methylpyrazolyl-1-carbonyl)-furan}palladium(II) (5)	49
2.4.6	Dichloro{bis-2-(pyrazolyl-1-carbonyl)furan}palladium(II) (6)	48
2.4.7	Dichloro{bis-2-(3,5-diphenylpyrazolyl-1- carbonyl)furan}palladium(II) (7)	48
2.4.8	Dichloro{bis-2-(3,5-diphenylpyrazolyl-1-carbonyl)thiophene}palladium(II) (8)	48
2.5	Results and discussion	49
2.5.1	Synthesis and characterisation of furoyl and thiophene carbonyl pyrazolyl Ligands and their palladium(II) complexes	49
2.5.2	Synthesis and characterisation of alkyl carbonyl pyrazolyl ligands and their palladium(II) complexes	68
2.5.3	Molecular structure determination by single crystal X-ray analysis	74
2.5.4	Molecular structure of ligand L1	76
2.5.5	Molecular structures of complexes 1 and 2	77

2.6 Conclusions	86
2.7 References	87
CHAPTER 3	
Ethylene oligomerisation and polymerisation catalyzed by furan and thiophene carbonyl pyrazolyl palladium(II) complexes	
3.1 Introduction	89
3.2 Materials and methods	92
3.2.1 Ethylene polymerisation procedure	92
3.2.2 Oligomerisation of ethylene procedure	93
	93
3.3 Results and discussion	
3.3.1 Evaluation of complexes 1 to 4 as catalyst for ethylene polymerisation	93
3.3.2 Effect of co-catalyst concentration on ethylene polymerisation.	95
3.3.3 The effect of trispentafluorophenylborane on the catalytic activity of catalyst 2	98
3.3.4 Evaluation of complexes 1 to 5 as catalyts for ethylene oligomerisation.	101
3.3.5 Effect of co-catalyst (EtAlCl ₂) concentration on ethylene oligomerisation	102
3.3.6 Effect of reaction time on ethylene oligomerisation	104
3.3.7 Effect of temperature on ethylene oligomerisation	106
3.3.8 Effect of ethylene pressure on oligomerisation.	108
3.4 Conclusion	109
3.5 References	111

CHAPTER 4

Synthesis and characterisation of bis(pyrazolyl)acetic acid ligands and their palladium(II) complexes

4.1 Introduction	112
4.2 Materials and methods	116
4.3 Synthesis of the ligands and their palladium(II) complexes	116
4.3.1. Bis(pyrazol-1-yl)acetic acid (L14)	116
4.3.2 Bis(3,5-dimethylpyrazol-1-yl)acetic acid (L15)	117
4.3.4. Bis(pyrazol-1-yl)ethyl acetate (L17)	118
4.3.5 Dichloro{bis(pyrazol-1-yl)acetic acid}palladium(II) (9)	118
4.3.6 Dichloro{bis(3,5-dimethylpyrazol-1-yl)acetic acid}palladium(II) (10)	119
4.3.7 Dichloro{bis(3,5-di- <i>tert</i> -butylpyrazol-1-yl)acetic acid}palladium(II) (11)	119
4.4 Results and discussion	120
4.5 Esterification reactions of bis(pyrazol-1-yl)acetic acid, L14 with ethanol	131
4.6 Evaluation of the acid dissociation constants of the bis(pyrazol-1-yl) acetic acid ligands and their palladium(II) complexes.	133
4.7 Conclusion	136
4.8 References	137

CHAPTER 5

5.1 Conclusions	139
5.2 Future directions	142

ABSTRACT

Reactions of furan, thiophene and alkyl carbonyl chlorides with unsubstituted and substituted pyrazoles produced the desired pyrazolyl ligands, [R₂pyrazole-CO-R'] (R= H, Me, ^tBu, Ph, R' = furan, thiophene, Me or ^tBu) in good yields. The reaction of these synthons with Pd(NCMe)₂Cl₂ as the metal precursor afforded the respective palladium(II) complexes in moderate to high yields. All compounds synthesised were characterised by a combination of ¹H NMR, ¹³C NMR and IR spectroscopic techniques for structure elucidation. Microanalyses were performed to confirm the purity of the compounds. Single crystal X-ray crystallography of complexes bis{2-(3,5-dimethylpyrazolyl-1-carbonyl)furan}PdCl₂, **1**, and bis{2-(3,5-dimethylpyrazolyl-1-carbonyl)thiophene}PdCl₂, **2**, was performed to determine the molecular structures of the compounds. The two structures show that the complexes formed are mononuclear. The ligands exhibit monodentate coordination with *trans*-geometry being favoured in the square planar complexes.

Activation of some of the complexes, **1-4**, with the methylaluminoxane (MAO) produced active catalysts for ethylene polymerisation at elevated temperatures giving high-density linear polyethylene. The optimum Al:Pd ratio was found to be 5000:1. The nature of the substituent on the pyrazolyl moiety affects the activity of these catalysts in ethylene polymerisation. In general, increase in steric bulk resulted in decreased catalytic activity and low molecular weight polyethylene. The use of the Lewis acid, B(C₆F₅)₃, with catalyst **2** resulted in enhanced catalytic activity towards ethylene polymerisation.

When ethylaluminium dichloride, EtAlCl₂, was used as the co-catalyst, these catalyst systems were found to be active towards ethylene oligomerisation producing mostly C₁₀ and C₁₂ oligomers. An optimum Al:Pd ratio of 1000: in the catalytic activity of catalyst **2** was observed. The nature of the alkyl substituent on the pyrazolyl system also shows significant influence in the oligomerisation process. The activity of the catalysts as well as the nature of the oligomers produced greatly depends on the oligomerisation conditions. For example, increase in both temperature and pressure resulted on significant increase in turnover number of catalyst **1** and **2**. Longer reaction times resulted in drastic drop in the catalytic activity of the complexes.

When acetic acid was reacted with the appropriate pyrazole in the presence of a phase transfer catalyst, the bidentate bis-pyrazolyl acetic acid ligands, {(pyrazole)₂CHCO₂H}, **L14**, {(Me₂pyrazole)₂CHCO₂H}, **L15**, and {(^tBu₂pyrazole)₂CHCO₂H} **L16** were obtained in good yields. The reaction of these ligands with Pd(NCMe)₂Cl₂ in a 1:1 ratio afforded the corresponding yellow complexes, Pd(**L14**)Cl₂, **9**, Pd(**L15**)Cl₂, **10**, and Pd(**L16**)Cl₂, **11**, in moderate yields. ¹H NMR, ¹³C NMR and IR spectroscopy have been used to characterise these compounds. Microanalysis confirmed the purity and empirical formulae of the complexes. Reaction of **L14** with ethanol under acidic conditions produced the respective ester, bis(pyrazol-1-yl)ethyl acetate, (**L17**) in good yield. The acid dissociation constants of the ligands and their palladium(II) complexes have been determined by titration using dilute NaOH. K_a values within the range of 1.8 × 10⁻⁴ to 1.75 × 10⁻² were obtained. Acidity was found to decrease with increase in the electron

donor ability of the alkyl pyrazolyl substituents. In general, the palladium(II) complexes were more acidic than their corresponding ligands.

LIST OF TABLES

Table	Page
2.1 Selected IR carbonyl frequencies of the ligands and complexes	54
2.2 Some m/z values for the important ions in the mass spectra of the ligands	64
2.3 Selected bond lengths [\AA] and angles [$^\circ$] for L1	76
2.4 Crystal data and structure refinement parameters for L1	78
2.5 Crystal data and structure refinement parameters for 1	80
2.6 Selected bond lengths [\AA] and angles [$^\circ$] for complex 1	82
2.7 Crystal data and structure refinement parameters for 2	83
2.8 Selected bond lengths [\AA] and angles [$^\circ$] for 2	85
3.1 Ethylene polymerisation data for complexes 1, 2, 3, and 4.	94
3.2 The dependence of ethylene polymerisation on the Al:Pd ratio	96
3.3 The effect of $\text{B}(\text{C}_6\text{F}_5)_3$ on ethylene polymerisation using complex 2	99
3.4 Effect of catalyst system on ethylene oligomerisation	101
3.5 Effect of co-catalyst (EtAlCl_2) concentration on ethylene oligomerisation	103
3.6 Effect of reaction time on ethylene oligomerisation	105
3.7 Effect of reaction temperature on ethylene oligomerisation	107
3.8 The effect of monomer concentration on ethylene oligomerisation	108

LIST OF FIGURES

Figure	Page
2.1 Infrared spectrum of complex 2	55
2.2 ¹ H NMR of 2-(3,5-dimethylpyrazolyl-1-carbonyl)thiophene L6	57
2.3 Homonuclear proton-proton shift correlation spectrum, COSY for L7 .	58
2.4 ¹ H NMR spectrum of complex 2	59
2.5 ¹³ C NMR spectrum of bis{2-(pyrazolyl-1- carbonyl)furan}PdCl ₂ 6	61
2.6 Mass spectrum showing the fragmentation pattern of L7 .	63
2.7 ¹ H NMR showing the decomposition of complex 1 to L1 by SnMe ₄	67
2.8 ¹³ C NMR spectrum of (3,5-di- <i>tert</i> -butylpyrazolyl-1-carbonyl)ethane L13	70
2.9 Mass spectrum showing the fragmentation pattern of L13	73
2.10 ORTEP diagram of single moiety of ligand L1	77
2.11 Molecular structure of complex 1	79
2.12 Molecular structure of complex 2	84
3.1 The turn-over numbers for catalysts 1 , 2 , 3 and 4 in the polymerisation of ethylene	98
3.2 The effect of Al:Pd ratio on ethylene polymerisation activity of catalyst 2	97
3.3 ¹³ C NMR spectrum of polyethylene produced from catalyst 2	100
3.4 The effect of Al:Pd on monomer conversion using catalyst 2 .	104
3.5 Effect of reaction time on monomer conversion using catalyst 1 .	106
3.6 The effect of temperature on ethylene oligomerisation activity of catalyst 1	107
3.7 Effect of ethylene pressure on turn-over number of catalyst 1	109

Figure	Page
4.1 Infrared spectrum of bis[(pyrazolyl)acetic acid]palladium dichloride 9 .	123
4.2 ¹ H NMR spectrum of bis(pyrazolyl)acetic acid L14	125
4.3 ¹ H NMR spectrum of bis[(pyrazolyl)acetic acid]palladium dichloride 9	126
4.4 ¹³ C NMR spectrum of bis(3,5-dimethylpyrazolyl)acetic acid L15	128
4.5 Mass spectrum of bis(3,5-di- <i>tert</i> -butylpyrazolyl)acetic acid L16	130
4.6 Figure 4.6 ¹ H NMR spectrum for bis(pyrazol-1-yl)ethyl acetate L17	132
4.7 pH titration curves of ligand L15 and complex 10 with NaOH	135
4.8 pH titration curve of bis(pyrazolyl)acetic acid, L14 with NaOH.	135

ABBREVIATIONS

COD	Cyclooctadiene
eV	Electron volt
EIMS	Electron impact mass spectrometry
GC-MS	Gas chromatography-mass spectrometry
GPC	Gel permeation chromatography
HDLPE	High density linear polyethylene
IR	Infrared spectroscopy
L	Ligand
LLDPE	Linear low density polyethylene
MAO	Methylaluminoxane
MS	Mass spectrometry
NMR	Nuclear magnetic resonance
pz	pyrazole

ACKNOWLEDGEMENTS

I wish to express my sincere gratitude to my supervisor Prof. James Darkwa and co-supervisor Prof. Selwyn Mapolie for their uncompromising professional guidance throughout this research work. DR. Ilia Guzei and Prof. Len Barbour are also greatly thanked for their services in X-ray analysis of the compounds. I am also very thankful to Mr. Timothy Lesch for the instrumental analysis especially the GC. The experience gained during the Organometallic research group seminars and cross-table consultations is highly applauded. I am also very grateful to the Chemistry department and the entire University of the Western Cape community for providing a conducive environment fundamental for this research work. I highly feel indebted to my family for their constant moral support and advice throughout this difficult moment. Lastly, I thank the Almighty Lord for His spiritual protection and guidance up to this particular time in my life.

CHAPTER 1

REVIEW OF LATE TRANSITION METAL CATALYZED OLEFIN

OLIGOMERISATION AND POLYMERISATION AND THE ROLE OF

CO-CATALYSTS

1.1 General

There is considerable effort to develop late transition-metal catalysts for oligomerisation and polymerisation of olefins both in the academic and industrial fields. Olefins particularly ethylene, propylene and butenes are the major building blocks of the petrochemical industry.¹ This is because they are readily available, cheap and could be easily transformed into a range of useful products. The past two decades have been marked by the increasing importance of higher linear olefins, which are used in the preparation of biodegradable detergents, polymers, surfactants and lubricants.²

Higher α -olefins are generally produced through thermal and catalytic cracking of paraffins, oligomerisation of ethylene, dimerization and metathesis of olefins, dehydration of alcohols, and electrolysis of C₃-C₃₀ straight chain carboxylic acids.³ Polymerisation of the lower α -olefins especially ethylene and propylene leads to the production of their respective higher molecular weight polymers.

Historically, heterogeneous catalysis is the most widely used route to making polymers in the polymer industry.⁴ Heterogeneous catalysts offer several important advantages over their soluble homogeneous counterparts in commercial production.⁵ These include the ease of separation of the products from the catalysts. However, they

also exhibit a considerable number of disadvantages. For instance, heterogeneous catalysts possess multiple active sites, each of which has its own properties for monomer insertion, stereoselectivity, comonomer incorporation, chain propagation and transfer.⁶ These factors result in the production of non-uniform polymers and hence a substantial amount of empirical optimization of these catalysts is paramount in order to produce polymers of uniform molecular weights, composition and stereochemistry.⁷

The last two decades have witnessed an increased impetus to develop homogeneous, single-site polymerisation and oligomerisation catalysts to address some of the problems associated with heterogeneous catalyts.⁸ These unique compounds have the general formula L_nMR , where L_n is an organic ligand(s) that bind the metal centre (M) and consequently modifies the reactivity⁹ of the catalyst and R is the polymer chain or initiating group. By controlling the coordination environment of the metal centre, single site catalysts can regulate the molecular weight, molecular weight distribution, yield and comonomer incorporation in a manner that is impossible with heterogeneous catalysts.¹⁰

This chapter is a review of the development of late transition metal compounds as single site catalysts for ethylene oligomerisation and polymerisation. It captures the structural properties of polyethylene, principles of ethylene oligomerisation and polymerisation and the development of nitrogen donor late transition metal complexes as catalysts for ethylene polymerisation. The role of organoaluminium and boron compounds as co-catalysts for metal-catalyzed olefin oligomerisation and polymerisation is also reviewed.

1.2 Ethylene oligomerisation and polymerisation

Oligomerisation generally refers to reactions in which a substrate (monomer) is converted to a higher molecular weight product by a series of repetitive interactions, Equation 1.1. The simplest form of oligomerisation ($n=2$) is dimerization.¹¹



When the number of repeating units is large, (n ranges from hundreds to hundreds of thousands) the area of polymerisation is reached. Chemically polymers are long-chain molecules of very high molecular weights, often in the hundreds of thousands daltons.¹¹ For this reason the term macromolecules is frequently used when referring to polymeric materials.¹² Some thirty different basic types of polymers, formed by linking together of one monomer or copolymers, are now commercially available.¹³ The end uses of polymers depend on their physical properties particularly chain length and varies from plastic buckets, electrical conductors to the production of artificial kidneys.¹⁴ Two of the largest volume polymers are polyethylene and polypropylene with polyethylene production alone in excess of 100 billion pounds per annum.¹⁵ It is for these two products that the discoveries of Ziegler in Germany and Natta in Italy remain significantly important in history.

1.2.1. Types and properties of polyethylene

The three major classes of polyethylene are classified according to their structure and stereochemistry. The three are high-density polyethylene (HDPE), linear low-density polyethylene (LLDPE) and low-density polyethylene (LDPE).¹⁶

The polymer produced depends entirely on the reaction conditions and the nature of the catalysts used.¹⁷ HDPE is a linear semi-crystalline ethylene homopolymer with a melting point of 135°C prepared by Ziegler-Natta and chromium based coordination polymerisation systems. LLDPE is a random copolymer of ethylene and other α -olefins e.g. 1-butene, 1-hexene, or 1-octene produced mainly by Ziegler-Natta, chromium and metallocene catalysts. This type of polyethylene contains considerable amount of short-chain branching. The third type, LDPE is a highly branched ethylene homopolymer prepared under high temperature and pressure free radical process. These extreme conditions have limited the production of this type of polyethylene at commercial levels.¹⁸

The physical and chemical properties of polyethylene produced depend entirely on their main chain stereochemistry. The dependence of physical and chemical properties of a polymer on its structure was predicted as early as 1929 by Staundinger.¹⁹ However, it took another two decades before this phenomenon was confirmed by Schildknecht.²⁰ The higher melting point (130-135°C) and higher density (0.941-0.941 g/cm³) of HDPE as compared to the low melting point (106 –112°C) (and low density (0.915-0.941 g/cm³) of LDPE could be credited to the tacticity and more uniform structure of the former.

1.2.2 Characterisation of polyethylene

The elucidation of polyethylene structure involves the determination of their physical properties and microstructure. These include molecular weight distributions, extent of branching, melting point and glass transition temperatures.²¹ Molecular weight distribution is generally determined by gel permeation chromatography (GPC) based

on polystyrene standards. The two most important molecular weight averages are the number-average molecular weight M_n given by Equation 1.2 where N_i is the number of molecules of molecular weight M_i .

$$M_n = \frac{\sum_i N_i M_i}{\sum_i N_i} \quad \text{Equation 1.2}$$

The weight-average molecular weight, M_w given by Equation 1.3

$$M_w = \frac{\sum_i N_i M_i^2}{\sum_i N_i M_i} \quad \text{Equation 1.3}$$

For unimodal distributions, M_n is usually near the peak. The weight-average molecular weight is always larger than M_n . Narrow molecular weight distributions may have M_w being 1.5 – 2.0 times M_n .²² The ratio M_w/M_n , called the polydispersity index, provides a simplified definition of the molecular weight distribution.

Polymer melting points and glass transition temperatures are commonly measured by thermal methods, which involve a combination of differential scanning calorimetry (DSC) and differential thermal analysis (DTA). Both methods yield peaks relating to endothermic and exothermic transitions and show changes in heat capacity. The DSC method also yields quantitative information relating to the enthalpy changes in the polymer. Other methods employed include dilatometry (volume - temperature and linear expansivity), mechanical strength (static and dynamic), dielectric and magnetic moments (dielectric loss and broad-line NMR) and melt viscosity.²³

The polyethylene structural analysis, which involves the extent of branching or linearity, is analysed by ^1H and ^{13}C NMR spectroscopic techniques. On the basis of

the NMR analysis of branching, it is possible to determine the relative probabilities of insertion or migration from each type of carbon atom in the polymer backbone.²⁴

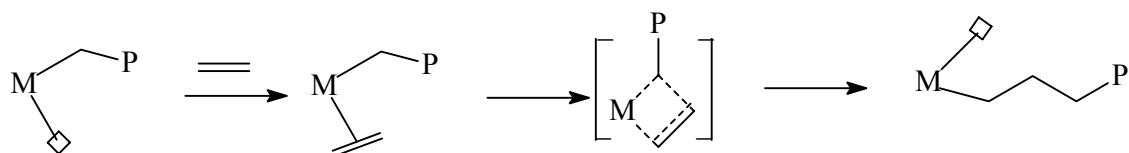
1.3 Principles of ethylene oligomerisation and polymerisation

1.3.1 Mechanistic considerations

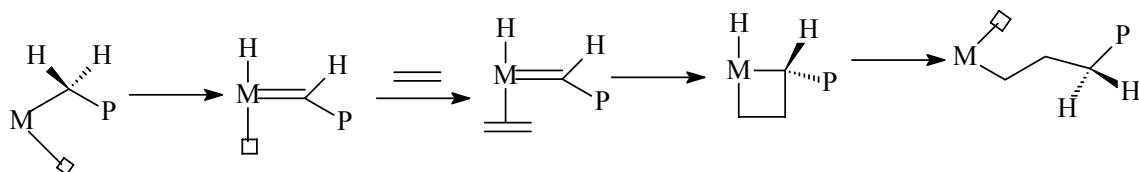
In the last four decades since the discovery of transition metal catalysts for olefin polymerisation by Ziegler and Natta, a considerable amount of research has been directed towards understanding the basic mechanistic steps involved in this process²⁵ Attention has been focused on the process of monomer enchainment, which is generally agreed to occur through olefin co-ordination and followed by insertion into a metal-carbon bond.²⁶

Three general mechanistic proposals for the nature of this insertion have since emerged with the early transition metal catalysts, Scheme 1.1. The first is alkyl migration to the coordinated olefin²⁷ and is known as Cossee-Arlman mechanism. The second type, put forward by Rooney and Green,²⁸ involves an oxidative 1,2 hydride shift from the α -carbon of the polymer chain generating a metal-alkylidene hydride. Olefin coordination follows to generate a metallacyclobutane, and reductive elimination completes the chain propagation.

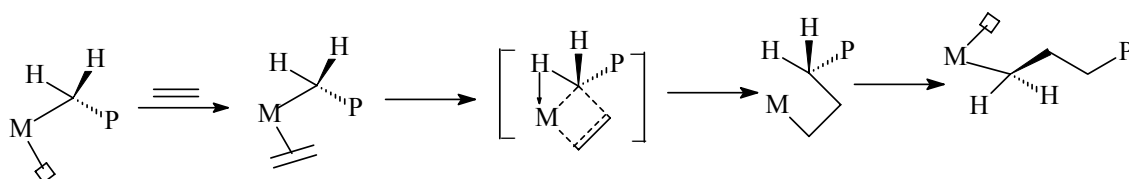
The third mechanistic possibility is the olefin insertion where a α -hydrogen interacts with the metal centre only during the transition state of the C-C bond formation. This model is a hybrid of the Cossee-Arlman and modified Green-Rooney²⁸ mechanisms.



Cossee-Arlman Mechanism (Direct Insertion)



Green-Rooney Mechanism (Hydride Shift)



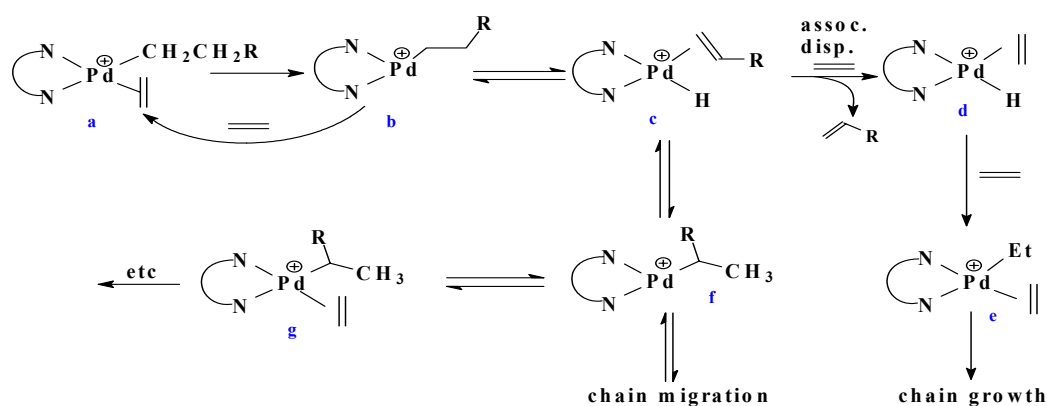
Transition State Agostic Mechanism

Scheme 1.1 Proposed mechanisms for olefin coordination into early transition metal-alkyl bonds

1.3.2 Ethylene oligomerisation and polymerisation mechanism using late transition α -diimine catalysts.

Most mechanistic and theoretical work published to date has been directed at the α -diimine complexes of Ni(II) and Pd(II). Insight into olefin polymerisation mechanisms has been gained through low-temperature NMR studies²⁹ with these catalysts. Under these conditions it has been established that the entire process takes

place via three vital steps, olefin coordination to the metal centre, chain propagation and chain termination³⁰ (Scheme 1.2).



Scheme 1.2. Ethylene polymerisation mechanism with late transition metal α -diimine complexes.

The alkyl ethylene complex **a**, is the catalyst resting state. This is in sharp contrast to early metal catalysts where such intermediates are not observed. The turn-over limiting step is the migratory insertion of the monomer to form a 14 electron system **b** which can be rapidly trapped by ethylene to reform to an alkyl complex **a**. However, in the square planar complexes conversion of **c** to **d** must be an associative process due to the low stability of the three co-ordinate system. It has been observed that the rates of associated displacement and chain transfer (**c** to **d**) are greatly reduced by the steric bulk of the diimine ligands. This is achieved by blocking the axial approach of the olefin monomers. The subsequent result is a much higher rate of chain propagation than chain transfer rate, hence production of higher molecular weight polyethylene. On the other hand complex **b** can undergo β -hydride elimination to

yield **c**. This could undergo further reinsertion with opposite regiochemistry to produce a branched alkyl group in **f**. Trapping and insertion of **f** produces a methyl branch, while further chain migration, β -hydride elimination and readdition results in longer branches. In a chain transfer process, complex **c** can release an olefin to yield **d**, this route results in the production of linear polyethylene. This complex **d** can initiate a new chain (chain propagation) and hence constitutes a whole catalytic cycle involved in the ethylene polymerisation.

1.3.3 Factors controlling the performance of the catalysts in ethylene oligomerisation and polymerisation

Various factors that influence activity of catalysts and the nature of the products obtained in ethylene polymerisation have been extensively investigated. These include catalyst to co-catalyst ratios, catalyst concentration, pressure and temperature, solvent type, reaction time and the nature of the ligand system. The nature of the ligand backbone of the catalyst plays a role in regulating the steric and electronic features around the metal centre. It has been established that increasing the steric bulk of the diimine ligands results in increased molecular weight of the polymers obtained.²⁹ This is by favouring chain propagation relative to chain transfer as earlier explained in section 1.2.1. Brookhart *et al.*³¹ found that increasing the steric bulk of the diimine ligand by substituting *o*-isopropyl groups for *o*-methyl resulted in increase of molecular weight from 110 000 to 390 000. However, there is a substantial body of evidence in literature that show reduced molecular weight with increased bulkiness contrary to theoretical calculations. One such example is the findings of Brookhart *et al.*³² in the ethylene polymerisation using cationic Pd(II) catalysts containing imine-phosphine ligands. It was observed that an increase of steric bulk at the

phosphorus from phenyl to *o*-toluene resulted in a drastic decrease of polymer molecular weight from 133 000 to 75 000.

The extent of branching has also been established to be dependent on the steric parameters of the ligand system. For instance palladium catalysts show decreased branching with decrease in steric bulk resulting in a more linear polymer with increased melting point as was observed by Killian and coworkers²⁹. In this study reduction of the number of branches per 1000 carbon atoms from 74 to 1.2 resulted in an increase in melting point from 97 to 132 °C.

It is well known that temperature has great influence on olefin polymerisation, especially on catalyst activity and polymer molar mass. As temperature increases polymer molecular weight and melting point decrease. Chen *et al.*³³ observed a drop in molecular weight from 101 000 at 0 °C to 52 000 at 40 °C. In general the increase in temperature would increase the catalyst activity if the catalyst is stable at higher temperature hence higher polymer yield. However, at very high temperatures low yields have been reported. This has been ascribed to catalyst decomposition and lower solubility of ethylene at elevated temperatures. The highest polymerisation activities occur in the temperature range from 25 to 40 °C. Malinoski and Brookhart³⁴ recorded highest polymer yields at 25 and 40 °C (productivities up to 320 000 kg of polymer per mol of catalyst per h) with a significant drop in yield at 60 °C of about 100 000 kg of polymer per mol. of catalyst per hour.

Pressure effect on the polymerisation process is well established especially the influence on the catalytic activity. Increase in the ethylene pressure results in an

increase in the polymer yield mainly due to the increase of the local concentration of the ethylene monomer.^{35a} The relationship between the molecular weight of the polymer produced and the pressure is determined by the type of chain termination process involved. For chain termination via β -hydride elimination the molecular weight is linearly dependent on the ethylene pressure.^{35b} Here, since β -hydride termination is independent of monomer concentration, the relative rates of propagation and termination, hence the molecular weight, would be strongly dependent on monomer concentration. Where chain transfer to monomer is predominant the molecular weight is observed to be independent on ethylene concentration. Here both propagation and termination rates would be dependent on upon monomer concentration hence monomer concentration dependency cancels out. In 1994 Brintzinger and co-workers reported^{35c} a polymer with molecular weight independent on of monomer concentration consistent with termination through transfer to monomer using zirconocene complexes containing indenyl rings. Introduction of methyl groups to the second position of indenyl rings generated a catalyst that produced polymer with molecular weight strongly dependent on monomer concentration consistent with β -hydride transfer.

Other factors that affect the catalytic activity and regulate the nature of the products formed include catalyst to co-catalyst ratio and reaction time. It has been found that Al:Pd ratio has a significant effect on ethylene polymerisation. The amount of co-catalyst required to produce the active catalyst varies from one catalyst precursor system to another. For some catalyst precursors, Al:Pd ratios as low as 100:1^{36a} has been reported to generate the active catalysts and activities as high as 3×10^6

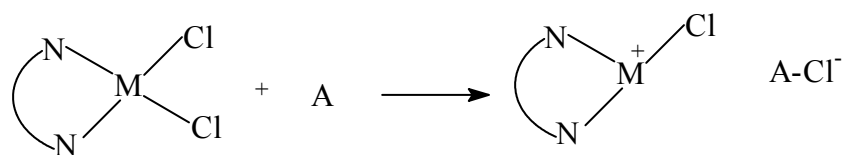
kg/h.mol have been obtained. On the other hand, Al:Pd ratios as high as 4000:1^{36b} have also been reported for some palladium complexes.

Reaction times have also been shown to influence the turn over frequencies depending on the catalyst life times. For catalysts with shorter life times, running polymerisation reactions for longer times significantly result in reduced productivity. Brookhart *et al.*³⁴ observed that experiments run for 15 minutes at 25 °C resulted in low productivity of only 1 200 kg/h.mol. Ni in ethylene polymerisation using cationic Ni(II) and Pd(II) complexes containing bidentate phenacyldiarylphosphine ligands. This was attributed to incomplete initiation of the catalyst species. The productivity reported after 45 minutes was significantly higher (23 000 kg/h.mol) suggesting that the number of active sites in solution is increasing with time. However, lower turnover frequencies were reported for 3 hours (9 000 kg/h.mol) as compared to 1 h (39 000 kg/h.mol) at 40 °C indicating that catalyst decomposition occurs even at lower temperatures.

1.4.1 The role of co-catalysts in metal-catalysed olefin oligomerisation and polymerisation.

Main-group organometallic compounds as co-catalysts in the Ziegler-Natta catalytic systems have played a substantial role in the development of the single-site olefin polymerisation.^{37a} Later discoveries of new and more effective co-catalysts have contributed significantly to the fundamental understanding and technological developments in this field.^{37b}

In general, the importance of the cocatalysts in metal catalysed olefin transformation is attributed to three major chemical processes. First is the conversion of the catalyst precursors to the active catalysts by the co-catalyst, activating species, (Scheme 1.3). Secondly, a successful activation requires special co-catalyst features that kinetically and thermodynamically favours the formation of the active species. Finally, the co-catalyst, which becomes an anion forms the vital part of a catalytically active cation-anion pair and significantly influences the polymerisation or oligomerisation efficiency and polymer or oligomer properties.^{37b}



A = co-catalyst, M = metal centre, N-N = ligand backbone

Scheme 1.3

The current theoretical studies has led to increased understanding of the role played by these group of compounds in metal-catalysed olefin transformations.³⁸ This section reviews the different types of activators and their principal role in olefin oligomerisation and polymerisation.

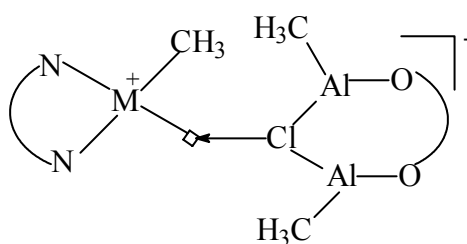
1.4.2 Aluminium alkyls as catalytic activators.

Organoaluminium compounds including trialkylaluminiums and alkylaluminium chlorides are the classical co-catalysts used in Ziegler-Natta oligomerisation and polymerisation catalysis.³⁹ Today, a wide range of homogeneous catalysts based on aluminium alkyls as co-catalysts are employed in the polymerisation and oligomerisation of olefins.⁴⁰ These compounds have been found to play a significant role in determining the nature of products formed when used with late transition metal

complexes in olefin transformations. Daugulis *et al.*³² have reported that the use of ethylaluminium dichloride, EtAlCl_2 , as co-catalyst with cationic Pd(II) complexes containing imine-phosphine ligands produce only butenes. Activation using diethylaluminium chloride led to the production of butenes and trace amount of polymer. While use of modified MAO gave exclusively polymeric material. They attributed this differences in products obtained to the variations in Lewis acidity of the co-catalysts used. Cavell *et al.*⁴¹ also observed that AlMe_3 is unable to activate these nickel complexes in ethylene oligomerisation. They suggested that this could be due to the low Lewis acidity of the compound. More recently, Speiser *et al.*⁴² reported the catalytic oligomerisation of ethylene based on nickel complexes with bidentate P, N phosphinitooxazoline and pyridine ligands using ethylaluminium dichloride, EtAlCl_2 , as co-catalyst. Turn-over frequencies as high as 50 000 with selectivities towards dimerization to butenes higher than 91% were obtained.

Since its discovery, methyl aluminoxane, MAO has been widely used as co-catalyst for Ziegler-Natta type polymerisation.⁴³ Its superb catalytic activity in olefin polymerisation has been attributed to its greater Lewis acidity as compared to the other alkyl aluminium compounds. To date, numerous publications abound in literature involving the use of MAO as co-catalyst in late-transition metal olefin polymerisation.⁵ However, despite its wide success in olefin polymerisation, MAO has several disadvantages: the need of large ratios of MAO to catalyst precursor (10^2 to 10^4 :1) to obtain high polymerisation activity leading to the high ash content (Al_2O_3) of the polymer products. On the same note, the exact nature of the species (ion pairs, free ions) including the role of the $[\text{MAO}]^-$ counter anion are important aspects of activation process under debate.⁴⁴ Recently, based on spectroscopic techniques,

Pedeutour *et al.*⁴⁵ reported the negative role of chloride counter anion in the activation process of Zirconocene chloride by MAO. They attributed this to the formation of a tight ion pair in which a strong interaction between chloride anion and zirconium vacant site, compound [1] still takes place and impedes olefin coordination and insertion. This might explain why replacement of chloride ligands by methyl groups allows much easier activation and hence higher activity.⁴⁶



[1]

The disadvantages associated with MAO has seen the introduction of other aluminoxanes such as ethylaluminoxane and isobutylaluminoxane which are synthesised by partial hydrolysis of triethylaluminium (TEA) and triisobutylbutylaluminium (TIBA), generally referred to as modified methylaluminxanes (MMAO).⁴⁷ However, these MMAOs, do not produce high activities as compared to the original MAO⁴⁸ owing to their low Lewis acidity. It has been reported in literature that tetrakis(*iso*-octyl) aluminoxane [(*i*-octyl)₂-O-Al-(*i*-octyl)₂]⁴⁹ exhibits significant co-catalyst activity comparable to that obtained using MAO.

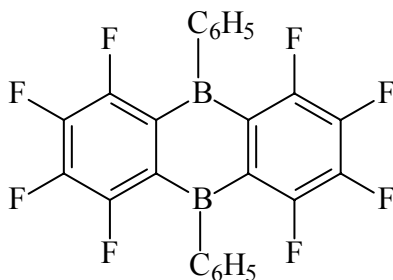
1.4.3 Perfluoroaryl boranes as co-catalysts

In the early 1990s, Marks and Ewen,⁵⁰ discovered that in combination with group 4 metallocene alkyls, strongly Lewis acidic tris(pentafluorophenyl)borane, promotes

highly efficient olefin polymerisation. The eventual isolation and characterisation of the cationic active species of this reagent has resulted in the extensive research of this compound both in the academic and industrial fields. Massey *et al.*⁵¹ recently reported cationic zirconocene ethylene polymerisation catalysts based on $B(C_6F_5)_3$. They showed from solid state ^{13}C NMR spectrum that the formation of electron deficient cationic species is similar to those generated by MAO and the other aluminium alkyls. They postulated that the higher activities reported is due to the high activation ability of the $B(C_6F_5)_3$ as compared to the organoaluminium activators. The organoaluminium activators are characterised by the formation of chloride-bridged complex, which is not an active catalyst.

Lee *et al.*⁵² recently reported the Lewis acidities of the aluminium compounds, $AlMe_3$, $Al(C_6F_5)_3$ and boron reagent $B(C_6F_5)_3$ based on the stretching frequencies of CN of the benzonitrile adducts formed. Their results show that the boron compound, $B(C_6F_5)_3$, is a stronger Lewis acid than the two aluminium compounds. However, high catalytic activity observed with $B(C_6F_5)_3$ as compared to other simple Lewis acids has resulted in the hypothesis that high Lewis acidity alone cannot guarantee effective cocatalyst system. For instance, although BX_3 reagents ($X = F, Cl, Br, I$) have comparable or even greater Lewis acidities than $B(C_6F_5)_3$,⁵³ they are poor activators. This has been accredited to either coordination of the halide atoms to or irreversible transfer to the metal cations.⁷⁵ Over the past few years, Marks and Piers⁵⁴ have developed a number of new and effective perfluoroarylborane activators as well as bifunctional boranes. Bis(pentafluorophenyl)borane, $[HB(C_6F_5)_2]_2$, tris(2,2,2-perfluorobiphenyl)borane, bis(pentafluorophenyl)(2-perfluorophenyl)borane and tris(perfluoronaththyl)borane are among the examples. Recently, the bifunctional

perfluoroarylborane, octafluoro-9,10-bis(pentafluorophenyl)-9,10-diboroanthracene⁵⁵ compound [2] was reported. When combined with group 4 metallocenes and other single-site catalyst precursors, catalytic activity 20 times greater than $B(C_6F_5)_3$ have been reported.



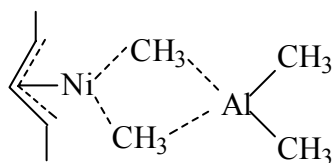
[2]

1.5 Late transition-metal complexes as catalysts for ethylene oligomerisation.

Catalytic oligomerisation is one of the most useful and commonly employed technologies for the conversion of the moderately cheap lower α -olefins (i.e. ethylene and butene) into industrially important higher olefins. The use of organometallic complexes as catalysts in this process has been widely studied.⁵⁶ Numerous catalyst systems involving late transition metal complexes are known to oligomerise lower alkenes to higher molecular weight olefins. Group 8 transition metals complexes, ferrocene and ferrous chloride⁵⁷ have been reported to convert ethylene to a mixture of butenes at 1-20 atm and at -10 to 50 °C. Recently, Brookhart *et al.*^{58a} reported a new Fe catalyst based on diimine tridentate pyridinebisimine ligand complex that oligomerise ethylene to higher olefins. They observed that by reducing the steric bulk of the ligand system, the catalysts oligomerise ethylene to linear α -olefins with remarkable high activity and selectivity. Turnover frequencies as high as 5×10^6 kg of oligomer per mol of Fe per hour were reported and were found to be dependent on catalyst structure, ethylene pressure and temperature. The Co complex of the same

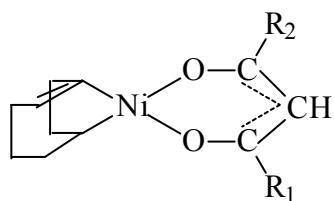
ligand system was also reported to dimerise and isomerise ethylene to higher olefins.^{58b}

One of the most active catalytic reactions have been reported with Ni and carried out at temperatures as low as $-100\text{ }^{\circ}\text{C}$.⁵⁹ These nickel complexes have the general formula of NiX_2L_2 (X = anionic ligand e.g. halogen, carboxyl, L = donor ligand e.g. PPh_3) and are reacted with an excess of an alkyl aluminium halide species such as $\text{Al}(\text{C}_2\text{H}_5)_x\text{Cl}_{3-x}$ (X = 1, 2 or 3) or $\text{Et}_3\text{Al}_2\text{Cl}_3$. Alternatively, organo nickel compounds of the type $\text{NiR}_x\text{X}_{2-x}\text{L}_n$ (where x and n are generally equal to one or two) may be used to provide the active nickel species [3]. In this system, the dimeric π -allyl nickel halides or their mono-tertiary-phosphine adducts have been frequently used and the subsequent reactions with the alkyl-aluminium compounds well characterised.

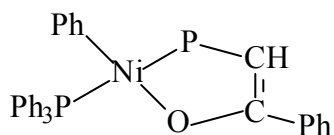


[3]

Today, Ni based complexes constitute one of the most important catalyst systems for olefin oligomerisation because of their high regioselectivity and remarkable catalytic activity. Many chelated Ni complexes have been reported to be highly active and selective in the ethylene oligomerisation. Chelate complexes of the type, [4], have been reported to be very high active with linearity of 80% and the C_8 oligomers as the major products.⁶⁰

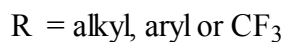
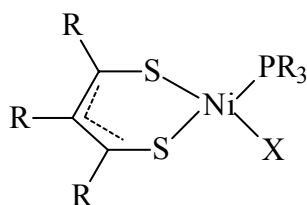


[4]



[5]

Keim *et al.*⁶¹ reported a very interesting Ni catalyst system, [5], which oligomerises ethylene at 50°C and 10-100 bar to α -olefins with 99% linearity and greater than 95% α -olefin content. Recently Cavell *et al.*⁴¹ reported a new system of Ni catalysts of the formula [Ni{RC(S)CR(S)R}₂] and [Ni{RC(S)CR(S)R}PR₃]X (R = alkyl, aryl or CF₃; X = Cl, Br or I), [6] that oligomerises ethylene, butene or propylene with preference to dimerization when activated with an appropriate cocatalyst.⁸⁶

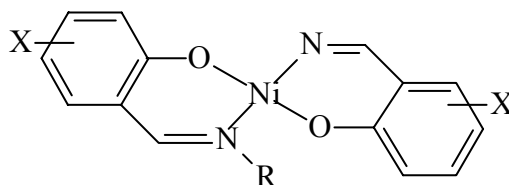


[6]

They observed that the catalytic activity and selectivity in ethylene oligomerisation are significantly affected by changes in the donor ligand, PR₃ while change in the halides, X, affected the catalytic activity only. For instance a change of PR₃ from PEt₃ to PBu₃ resulted in an increase in turnover number from 3 500 to 6 000 kg of oligomer per mol of Ni per hour.

Ni(II) catalysts based on salicylaldiminato complexes have also been reported to oligomerise ethylene to higher olefins. Carlini *et al.*⁶² investigated the ability of Ni

complexes, [7] to oligomerise ethylene when activated with various organoaluminium compounds as co-catalysts. Activities as high as 1.65×10^6 when systems of type [7] are activated with MAO (Al:Ni molar ratio of 100) with $C_4 - C_8$ being the main products are obtained.



X = 5-OMe, H

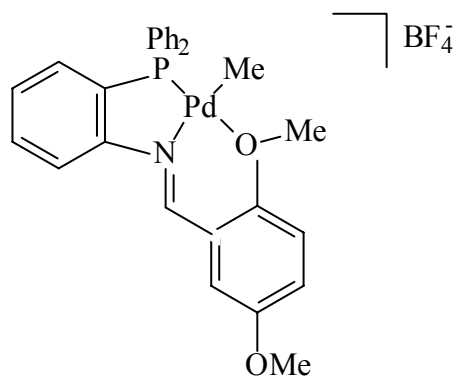
R = *i*Pr, *t*Bu, 2, 6-diisopropylphenyl

[7]

It was observed that an increase in Al/Ni molar ratio to 1000 resulted in a significant increase in turnover frequency to 1×10^7 mol of converted ethylene per mol of Ni per hour, though only butenes were obtained. This suggests that an increase in co-catalyst concentration enhanced activity but favoured the production of lower molecular weight olefins. When activated by Et_2AlCl (Al:Ni molar ratio of 20), an appreciable activity, (TOF = 1×10^5 mol C_2H_4 /mol. Ni. h) was observed with oligomerisation favoured towards the formation of C_4 and C_6 oligomers. More recently, Brookhart *et al.*⁶³ reported cationic Ni(II) α -diimine complexes that are effective in ethylene oligomerisation.

The use of Pd in ethylene oligomerisation is less prevalent presumably due to its low activity and poor selectivity.⁶⁴ Few literature reports exist hitherto on Pd complexes as ethylene oligomerisation catalysts. The dimerisation of ethylene by tetrachlorobis(ethylene)dipalladium in non-hydroxyl media (benzene or dioxane) has

been reported.⁶⁴ Recently, Liu and co-workers⁶⁵ reported Pd(II) complexes containing P-N-O ligands [8] as ethylene oligomerisation catalysts.

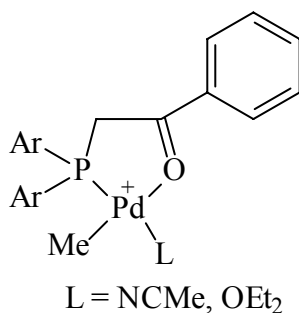


[8]

This catalyst system does catalyse the conversion of ethylene to oligomers (C₆-C₁₆) though with low activity (49.5 g of product/mol. Pd.h) presumably due to the non-symmetric P-N bidentate ligand. They also observed significant effect of the reaction conditions on the activity of these catalyst systems. For example, an increase of temperature from 30 to 110 °C resulted in an increase in activity from 2.6 to 49.5 g oligomer per mol of catalyst per hour with product distribution of C₆-C₈ and C₁₂-C₁₆ being obtained respectively.

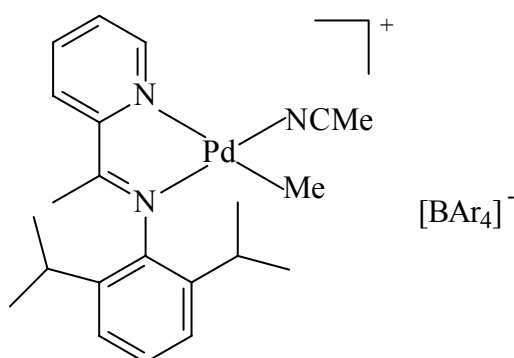
Brookhart and co-workers³⁴ recently reported the oligomerisation of ethylene by cationic Pd(II) complexes containing bidentate phenacyldiarylphosphine ligands [9] of the well known SHOP systems. The Pd analogues were found to be about an order of magnitude less active than their Ni counterparts.⁶⁶ They also observed that when L = NCMe and Ar = C₆H₅, only butenes were generated while when Ar = 2,4,6-(CH₃)₃C₆H₅, a mixture of butenes and hexenes were produced. In all cases the

products formed were greater than 90% α -olefin. However, these catalysts exhibit shorter lifetime as majority of the catalyst were found to deactivate after 1 h.



[9]

Kress *et al.*⁶⁷ recently reported the oligomerisation of ethylene by cationic Pd(II) complexes containing unsymmetrical α -diimine ligand [10]. Activities of 105 kg/mol.h of catalyst were obtained. The activity of this catalyst system increases markedly with increase in temperature. Interestingly, the nature of the oligomeric materials obtained (C₄–C₂₀) does not change significantly with the reaction conditions.

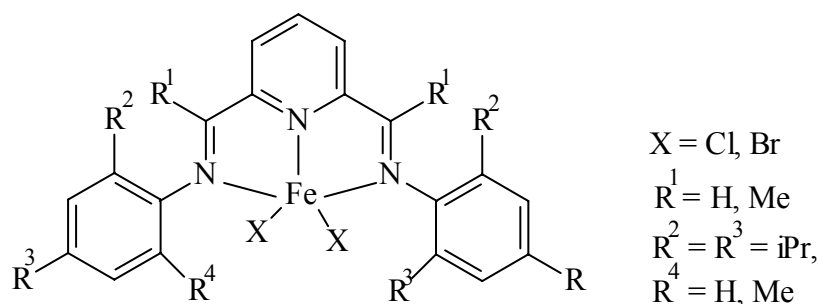


[10]

1.7 Late transition-metal complexes as catalysts for ethylene polymerisation.

The discovery by Brookhart and co-workers of highly active Pd(II) and Ni(II) α -diimine catalysts has resulted in renewed interests in the development of late transition metal catalysts for olefin polymerisation.^{29, 68} It is believed that the key to the production of high molecular weight polymers is the incorporation of bulky substituents onto the aryl rings. This has the overall effect of retarding the rate of ethylene associative chain transfer.

One of the most recent reports of highly active late transition catalysts is that of group 8 nitrogen-donor complexes. Systems of type [11] based on a five coordinate Fe centre supported by a neutral tridentate 2,6-bis(imino)pyridine ligand⁶⁹ when activated with MAO show exceptionally high activity. Activities are comparable to, or even higher than those found for Group 4 metallocenes under similar conditions. The molecular weights of polyethylene produced show significant dependency on the aryl substituents. Increasing the size of these substituents or having substituents on both of the *ortho* positions of the aryl rings results in the formation of high molecular weight polyethylene. Chen *et al.*⁷⁰ recently reported an Fe complex based on the same ligand backbone as ethylene polymerisation catalysts but using halogens instead of the alkyls as the substituents on the aryl rings. The halogen substituents impart not only steric effects but also electronic effects. As opposed to the small difference in electronic effect resulting from changing the alkyl substituents, the electronic effect resulting from varying the halogens is much more significant due to the large difference in their electronegativities.

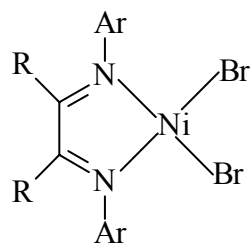


[11]

The complex containing the chloro substituent was found to be more active (12.8×10^3 kg/mol.h) than the bromo analogue (8.6×10^3 kg/mol.h). Gratifyingly, the bromo analogue was found to be more active in ethylene polymerisation (12.2×10^3 kg/mol.h) than the *iso*-propyl substituted Fe complex (5.4×10^3 kg/mol.h) under similar conditions. This was attributed to the electron-withdrawing nature of the chloro and bromo substituents, which results in a more electrophilic Fe centres in the complexes. In this study, the Co(II) complex based on this ligand system was also reported to polymerise ethylene with lower activity (0.6×10^3 kg/mol.h) when treated with MAO than the respective Fe analogue. The other Group 8 ethylene polymerisation catalyst that has been reported is the Ru complex containing triphenyl phosphine donor ligand.⁷¹ This catalyst system shows low activity with branched polyethylene being produced.

The Ni(II) dibromide complex of the type [12] when treated with MAO shows very high activity in ethylene polymerisation (11.0×10^3 kg/mol.h.bar).⁷² The formation of high molecular weight polymers is attributed to the steric protection of the vacant coordination site provided by the bulky substituents. Polyethylene with molecular weights of 1.0×10^6 and degree of branching from linear to over 70 branches per 1000 carbons under various polymerisation conditions have been reported for these

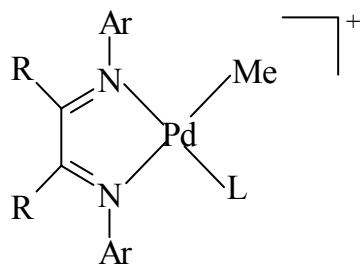
type of catalysts. The analogous Pd(II) [13] complexes show moderate activity producing highly branched amorphous polyethylene with up to 100 branches per 1000 carbon atoms.



[12]

R = H, Me,

Ar = 2,6-*i*Pr₂C₆H₃



X⁻

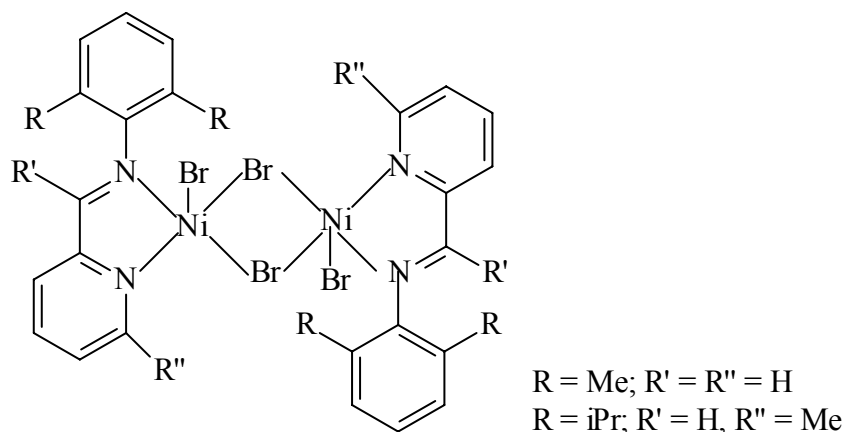
Ar = 2,6-*i*Pr₂C₆H₃

X = B[3,5-(CF₃)₂C₆H₃]₄

L = Et₂O, MeCN

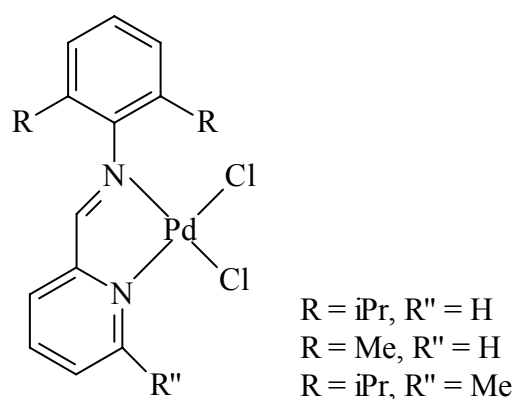
[13]

Laine *et al.*⁷³ have reported pyridinyl-based Ni(II) and Pd(II) complexes as catalysts for polymerisation of ethylene. The dimeric Ni(II) complex [14] showed moderate ethylene activity when activated with MAO.



[14]

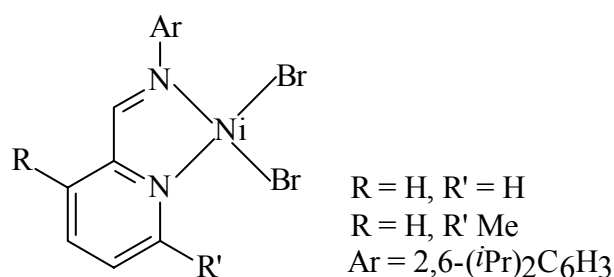
They reported that activities for the system that contains the methyl substituents are one order of magnitude lower than that of the unsubstituted complex. This was attributed to the obstruction of the equatorial coordination sites by the methyl groups. Another interesting phenomenon observed is the dependence of the degree of polymer branching on the substituents on the ligand backbone. Decreasing the steric bulk in the aryl ring by replacing the two *iso*-propyl groups with methyls in the 2 and 6-positions gives more linear polymers. The Pd(II) analogues of these complexes, [15], also produce active catalysts for ethylene polymerisation when activated with MAO.



[15]

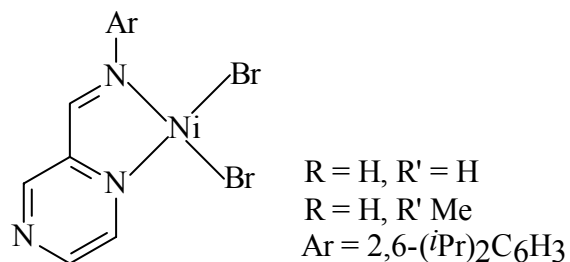
Ni(II) and Pd(II) metal complexes based on bulky arylimino substituents on one side and a relatively unhindered heterocyclic donor ligand on the other have also been

reported as ethylene polymerisation catalysts by Britovsek and co-workers.⁷⁴ These ligands provide only half the steric protection of derivatives with bulky substituents on both donor atoms. The activities reported for the Ni(II) iminopyridine **[16]**, (0.69×10^3 kg/mol Ni. h.) is considerably lower than those reported for similar (α -diimine)NiBr₂ complex, R = H and Ar = 2,6-diisopropylphenyl, (11.0×10^3 kg/mol.Ni.h) described above.



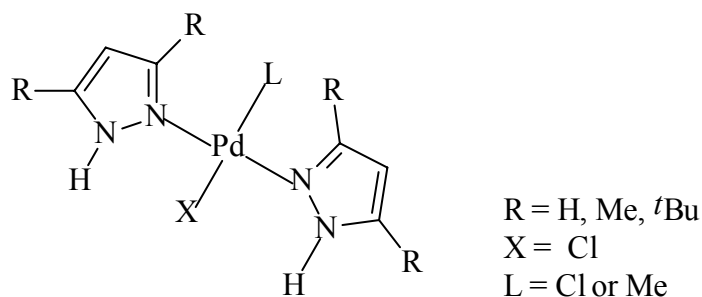
[16]

More interesting in this study was the inactivity towards ethylene polymerisation reported for the pyrazine Ni(II) analogue, **[17]**, though it is sterically identical to the iminopyridine catalyst **[16]**. The reduced basicity of the pyrazine nitrogen donor atom (pK_a = 0.4 vs 5.2 for pyridine) which may lead to catalyst deactivation (via ligand dissociation) could account for this observation.⁷⁵ Another explanation is the coordination of the non-coordinating nitrogen donor of the pyrazine moiety to the Lewis-acidic aluminium centre of the co-catalyst, MAO, leading to catalyst deactivation as well.



[17]

Currently our research group has embarked on the synthesis of Ni(II) and Pd(II) with pyrazole and pyrazolyl ligands and their evaluation as potential catalysts for ethylene polymerisation. The choice of the pyrazole ligand is based on the easily varied steric and electronic properties of the systems, which helps in fine-tuning the eventual properties of the complexes towards the desired active polymerisation catalysts. Darkwa *et al.*⁷⁶ have reported the synthesis and ethylene polymerisation results of pyrazole Pd(II) complexes of type [18]. They reported moderate catalytic activity (1.768×10^3 kg/mol of Pd. h.) and high molecular weight polyethylene of up to 1×10^6 comparable to the Brookhart systems. The catalyst system (3,5-*t*Bu₂pz)₂Pd(Me)Cl was found to be the most active, a feature attributed to the existence of the Pd-Me bond while the others contain Pd-Cl bonds. The activities of the complexes were found to be temperature, pressure, time and catalyst concentration dependent. For instance the activity almost doubled when the temperature was increased from 30 °C to 70 °C.

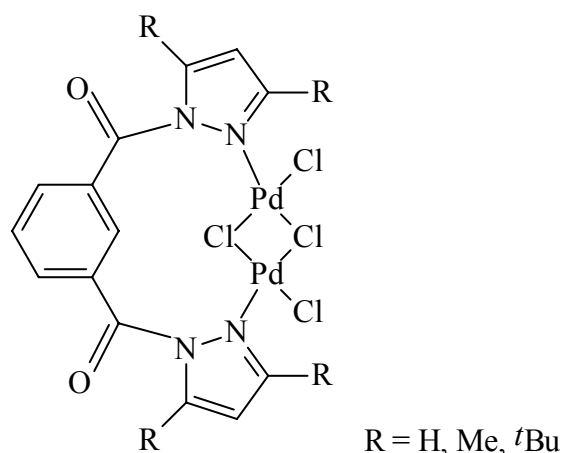


[18]

The Ni(II) analogues⁷⁷ of these systems have also been evaluated for ethylene polymerisation and were found to have activity comparable to that of their Pd(II) counterparts, but produce higher molecular weight polyethylene. For instance at 25°C and 5 atm ethylene pressure, catalyst (3,5-Me₂pz)₂PdCl₂ showed activity of 2.14 × 10² kg/mol.h with *M_w* of 5.53 × 10⁵ compared to 2.50 × 10² kg/mol.h and *M_w* of 1.44 × 10⁶ produced by (3,5-Me₂pz)₂NiCl₂ under similar experimental conditions.

In an attempt to increase the electrophilicity of the metal centre for easy coordination of ethylene to increase catalytic activity of the Pd complexes, Darkwa *et al.*⁷⁸ introduced electron withdrawing carbonyl linkers in the pyrazole systems. In this work, the ethylene polymerisation results by the benzenedicarbonyl and benzenetricarbonyl pyrazolyl Pd(II) complexes [19] were reported. Significantly, the activity of these complexes showed remarkable improvement as compared to the simple systems. For example, the turn-over number of compound [19] is reported as 2591 kg/mol.h compared to 1005 kg/mol.h of the analogous (3,5-*t*Bu₂pz)₂PdCl₂ compound. It can thus be confidently concluded that the presence of the carbonyl functionality in the pyrazolyl ligands improves the electrophilic nature of the metal centre hence leading to higher catalytic activity. The dinuclear coordination environment of this system could also contribute to its observed higher activity. It is

on this basis, that we undertook to study the catalytic ability of monocarbonyl thiophene and furan pyrazolyl Pd(II) complexes in this thesis.



[19]

1.8 Objectives of this research work

As part of the on-going research to develop other active nitrogen containing late transition metal catalysts for olefin catalysis worldwide, we set out to investigate the catalytic ability of monocarbonyl furan and thiophene pyrazolyl Pd(II) complexes in ethylene oligomerisation and polymerisation. Earlier findings have shown that the introduction of carbonyl functionalities in the pyrazole unit enhances the catalytic activity of the resultant complexes. However, the activity is also shown to be dependent on the structure of the complexes. Low activities are reported for the systems having a non-coordinating pyrazole unit. While on the other hand, higher activities were reported for dinuclear complexes. In this work therefore, we undertook to explore any significant effect that could arise from the donor atoms oxygen and

sulfur in the furan and thiophene units respectively on the coordination and eventual catalytic activity of their Pd(II) complexes. To further understand the role of these heterocycles, we attempted to synthesise the acyl pyrazolyl Pd(II) complexes with the aim of evaluating their catalytic activity in ethylene polymerisation.

The second chapter of the thesis deals with the synthesis and characterisation of a series of substituted pyrazolyl ligands containing furoyl and thiophene carbonyl units. The synthesis and characterisation of their resultant Pd(II) complexes is also reported in this section. In addition, we also report the synthesis of the acyl pyrazolyl ligands and attempted preparation of their respective Pd(II) complexes. Chapter 3 reports the preliminary catalytic studies of some of the synthesised complexes in ethylene oligomerisation and polymerisation.

In Chapter 4, we discuss the synthesis and characterisation of bis(pyrazolyl)acetic acid ligands and their Pd(II) complexes with the objective of testing their catalytic potential in ethylene oligomerisation and polymerisation. We also report the acidities of these ligands and their Pd(II) complexes. The ability of these bis(pyrazolyl)acetic acid ligands to undergo the classical esterification reactions is also investigated in this section.

1.8 References

1. J. Skupinska, *Chem. Rev.* **91** (1991) 613.
2. P. Pino, *Adv. Polym. Sci.* **4** (1965) 394.
3. P. Schwab, M. B. France, J.W. Ziller, R. H. Grubbs, *Angew. Chem. Int. Ed. Engl.* **34** (1995) 2039.
4. G. W. Coates, *Chem. Rev.* **100** (2000) 1223.
5. S. Ittel, M. Brookhart, L. Johnson, *Chem. Rev.* **100** (2000) 1169.
6. W. M. Kelly, N. J. Taylor, S. Collins, *Macromolecules* **27** (1994) 4477.
7. W. K. Doak, *Encyclopaedia of Polymer Science and Engineering* John Wiley and Sons, New York (1986) 386.
8. L. H. Sperling, *J. Chem. Ed.* **62** (1985) 867.
9. G.T. Davis and R.K. Eby, *J. Appl. Phys.* **44** (1973) 4274.
10. F. C. and L. Mandelkern, *Macromolecules* **3** (1970) 242.
11. J. M. Widmaier and G. C. Meyer, *Macromolecules* **14** (1981) 450.
12. L.H. Sperling, *Introduction to Polymer Science*, 2nd edition John Wiley and Sons, New York (1991) 303.
13. C. Masters, *Homogeneous Transition-Metal Catalysis*, Chapman and Hall, London (1981) 159.
14. L. A. Waddams, *Chemicals From Petroleum*, 4th edition, John Murray, London (1978).
15. J.I. Kroschwitz, *Encyclopedia of Polymer Science and Engineering* 2nd ed, Wiley, New York (1990).
16. F. C. Chen, C. L. Choy, S. P. Wong, and K. Young, *Polymer* **21** (1980) 1139.
17. T. R. Youngkin, E. F. Connor, J. R. Henderson, S. K. Friedrich, R. H. Grubbs, D. A. Bansleben, *Science* **287** (2000) 460.

18. W. Keim, R. Appel, S. Gruppe, F. Knoch, *Angew. Chem. Int. Ed. Engl.* **26** (1987) 1012.
19. S. Y. Desjardins, K. J. Cavell, H. Jin, B. W. Skeleton, A. H. White, *J. Organomet. Chem.* **515** (1996) 233.
20. C. Wang, S. Friedrich, T. R. Younkin, R. H. Grubbs, D. A. Bansleben, M. W. Day, *Organometallics* **17** (1998) 314.
21. A. Tomov, K. Kurtev, *J. Mol. Catal. A. Chem.* **103** (1995) 95.
22. G. Allen Ed. *Comprehensive Polymer Science*, Pergamon, Oxford (1989)
23. G. Natta, P. Pino, P. Corradini, F. Dannusso, E. Mantica, *J. Am. Chem. Soc.* **77** (1955) 1708.
24. U. Klabunde, S. D. Ittel, *J. Mol. Catal.* **41** (1987) 123.
25. C. P. Cassey, S. L. Hallenbeck, D. W. Pollock, C. R. Landis, *J. Am. Chem. Soc.* **117** (1995) 9770.
26. E. J. Arlman, P. Cossee, *J. M. Catal.* **3** (1964) 99.
27. K. J. Ivin, J. J. Rooney, C. D. Stewart, M. L. H. Green, R. Mahtab, *J. Chem. Soc. Chem Commun.* (1978) 604.
28. M. Brookhart, M. L. H. Green, *J. Organomet. Chem.* **250** (1983) 395.
29. C. M. Killian, L. K. Johnson, M. Brookhart, *J. Am. Chem. Soc.* **117** (1995) 6414.
30. (a) G. W. Coates, R. M. Waymouth, *J. Am. Chem. Soc.* **115** (1995) 6465. (b) R. Cramer, *J. Am. Chem. Soc.* **87** (1965) 4717.
31. M. Brookhart, M. L. H. Green, *J. Organomet. Chem.* **250** (1983) 395.
32. O. Daugulis, M. Brookhart, *Organometallics* **21** (2002) 5926.
33. Y. Chen, R. Chen, C. Qian, X. Dong, J. Sun, *Organometallics* **22** (2003) 4312.

34. J. M. Malinoski, M. Brookhart, *Organometallics* **22** (2003) 5324.
35. (a) D. W. Coater, J. E. Bercaw, *J. Organomet. Chem.* **417** (1991) 1. (b) A. K. Rappe, W. M. Skiff, C. J. Casewit, *Chem. Rev.* **100** (2000) 1435. (c) U. Stehling, J. Diebold, R. Kirsten, W. Roll, H. Brintzinger, F. Langhauser, S. Jungling, *Organometallics* **13** (1994) 964.
36. (a) T. Yoshinda, N. Koga, K. Morokuma, *Organometallics* **14** (1995) 746. (b) J. R. Hart, A. K. Rappe, *J. Am. Chem. Soc.* **115** (1993) 6159.
37. (a) E. Y. Chen, T. J. Marks, *Chem Rev.* **100** (2000) 1391. (b) X. Yang, C. L. Stern, T. J. Marks, *J. Am. Chem. Soc.* **116** (1994) 10015.
38. G. Erker, M. Aulbach, C. Kruger, S. Werner, *J. Organomet. Chem.* **450** (1993) 1.
39. J. C. W. Chien, Ed. *Coordination Polymerisation*, Academic Press, New York (1975) 15.
40. W. Keim, F. H. Kowarldt, R. Goddard, C. Kruger, *Angew. Chem. Int. Ed. Engl.* **17** (1978) 466.
41. R. Abeywickrema, M. A. Bennett, K. J. Cavell, M. Kony, A.F. Masters, A. G. Webb, *J. Chem. Soc. Dalton Trans.* (1993) 59.
42. F. Speiser, P. Braunstein, L. Saussine, R. Welter, *Inorg. Chem.* **43** (2004) 1649.
43. (a) H. Sinn, W. Kaminsky, H. J. Vollmer, R. Woldt, *Angew. Chem. Int. Ed. Engl.* **19** (1980) 390. (b) P. Pino, R. Mulhaupt, *Angew. Chem. Int. Ed. Engl.* **19** (1980) 857. (c) A. R. Barron, *Organometallics* **14** (1995) 3581. (d) C. J. Harlan, S. G. Bott, A.R. Barron, *J. Am. Chem. Soc.* **117** (1993) 91.
44. A. G. Massey, A. J. Park, *J. Organomet. Chem.* **5** (1966) 218.

45. J. N. Pedeutour, H. Cramail, A. Deffieux, *J. Mol. Catal. A. Chem.* **174** (2001) 81.
46. Y-X. Chen, P-F. Fu, C. L. Stern, T. J. Marks, *Organometallics* **16** (1997) 5958.
47. K. Peng, S. Xiao, *J. Mol. Cat.* **90** (1994) 201.
48. W. Kaminsky, R. Steiger, *Polyhedron* **7** (1988) 3375.
49. Y. X. Chen, M. V. Metz, L. Li, C. L. Stern, T. J. Marks, *J. Am. Chem. Soc.* **120** (1998) 6287.
50. X. Yang, C. L. Stern, T. J. Marks, *J. Am. Chem. Soc.* **113** (1991) 3623.
51. (a) A. G. Massey, A. J. Park, *J. Organomet. Chem.* **2** (1964) 245.
52. C. H. Lee, S. Jin Lee, J. W. Park, K. H. Kim, B. Y. Lee, J. S. Oh, *J. Mol. Catal. A. Chem.* **132** (1998) 231.
53. (a) M. Bochmann, L. M. Wilson, *J. Chem. Soc. Chem Commun.* (1986) 1610.
(b) R. F. Jordan, W.E. Dasher, S. F. Schols, *J. Chem. Soc. Chem Commun.* **108** (1986) 1718.
54. (a) D. J. Perks, R. E. Spence, W. E. Piers, *Angew. Chem. Int. Ed. Engl.* **34** (1995) 857. (b) X. Yang, C. L. Stern, T. J. Marks, *J. Am. Chem. Soc.* **118** (1996) 12451.
55. V.C. Williams, C. Dai, Z. Li, S. Collins, W. E. Piers, W. Clegg, M. R. J. Elsegood, T. B. Marder, X. Yang, C. L. Stern, T. J. Marks, *J. Am. Chem. Soc.* **38** (1999) 3695.
56. B. Bogdanovic, B. Spliethoff, G. Wilke, *Angew. Chem. Int. Ed. Engl.* **19** (1980) 622.
57. V. Sh. Feldblyum, L. S. Korotova, A. I. Leshcheva, L. D. Kononova, French Patent, 1588162 (1970) *Chem Abstr.* **76** 153182 (1972).

58. (a) B. L. Small, M. Brookhart, *J. Am. Chem. Soc.* **120** (1998) 7143. (b) B. L. Small, *Organometallics* **22** (2003) 3178.
59. B. Bogdanovic, *Adv. Organometal. Chem.* **17** (1979) 105.
60. W. Keim, E. Hoffman, R. Lodewick, M. Pauckert, G. Schmitt, J. Fleischhauer, U. Meier, *J. Mol. Catal.* **6** (1979) 79.
61. W. Keim, F. H. Kowarldt, R. Goddard, C. Kruger, *Angew. Chem. Int. Ed. Engl.* **90** (1978) 493.
62. C. Carlini, M. Isola, V. Liuzzo, A. R. Galletti, G. Sbrana, *Appl. Catal. A. Gen.* **231** (2002) 307.
63. C. M. Killian, L. K. Johnson, M. Brookhart, *Organometallics* **16** (1997) 2005.
64. J. T. Vangermert, P. R. Wilkinson, *J. Phys. Chem.* **68** (1994) 645.
65. P. Y. Shi, Y. H. Liu, S. M. Peng, S. T. Liu, *Organometallics* **21** (2002) 3203.
66. W. Liu, J. M. Malinoski, M. Brookhart, *Organometallics* **21** (2002) 2836.
67. (a) S. P. Meneghetti, P. J. Lutz, J. Kress, *Organometallics* **18** (1999) 2734. (b) S. P. Meneghetti, P. J. Lutz, J. Kress, *Organometallics* **20** (2001) 5050.
68. S. K. Mecking, L. K. Johnson, M. Brookhart, *J. Am. Chem. Soc.* **118** (1996) 267.
69. (a) B. L. Small, M. Brookhart, A. M. A. Bennet, *J. Am. Chem. Soc.* **120** (1998) 4049. (b) G. J. P. Brtovsek, B. S. Kimberly, P. J. Maddox, S. J. McTavish, G. A. Solan, A. J. P. White, D. J. Williams, *Chem Commun.* (1998) 849.
70. Y. Chen, R. Chen, C. Qian, X. Dong, J. Sun, *Organometallics* **22** (2003) 4312.

71. (a) Z. Guan, J. W. Marshall, *Organometallics* **21** (2002) 3580. (b) G. M. Kapteijn, M. P. R. Spee, D. M. Grove, H. Kooijman, A. L. Spek, G. van Koten, *Organometallics* **15** (1996) 1405.
72. M. Brookhart, D. M. Lincoln, *J. Am. Chem. Soc.* **110** (1988) 8719.
73. T. V. Laine, U. Piironen, K. Lappalainen, M. Klinga, E. Aitola, M. Leskela, *J. Organomet. Chem.* **606** (2000) 112.
74. J. P. G. Britovsek, P.D. S. Baugh, O. Hoarau, V. C. Gibson, D. F. Wass, J. P. Andrew, D. J. Williams, *Inorg. Chim. Acta*, **345** (2003) 279.
75. A. R. Katritzky, A. F. Pozharskii, (Eds), *Handbook of Heterocyclic Chemistry*, 2nd ed, Elsevier, Amsterdam (2000) 17.
76. K. Li, J. Darkwa, I. A. Guzei, S. F. Mapolie, *J. Organomet. Chem.* **660** (2002) 108.
77. S. M. Nelana, J. Darkwa, I. A. Guzei, S. F. Mapolie, *J. Organomet. Chem.* **689** (2004) 1835.
78. K. Li, J. Darkwa, I. Guzei, G. A. Bikzhanova, S. F. Mapolie, *Dalton. Trans.* (2003) 715.

CHAPTER 2

SYNTHESIS AND CHARACTERISATION OF HETEROCYCLIC CARBONYL PYRAZOLYL PALLADIUM(II) COMPLEXES

2.1 Introduction

Pyrazole type heterocycles represent an important class of nitrogen containing donor ligands in coordination chemistry of late transition metal elements.¹ They have been widely used as terminal ligands,² bridging ligands³ and precursors for the synthesis of various multi-nitrogen bearing ligands in coordination chemistry, bioinorganic chemistry and organometallic chemistry. The synthesis, characterisation and molecular structures of pyrazole and pyrazolyl complexes with transition metals have been extensively reviewed.⁴

Pyrazolyl ligands provide hard donor sites for transition metals hence suitable for stabilizing higher oxidation states metal complexes. Their donor ability also accounts for the ease of coordination of these ligands to transition metals.⁵ The five membered pyrazole ligands have also been used to modify π -deficient six membered heterocyclic ligands like pyridine⁶ and 1,10 phenanthroline.⁶ For example a planar tridentate bis(pyrazolyl-3-yl)pyridine has been synthesised by Gamez *et al.*⁷ and found to stabilize copper(II) complexes. Homoleptic bis-tridentate Ru(II) complexes of the ligand 3,5-dimethylpyrazol-1-yl) bipyridine⁸ have also been prepared by the reaction of the ligand with ruthenium trichloride in a mixture of refluxing ethanol/water.

However, the best known pyrazolyl ligand is poly(pyrazol-1-yl)borates. This was first synthesised by Trofimenko and co-workers,⁴ and improved synthetic methods developed by Elguero and co-workers⁹ have led to extensive studies of the physical and chemical properties of transition metal complexes containing multidentate pyrazole and pyrazolyl ligands. These ligands are dominated by BR and BR₂ linkers as is the case with hydrotris(3-tert-butylpyrazol-1-yl)borate¹⁰ and hydrotris(3-tert-butyl-5-methylpyrazol-1-yl)borate.¹¹

The choice of the substituents and linkers in the pyrazolyl ligands affects the electron donor ability of the nitrogen atoms and hence the strength of the bonding to the ligated metal. The use of linkers hitherto was still limited to boron compounds. However, there are few examples of non boron linker compounds, such as 2,6-bis(pyrazolylmethyl)pyridine¹² and (2-hydroxy-3-*t*-butyl-methylphenyl)bis(3,5-dimethylpyrazolyl)methane.¹³ Such modification of linkers confer different electronic properties on the ligand and the resultant complexes. Darkwa and coworkers recently reported the use of the carbonyl linkers to modify the electronic nature of the pyrazolyl ligands. They observed enhanced catalytic behaviour in ethylene polymerisation of these pyrazolyl palladium complexes¹⁴ compared to their simple pyrazole palladium analogues.¹⁵

In this Chapter, we report the synthesis and characterisation of furan and thiophene carbonyl pyrazolyl ligands as modifications of linkers in pyrazolyl ligands that could be used in ethylene oligomerisation and polymerisation reactions. The synthesis and

characterisation of their respective palladium(II) complexes is also discussed. This part of the thesis, also reports the successful synthesis of acyl pyrazolyl ligands and attempts to prepare their palladium(II) complexes.

2.2 Materials and instrumentation

All ligand and complex syntheses were performed under a nitrogen atmosphere using standard Schlenk techniques. All solvents were of analytical grade and were dried and distilled prior to use. Toluene and dichloromethane were dried and distilled from sodium/benzophenone and P₂O₅ respectively. The carbonyl linkers, 2-thiophene carbonyl chloride and 2-furoyl chloride were obtained from Sigma-Aldrich and used as received. The NMR spectra were recorded on a Varian Gemini 2000 instrument (¹H at 200 MHz, ¹³C at 50.3 MHz) at room temperature. The chemical shifts are reported in δ (ppm) and referenced to the residual CDCl₃ in NMR solvent. Elemental analysis and IR spectroscopy were performed on a Carlo Erba NA analyzer and PerkinElmer, FT-IR Paragon 1000PC respectively at the Chemistry Department, University of the Western Cape. GC-MS analysis was performed using a Finnigan-Matt GCQ-Gas Chromatography equipped with an electron impact ionization source at 70eV, a 30 m HP-MS capillary column with a stationary phase based on 5 % phenyl-methylpolysiloxane. The X-ray crystal evaluation and data collection were performed on a Bruker CCD-1000 diffractometer with Mo K_α (λ = 0.71073 Å) radiation and a diffractometer to crystal distance of 4.9 cm.

2.3 Synthesis of the ligands

2.3.1 2-(3,5-dimethylpyrazolyl-1-carbonyl)furan (L1)

To a solution of 2-furoyl chloride (2.12 g, 15.60 mmol) in toluene (40 mL) was added 3,5-dimethylpyrazole (1.49 g, 15.60 mmol) and Et₃N (2 mL). The mixture was refluxed for 24 h, filtered to remove the Et₃NH⁺Cl⁻ by-product and the solvent removed in *vacuo* to give a white residue, which was purified by recrystallization from CH₂Cl₂/hexane. Yield = 2.52 g (85%). ¹H NMR, (CDCl₃): δ 2.29 (s, 3H, CH₃, pz); 2.62 (s, 3H, CH₃, pz); 6.02 (s, 1H, pz); 6.61 (dd, 1H, furan, ⁴J_{HH} = 1.6 Hz, ³J_{HH} = 3.6 Hz); 7.71 (dd, 1H, furan, ⁴J_{HH} = 0.8 Hz, ³J_{HH} = 3.6 Hz); 7.94 (dd, 1H, furan, ⁴J_{HH} = 0.8 Hz, ³J_{HH} = 3.8 Hz). ¹³C{¹H} NMR (CDCl₃): δ 13.2; 13.8; 110.4; 111.7; 123.4; 144.8; 146.9; 152.1; 156.1; 161.8. IR (Nujol, cm⁻¹): ν_(C=O) = 1702. EIMS (70 eV): m/z (%) = 190 (20) [M⁺]; 162 (100) [M⁺-C₂H₄]; 95 (40) [M⁺-C₅N₂H₇]; 67 (5) [M⁺-C₆N₂H₇CO]. Anal. Calc. for C₁₀H₁₀N₂O₂: C, 63.25; H, 5.32; N, 14.71. Found: C, 62.76; H, 4.88; N, 14.49%.

2.3.2 2-(pyrazolyl-1-carbonyl) furan (L2)

This compound was prepared in a similar manner to **L1** by reacting 2-furoyl chloride (2.97 g, 22.12 mmol) and unsubstituted pyrazole (1.50 g, 22 mmol). Purification by column chromatography on silica gel with dichloromethane:hexane (1:1) as eluent gave a colourless oil, which solidified after a period of ten days at room temperature. Yield = 2.40 g (75%). ¹H NMR (CDCl₃): δ 6.50 (dd, 1H, pz, ⁴J_{HH} = 1.4 Hz, ³J_{HH} = 3.0 Hz); 6.65 (dd, 1H, furan, ⁴J_{HH} = 1.8 Hz, ³J_{HH} = 3.6 Hz); 7.78 (dd, 2H, pz, ⁴J_{HH} = 1.6 Hz, ³J_{HH} = 3.8 Hz); 8.08 (dd, 1H, furan, ⁴J_{HH} = 0.8 Hz, ³J_{HH} = 3.8 Hz); 8.44 (dd, 1H, furan, ⁴J_{HH} = 0.8 Hz, ³J_{HH} = 3.8 Hz). ¹³C{¹H} NMR (CDCl₃): δ 111.4; 117.4; 124.3; 132.6; 144.9; 145.9;

147.8; 161.8. IR (Nujol cm^{-1}): $\nu_{(\text{C}=\text{O})} = 1685$. EIMS (70 eV): m/z (%) = 162 (20) [M^+]; 134 (100) [$\text{M}^+ - \text{CN}_2\text{H}_2$]; 95 (40) [$\text{M}^+ - \text{C}_3\text{N}_2\text{H}_3$]; 67 (5) [$\text{M}^+ - \text{C}_3\text{N}_2\text{H}_3\text{CO}$]. Anal. Calc. for $\text{C}_8\text{H}_6\text{N}_2\text{O}_2$: C, 59.32; H, 3.72; N, 17.34. Found: C, 58.89; H, 3.35; N, 16.81%.

The remaining ligands, **L3** to **L13**, were prepared using the same procedure as **L2**.

2.3.3 2-(3-methylpyrazolyl-1-carbonyl)furan (**L3**)

This compound was prepared by reacting 2-furoyl chloride (1.42 g, 10.48 mmol) and 3-methylpyrazole (1.2 g, 10.52 mmol) Yield = 1.42 (55%). ^1H NMR (CDCl_3): δ 2.36 (s, 3H, CH_3 , pz); 6.30 (dd, 1H, pz, $^4J_{\text{HH}} = 1.2$ Hz, $^3J_{\text{HH}} = 2.6$ Hz); 6.60 (dd, 1H, pz, $^4J_{\text{HH}} = 1.8$ Hz, $^3J_{\text{HH}} = 3.6$ Hz); 7.75 (s, 1H, furan); 8.07 (dd, 1H, pz, $^4J_{\text{HH}} = 1.6$ Hz, $^3J_{\text{HH}} = 3.8$ Hz); 8.32 (dd, 1H, furan, $^4J_{\text{HH}} = 1.6$ Hz, $^3J_{\text{HH}} = 3.8$ Hz). $^{13}\text{C}\{^1\text{H}\}$ NMR (CDCl_3): δ 13.4; 109.5; 111.9; 123.7; 130.0; 144.4; 147.3; 154.0. IR (nujol cm^{-1}): $\nu_{(\text{C}=\text{O})} = 1701$. EIMS (70 eV): m/z (%) = 176 (60) [M^+]; 145 (100) [$\text{M}^+ - \text{CNH}_5$]; 95 (30) [$\text{M}^+ - \text{C}_4\text{N}_2\text{H}_5$]; 67 (5) [$\text{M}^+ - \text{C}_4\text{N}_2\text{H}_5\text{CO}$]. Anal. Calc. for $\text{C}_9\text{H}_8\text{N}_2\text{O}_2$: C, 61.46; H, 4.53; N, 15.91. Found: C, 61.08; H, 4.30; N, 15.53%.

2.3.4 2-(pyrazolyl-1-carbonyl)thiophene (**L4**)

Compound **L4** was synthesised by reacting 2-thiophene carbonyl chloride (1.44 g, 10.52 mmol) and pyrazole (0.98 g, 10.52 mmol). Yield = 1.49 (81%). ^1H NMR (CDCl_3): δ 6.52 (dd, 1 H, pz, $^4J_{\text{HH}} = 1.4$ Hz, $^3J_{\text{HH}} = 3.0$ Hz); 7.20 (dd, 1H, thiophene, $^4J_{\text{HH}} = 1.8$ Hz $^3J_{\text{HH}} = 3.6$ Hz); 7.80 (dd, 2H, pz, $^4J_{\text{HH}} = 1.8$ Hz $^3J_{\text{HH}} = 5.2$ Hz); 8.45 (dd, 2H, thiophene, $^4J_{\text{HH}} = 1.8$ Hz $^3J_{\text{HH}} = 3.8$ Hz). $^{13}\text{C}\{^1\text{H}\}$ NMR (CDCl_3): δ 110.5; 123.7; 130.0; 132.9; 144.4;

147.3; 155.4; 160.7. IR (nujol cm^{-1}): $\nu_{(\text{C}=\text{O})} = 1690, 1701$. EIMS (70 eV): m/z (%) = 178 (25) [M^+]; 149 (100) [$\text{M}^+ - \text{CNH}_3$]; 111 (25) [$\text{M}^+ - \text{C}_3\text{N}_2\text{H}_3$]; 83 (1) [$\text{M}^+ - \text{C}_3\text{N}_2\text{H}_3\text{CO}$]. Anal. Calc. for $\text{C}_8\text{H}_6\text{N}_2\text{OS}$: C, 53.95; H, 3.46; N, 15.71. Found: C, 52.42; H, 2.98; N, 15.05%.

2.3.5 2-(3,5-di-tert-butylpyrazolyl-1-carbonyl)furan (L5)

This compound was prepared using 2-furoyl chloride (1.42 g, 10.52 mmol) and 3,5-di-tert-butylpyrazole (2.9 g, 10.52 mmol). Yield = 2.31 g (80%). ^1H NMR (CDCl_3): δ 1.35 (s, 9H, CH_3 , pz); 1.46 (s, 9H, CH_3 , pz); 6.18 (s, 1H, pz); 6.60 (dd, 1H, furan, $^4J_{\text{HH}} = 1.6$ Hz, $^3J_{\text{HH}} = 3.4$ Hz); 7.71 (dd, 1H, furan, $^4J_{\text{HH}} = 0.8$ Hz, $^3J_{\text{HH}} = 1.6$ Hz); 7.82 (dd, 1H, furan, $^4J_{\text{HH}} = 0.8$ Hz, $^3J_{\text{HH}} = 3.8$ Hz). $^{13}\text{C}\{^1\text{H}\}$ NMR (CDCl_3): δ 29.0; 29.3; 31.9; 32.8; 105.5; 111.7; 123.1; 146.5; 156.1; 158.0; 161.6. IR (Nujol cm^{-1}): $\nu_{(\text{C}=\text{O})} = 1716$. EIMS (70 eV): m/z (%) = 274 (45) [M^+]; 244 (30) [$\text{M}^+ - \text{C}_2\text{H}_6$]; 232 (100) [$\text{M}^+ - \text{C}_3\text{H}_6$]; 217 (95) [$\text{M}^+ - \text{C}_{11}\text{N}_2\text{H}_{19}$]; 67 (5) [$\text{M}^+ - \text{C}_{11}\text{N}_2\text{H}_{19}\text{CO}$]. Anal. Calc. for $\text{C}_{16}\text{H}_{22}\text{N}_2\text{O}_2$: C, 69.82; H, 8.36; N, 10.18. Found: C, 69.77; H, 8.26; N, 10.02%.

2.3.6 2-(3,5-dimethylpyrazolyl-1-carbonyl)thiophene (L6)

This ligand was synthesised using 3,5-dimethylpyrazole (1.50 g, 15.60 mmol) and 2-thiophene carbonyl chloride (2.28 g, 15.60 mmol). Yield = 2.41 g (75%). ^1H NMR (CDCl_3): δ 2.32 (s, 3H, CH_3 , pz); 2.63 (s, 3H, CH_3 , pz); 6.03 (s, 1H, pz); 7.15 (dd, 1H, thiophene, $^4J_{\text{HH}} = 1.6$ Hz, $^3J_{\text{HH}} = 4.8$ Hz); 7.71 (dd, 1H, thiophene, $^4J_{\text{HH}} = 1.4$ Hz, $^3J_{\text{HH}} = 4.8$ Hz); 8.34 (d, 1H, thiophene, $^4J_{\text{HH}} = 1.4$ Hz, $^3J_{\text{HH}} = 4.0$ Hz). $^{13}\text{C}\{^1\text{H}\}$ NMR (CDCl_3): δ 13.3; 14.0; 110.8; 126.4; 127.9; 137.2; 144.5; 151.5; 156.0; 160.0. IR (Nujol cm^{-1}): $\nu_{(\text{C}=\text{O})} = 1675$. EIMS (70 eV): m/z (%) = 206 (100) [M^+]; 178 (50) [$\text{M}^+ - \text{C}_2\text{H}_4$]; 111 (50) [M^+ -

C₅N₂H₇]; 83 (5) [M⁺-C₆N₂H₇ CO]. Anal. Calc. for C₁₀H₁₀N₂OS: C, 58.32; H, 4.87; N, 13.65. Found: C, 58.15; H, 4.26; N, 13.68%.

2.3.7 2-(3,5-di-*tert*-butylpyrazolyl-1- carbonyl)thiophene (L7)

Compound **L7** was prepared by reacting 3,5-di-*tert*-butylpyrazole (1.82 g, 10.34 mmol) with 2-thiophene carbonyl chloride (1.37 g, 9.35 mmol). Yield = 1.50 g (52%). ¹H NMR (CDCl₃): δ 1.37 (s, 9H, CH₃, pz); 1.46 (s, 9H, CH₃, pz); 6.17 (s, 1H, pz); 7.12 (dd, 1H, thiophene, ⁴J_{HH} = 1.8 Hz, ³J_{HH} = 5.2 Hz); 7.71 (dd, 1H, thiophene, ⁴J_{HH} = 1.4 Hz, ³J_{HH} = 5.2 Hz); 8.83 (dd, 1H, thiophene, ⁴J_{HH} = 1.6 Hz, ³J_{HH} = 4.0 Hz). ¹³C{¹H} NMR (CDCl₃): δ 28.9; 29.4; 32.1; 32.8; 106.0; 125.8; 137.2; 157.4; 159.7; 169.8. IR (Nujol cm⁻¹): ν_(C=O) = 1686. EIMS (70 eV): m/z (%) = 290 (63) [M⁺]; 275 (20) [M⁺-CH₃]; 233 (65) [M⁺-C₄H₉]; 191 (30) [M⁺-C₇H₁₅]; 111 (100) [M⁺-C₁₁N₂H₁₉]; 83 (5) [M⁺-C₁₁N₂H₁₉CO]. Anal. Calc. for C₁₆H₂₂N₂OS: C, 65.98; H, 7.90; N, 9.62. Found: C, 65.86; H, 8.32; N, 9.34%.

2.3.8 2-(3-methylpyrazolyl-1-carbonyl)thiophene (L8)

This compound was synthesised using 3-methylpyrazole (1.23 g, 15.60 mmol) and 2-thiophene carbonyl chloride (2.28 g, 15.60 mmol). Yield = 2.38 g (83%). ¹H NMR (CDCl₃): δ 2.40 (s, 3H, CH₃, pz); 6.31 (d, 1H, pz, ³J_{HH} = 3.8 Hz); 7.20 (d, 1H, thiophene, ³J_{HH} = 3.6 Hz); 7.76 (dd, 1H, thiophene, ⁴J_{HH} = 1.4 Hz, ³J_{HH} = 3.6 Hz); 8.42 (dd, 1H, pz, ⁴J_{HH} = 1.8 Hz, ³J_{HH} = 3.8 Hz). 8.44 (dd, 1H, pz, ⁴J_{HH} = 1.6 Hz, ³J_{HH} = 3.6 Hz). ¹³C{¹H} NMR (CDCl₃): δ 13.5; 109.8; 126.7; 128.5; 136.3; 137.6; 141.8; 153.5; 158.1. IR (nujol, cm⁻¹): ν_(C=O) = 1682. EIMS (70 eV): m/z (%) = 162 (40) [M⁺]; 164 (100) [M⁺-C₂H₄]; 111 (45) [M⁺-C₄N₂H₅]; 83 (5) [M⁺-C₄N₂H₅CO].

2.3.9 2-(3,5-diphenylpyrazolyl-1-carbonyl)furan (L9)

This compound was synthesised by reacting 2-furoyl chloride (0.90 g, 6.81 mmol) and 3,5-diphenylpyrazole (1.50 g, 6.81 mmol). Yield = 0.36 g (50%). ^1H NMR: δ 6.51 (s, 1H, pz); 6.65 (d, 1H, furan, $^3J_{HH} = 3.8$ Hz); 7.31 (m, 10H, benzene); 7.74 (d, 1H, furan, $^3J_{HH} = 4.4$ Hz) 7.86(d, 1H, furan, $^3J_{HH} = 3.6$ Hz). IR (nujol cm^{-1}): $\nu_{(\text{C}=\text{O})} = 1690$. EIMS (70 eV): m/z (%) = 314 (78) [M^+]; 286 (100) [$\text{M}^+ - \text{C}_2\text{H}_4$]; 269 (50) [$\text{M}^+ - \text{C}_3\text{H}_9$]; 95 (20) [$\text{M}^+ - \text{C}_{15}\text{H}_{11}\text{N}_2$]; 67 (2) [$\text{M}^+ - \text{C}_{15}\text{H}_{11}\text{N}_2 \text{CO}$]. Anal. Calc. for $\text{C}_{20}\text{H}_{14}\text{N}_2\text{O}_2$: C, 76.42, H, 4.49, N, 8.91. Found: C, 75.72 H, 4.30, N, 8.60%.

2.3.10 2-(3,5-diphenylpyrazolyl-1-carbonyl)thiophene (L10)

Compound **L10** was synthesised by reacting 2-thiophene carbonyl chloride (1.73 g, 11.85 mmol) and 3,5-diphenylpyrazole (2.61 g, 11.86 mmol). Yield = 3.07 g (75%). ^1H NMR: δ 6.61 (s, 1H, pz); 6.98 (d, 1H, thiophene, $^3J_{HH} = 3.6$ Hz); 7.32 (m, 8H, ph); 7.63 (d, 1H, thiophene, $^3J_{HH} = 3.8$ Hz); 7.82 (m, 2H, ph); 8.14 (d, 1H, thiophene, $^3J_{HH} = 3.8$ Hz). $^{13}\text{C}\{^1\text{H}\}$ NMR (CDCl_3): δ 109.2; 125.9; 126.5; 127.5; 128.3; 128.8; 130.6; 131.2; 133.0; 137.1; 137.9; 147.8; 153.1; 159.2. IR (Nujol cm^{-1}): $\nu_{(\text{C}=\text{O})} = 1689$. EIMS (70 eV): m/z (%) = 330 (100) [M^+]; 302 (85) [$\text{M}^+ - \text{C}_2\text{H}_4$]; 189 (20) [$\text{M}^+ - \text{C}_{13}\text{H}_9$]; 111 (85) [$\text{M}^+ - \text{C}_{15}\text{H}_{11}\text{N}_2$]; 83 (4) [$\text{M}^+ - \text{C}_{15}\text{H}_{11}\text{N}_2\text{CO}$]. Anal. Calc. for $\text{C}_{20}\text{H}_{14}\text{N}_2\text{OS}$: C, 72.70; H, 4.27; N, 8.48. Found: C, 72.68; H, 4.05; N, 8.36%.

2.3.11 (3,5-dimethylpyrazolyl-1-carbonyl)methane (L11)

Ligand **L11** was synthesised using 3,5-dimethylpyrazole (0.62 g, 6.41 mmol) and acetyl chloride (0.50 g, 6.41 mmol). Yield = 0.44 g (50%). ^1H NMR (CDCl_3): δ 2.22 (s, 3H,

CH₃); 2.51 (s, 3H, CH₃, pz); 2.64 (s, 3H, CH₃, pz); 5.94 (s, 1H, pz). ¹³C{¹H} NMR (CDCl₃): δ 13.2; 14.0; 22.9; 110.6; 143.4; 151.4; 170.9. IR (nujol, cm⁻¹): ν_(C=O) = 1730. EIMS (70 eV): m/z (%) = 138 (100) [M⁺]; 110 (10) [M⁺-C₂H₄]; 95 (30) [M⁺-C₃H₇]; 43 (4) [M⁺-C₅N₂H₇].

2.3.12 Synthesis of (3,5-di-*tert*-butylpyrazolyl-1- carbonyl)methane (L12)

Ligand **L10** was prepared by reacting 3,5-di-*tert*-butylpyrazole (1.23 g, 6.80 mmol) with acetyl chloride (0.72 g, 9.00 mmol). Yield = 1.29 g (65%). ¹H NMR (CDCl₃): δ 1.81 (s, 9H, pz); 1.39 (s, 9H, pz); 2.68 (s, 3H, CH₃); 6.10 (s, 1H, pz). ¹³C{¹H} NMR (CDCl₃): δ 24.5; 28.7; 29.2; 31.7; 32.6; 105.7; 156.4; 162.4; 170.6. IR (nujol, cm⁻¹): ν_(C=O) = 1745. EIMS (70 eV): m/z (%) = 223 (75) [M⁺]; 180 (40) [M⁺-C₃H₆]; 165 (100) [M⁺-C₄H₉]; 108 (10) [M⁺-C₈H₁₈]; 57 (4) [M⁺-C₁₁N₂H₁₉].

2.3.13 (3,5-di-*tert*-butylpyrazolyl-1- carbonyl)ethane (L13)

This compound was synthesised using 3,5-di-*tert*-butylpyrazole (1.70 g, 9.44 mmol) and propionyl chloride (0.87 g, 9.44 mmol). Yield: 1.33 g (60%). ¹H NMR (CDCl₃): δ 1.18 (t, 3H, CH₃, ³J_{HH} = 3.0 Hz); 1.26 (s, 9H, pz); 1.41 (s, 9H, pz); 3.20 (q, 2H, CH₂, ³J_{HH} = 5.8 Hz); 6.09 (s, 1H, pz). ¹³C{¹H} NMR (CDCl₃): δ 9.1; 29.3; 29.9; 30.4; 32.4; 33.3; 106.0; 157.0; 162.9; 174.7. IR (Nujol, cm⁻¹): ν_(C=O) = 1741. EIMS (70 eV): m/z (%) = 237 (100) [M⁺]; 207 (20) [M⁺-C₂H₆]; 165 (65) [M⁺-C₅H₁₂]; 138 (20) [M⁺-C₇H₁₅]; 57 (4) [M⁺-C₁₁N₂H₂₀]. Anal. Calc. for C₁₄H₁₅N₂O: C, 71.14; H, 10.23; N, 11.86. Found: C, 71.45; H, 10.01; N, 11.67%.

2.4 Synthesis of the complexes

2.4.1 Dichloro{bis-2-(3,5-dimethylpyrazolyl-1-carbonyl)furan}palladium(II) (1)

To a solution of Pd(NCMe)₂Cl₂ (0.20 g, 0.68 mmol) in dichloromethane (20 mL), 2-(3,5-dimethylpyrazolyl-1-carbonyl)furan (0.26 g, 1.43 mmol) was added. The mixture was stirred at room temperature for 6 h. The solution was concentrated in *vacuo* to about 10 mL and an analytically pure yellow powder was obtained upon addition of an equal volume of hexane. Yield = 0.28 g (79%). ¹H NMR (CDCl₃): δ 2.34 (s, 6H, CH₃, pz); 2.44 (s, 6H, CH₃, pz); 6.03 (s, 2H, pz); 6.77 (d, 2H, furan, ³J_{HH} = 3.6 Hz); 7.70 (d, 2H, furan, ³J_{HH} = 3.6 Hz); 7.91 (d, 2H, furan, ³J_{HH} = 3.6 Hz). ¹³C{¹H} NMR (CDCl₃): δ 12.8; 15.1; 110.9; 113.3; 126.8; 146.1; 147.1; 149.4; 154.8; 155.9. IR (Nujol cm⁻¹): ν(C=O) = 1694. Anal. Calc. for C₂₀H₂₀N₄O₄PdCl₂: C, 43.09; H, 3.59; N, 10.05. Found: C, 42.57; H, 3.20; N, 9.65%.

2.4.2 Dichloro{bis-2-(3,5-dimethylpyrazolyl-1-carbonyl)thiophene}palladium(II) (2)

Complex **2** was prepared in the same way as **1** using ligand **L6** (0.50 g, 3.42 mmol) and PdCl₂(NCMe)₂ (0.45 g, 1.71 mmol). Recrystallization from dichloromethane-hexane gave yellow single crystals suitable for X-ray analysis. Yield = 0.61 g (62%). ¹H NMR (CDCl₃): δ 2.30 (s, 6H, CH₃, pz); 2.32 (s, 6H, CH₃, pz); 6.00 (s, 2H, pz); 7.29 (dd, 2H, thiophene, ⁴J_{HH} = 1.6 Hz, ³J_{HH} = 3.8 Hz); 7.73 (dd, 2H, thiophene, ⁴J_{HH} = 1.6 Hz, ³J_{HH} = 3.8 Hz); 8.02 (dd, 2H, thiophene, ⁴J_{HH} = 6 Hz, ³J_{HH} = 3.8 Hz). ¹³C{¹H} NMR (CDCl₃): δ 12.6; 14.4; 110.1; 126.4; 128.4; 136.2; 136.5; 140.1; 146.1; 155.2; 160.0. IR (Nujol cm⁻¹): ν(C=O) = 1688. Anal. Calc. for C₂₀H₂₀N₄O₂S₂PdCl₂: C, 40.83; H, 3.43; N, 9.51. Found: C, 40.84; H, 2.69; N, 9.53%.

2.4.3 Dichloro{bis-2-(3,5-di-tert-butylpyrazolyl-1-carbonyl)furan}palladium(II) (3)

Complex **3** was prepared following the same procedure for complex **1** but using ligand **L5** (0.37 g, 1.35 mmol) and Pd(NCMe)₂Cl₂ (0.18 g, 0.68 mmol). Yield = 0.25 g (52%).

¹H NMR (CDCl₃): δ 1.32 (s, 18H, CH₃, pz); 1.46 (s, 18H, CH₃, pz); 6.17 (s, 2H, pz); 6.58 (dd, 2H, furan, ⁴J_{HH} = 1.7 Hz, ³J_{HH} = 3.6 Hz); 7.71 (dd, 2H, furan, ⁴J_{HH} = 1.8 Hz, ³J_{HH} = 3.4 Hz); 7.82 (dd, 2H, furan, ⁴J_{HH} = 1.8 Hz, ³J_{HH} = 3.4 Hz). ¹³C{¹H} NMR (CDCl₃): δ 28.8; 29.7; 30.5; 31.6; 100.1; 111.7; 119.3; 125.8; 137.2; 146.7; 156.1; 157.8. IR (Nujol cm⁻¹): ν_(C=O) = 1705. Anal. Calc. for C₃₄H₅₀N₄O₄PdCl₆·2CH₂Cl₂: C, 45.53; H, 5.58; N, 6.25. Found: C, 46.05; H, 5.03; N, 6.55%.

2.4.4 Dichloro{bis-2-(3,5-di-tert-butylpyrazolyl-1-carbonyl)thiophene}palladium(II) (4)

This complex was prepared in the same way as complex **1** but using ligand **L7** (0.44 g, 1.52 mmol) and PdCl₂(NCMe)₂ (0.20 g, 0.76 mmol). Yield = 0.32 g (58%). ¹H NMR (CDCl₃): δ 1.32 (s, 18H, CH₃, pz); 1.46 (s, 18H, CH₃, pz); 6.19 (s, 2H, pz); 7.13 (dd, 2H, thiophene, ⁴J_{HH} = 1.6 Hz, ³J_{HH} = 5.0 Hz); 7.72 (dd, 2H, thiophene, ⁴J_{HH} = 1.2 Hz, ³J_{HH} = 5.4 Hz); 8.26 (dd, 2H, thiophene, ⁴J_{HH} = 1.6 Hz, ³J_{HH} = 4.2 Hz). IR (Nujol cm⁻¹): ν_(C=O) = 1694. Anal. Calc. for C₃₂H₄₆N₂O₂S₂PdCl₂: C, 49.05; H, 6.27; N, 7.63. Found: C, 48.75; H, 5.06; N, 7.66%.

2.4.5 Dichloro{bis-2-(3-methylpyrazolyl-1-carbonyl)-furan}palladium(II) (5)

To a solution of ligand **L3** (0.68 g, 4.00 mmol) in dichloromethane (30 mL), Pd(NCMe)₂Cl₂ (0.50 g, 1.93 mmol) was added. A light brown precipitate was formed immediately. The resultant mixture was filtered and the yellow solid dried. Yield = 0.75 g

(75%). ^1H NMR (dms o-d_6): δ 2.30 (s, 3H, CH_3 , pz); 6.51 (d, 2H, pz, $^3J_{\text{HH}} = 2.8$ Hz); 6.82 (dd, 2H, furan, $^4J_{\text{HH}} = 1.6$ Hz, $^3J_{\text{HH}} = 3.8$ Hz); 8.01 (d, 2H, pz, $^3J_{\text{HH}} = 2.8$ Hz); 8.16 (dd, 2H, pz, $^4J_{\text{HH}} = 1.6$ Hz, $^3J_{\text{HH}} = 3.8$ Hz); 8.41 (d, 2H, furan, $^3J_{\text{HH}} = 2.8$ Hz). IR (nujol cm^{-1}): $\nu_{(\text{C}=\text{O})} = 1703$. Anal. Calc. for $\text{C}_{21}\text{H}_{19}\text{N}_4\text{O}_4\text{PdCl}_5 \cdot 1.5\text{CH}_2\text{Cl}_2$: C, 35.78; H, 2.91; N, 9.14. Found: C, 35.79; H, 2.22; N, 10.44%.

2.4.6 Dichloro{bis-2-(pyrazolyl-1- carbonyl)furan}palladium(II) (6)

Complex **6** was prepared in the same way as complex **5** using ligand **L2** (0.80, 4.94 mmol) and $\text{Pd}(\text{NCMe})_2\text{Cl}_2$ (0.63 g, 2.47 mmol). Yield = 1.01 g (80%). ^1H NMR (dms o-d_6): δ 6.64 (dd, 2H, pz, $^4J_{\text{HH}} = 1.6$ Hz, $^3J_{\text{HH}} = 3.0$ Hz); 6.78 (dd, 2H, furan, $^4J_{\text{HH}} = 1.6$ Hz, $^3J_{\text{HH}} = 3.6$ Hz); 7.79 (dd, 4H, pz, $^4J_{\text{HH}} = 0.8$ Hz, $^3J_{\text{HH}} = 3.6$ Hz); 8.15 (dd, 2H, furan, $^4J_{\text{HH}} = 0.8$ Hz, $^3J_{\text{HH}} = 3.0$ Hz); 8.52 (dd, 2H, furan, $^4J_{\text{HH}} = 0.8$ Hz, $^3J_{\text{HH}} = 1.8$ Hz). $^{13}\text{C}\{^1\text{H}\}$ NMR (CDCl_3): δ 106.4; 110.1; 112.2; 113.2; 117.8; 125.0; 130.5; 145.3; 147.1; 149.8; 154.3; 159.4. IR (Nujol cm^{-1}): $\nu_{(\text{C}=\text{O})} = 1712$. Anal. Calc. for $\text{C}_{16}\text{H}_{12}\text{N}_4\text{O}_4\text{PdCl}_2$: C, 38.31; H, 2.41; N, 11.17. Found: C, 38.06; H, 2.30; N, 10.33%.

2.4.7 Dichloro{bis-2-(3,5-diphenylpyrazolyl-1- carbonyl)furan}palladium(II) (7)

This compound was synthesised by reacting **L8**, 2-(3,5-diphenylpyrazolyl-1-carbonyl)furan (0.20 g, 0.64 mmol) and $\text{Pd}(\text{NCMe})_2\text{Cl}_2$ (0.10 g, 0.32 mmol). Yield = 0.13 g (50%). ^1H NMR (dms o-d_6): δ 6.85 (s, 1H, pz); 7.27 (d, 1H, furan, $^3J_{\text{HH}} = 3.6$ Hz); 7.48 (m, 10H, benzene); 7.96(d, 1H, furan, $^3J_{\text{HH}} = 3.8$ Hz) 8.10(d, 1H, furan, $^3J_{\text{HH}} = 4.0$ Hz). IR (nujol cm^{-1}): $\nu_{(\text{C}=\text{O})} = 1690$.

2.4.8 Dichloro{bis-2-(3,5-diphenylpyrazolyl-1-carbonyl)thiophene}palladium(II) (**8**)

Compound **8** was synthesised using the same procedure as complex **1** by reacting 2-(3,5-diphenylpyrazolyl-1-carbonyl)thiophene, **L9** (0.50 g, 1.53 mmol) and Pd(NCMe)₂Cl₂ (0.20 g, 0.77 mmol). Yield = 0.23 g (37%). ¹H NMR (CDCl₃): δ 7.20 (s, 1H, pz); 7.46 (d, 1H, thiophene, ³J_{HH} = 4.0 Hz); 8.16 (m, 10H, benzene); 8.37 (d, 1H, thiophene, ³J_{HH} = 3.6 Hz) 8.42 (d, 1H, thiophene, ³J_{HH} = 3.8 Hz). ¹³C{¹H} NMR (CDCl₃): δ 109.2; 125.9; 126.5; 127.5; 127.7; 128.4; 128.7; 130.5; 131.2; 133.0; 137.0; 137.9; 147.8; 153.1; 158.2. IR (Nujol cm⁻¹): ν_(C=O) = 1694. Anal. Calc. for C₄₀H₂₈N₂O₂S₂PdCl₂: C, 57.32; H, 4.37; N, 6.63. Found: C, 56.82; H, 4.15; N, 6.16%.

2.5 Results and discussion

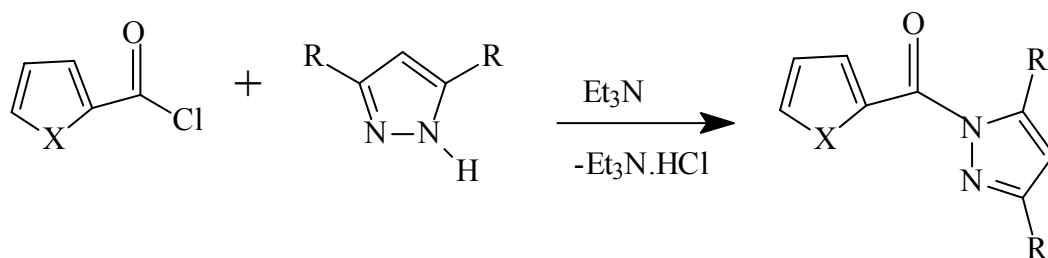
2.5.1 Synthesis and characterisation of furoyl and thiophene carbonyl pyrazolyl ligands and their palladium(II) complexes.

Ligands **L1** to **L10** were prepared by reacting 2-furoyl chloride or 2-thiophene carbonyl chloride with an equivalent amount of the appropriate pyrazole in a 1:1 ratio with toluene as a solvent, Scheme 2.1. Triethylamine was used as a base to abstract the acidic N-H proton in the pyrazole, leading to the immediate formation of the insoluble Et₃NH⁺.Cl⁻ salt during the reaction. The reactions were refluxed for 24 h after which the Et₃NH⁺.Cl⁻ by-product formed was filtered off and the solvent removed in *vacuo* to obtain the crude products.

Ligands **L3** to **L10** were purified by column chromatography on silica gel using solvent mixtures of dichloromethane and hexane as eluent in a ratio 1:1 and were obtained in moderate to high yields (53 to 82%). The use of a 3:2 solvent ratio instead of 1:1 for

purification of **L5** resulted in remarkable increased yield from 18 to 80%. Ligands **L1** and **L2** did not require purification using column chromatography and analytically pure compounds were obtained in high yields, (85 and 75% respectively), upon evaporation of the solvent in *vacuo* after the ammonium salt was removed by filtration. Attempts to reflux the reactions for longer periods neither improved the yields nor the purity of the products. All the ligands synthesised (**L1–L10**) showed good solubility in most polar solvents such as, dichloromethane, diethyl ether, chloroform and in aromatic solvents like toluene and benzene. However, they were all insoluble in hexane. A schematic route to the synthesis and the various variations of the ligands are provided in Scheme 2.1

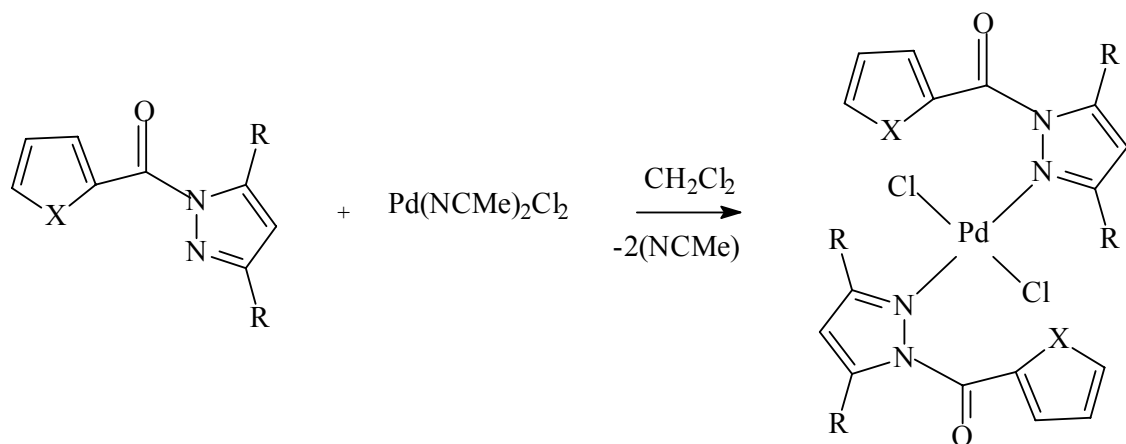
The reactions of ligands **L1**, **L6**, **L5**, **L7**, **L2**, **L3**, **L9** and **L10** with Pd(NCMe)₂Cl₂ in 2:1 ratio in dichloromethane according to Scheme 2.2 produced complexes **1** to **8** respectively. Complexes **1-4** and **7-8** were isolated as analytically pure solids in moderate to high yields (40 to 80%) after stirring for 6 h at room temperature followed by recrystallization from CH₂Cl₂/Hexane. Initial experiments to prepare the complexes using shorter reaction times such as 3 h produced a mixture of the complexes and the starting materials. Similar behaviour was observed when the reaction time was prolonged to 24 h indicating decomposition of the products to the palladium metal and the ligands. It is not clear to us why longer reaction times resulted in decomposition. It is interesting to note



Ligand	X	R	Ligand	X	R
L1	O	Me	L6	S	Me
L2	O	H	L7	S	^t Bu
L3	O	H, Me	L8	S	H, Me
L4	S	H	L9	O	Ph
L5	O	^t Bu	L10	S	Ph

Scheme 2.1

that unlike the other complexes, bis{2-(3,5-diphenylpyrazolyl-1-carbonyl)furan}PdCl₂, **7**, produced insoluble material on prolonged reaction time. This could be due to the formation of some dimeric complex. Complexes **5** and **6** were found to be insoluble in most organic solvents. The products were isolated as pure yellow solids in high yields (75 and 80% respectively) upon filtration of the precipitates. This observation confirmed the role played by the bulkiness of the substituent groups in enhancing complex solubility. A similar trend has been reported in the synthesis of benzenedicarbonyl and benzenetricarbonyl complexes of palladium.¹⁴



Complex	X	R	Complex	X	R
1	O	Me	5	O	Me, H
2	S	Me	6	O	H
3	O	^t Bu	7	O	Ph
4	S	^t Bu	8	S	Ph

Scheme 2.2

While there was no significant effect of the nature of the substituents on the percentage yield of the ligands reported, we observed a significant effect of the substituent bulkiness on the yield of the complexes. For instance, complex **3**, bis{2-(3,5-di-*tert*-butylpyrazolyl-1-carbonyl)furan}PdCl₂ was obtained in 52% as compared to 79% for the corresponding methyl analogue, complex **1**. The same trend was reported for the thiophene complexes with the diphenyl complex, **8** reported in 37% yield compared to 62% for the dimethyl analogue, complex **2**. From the data collected, it was evident that increase in bulkiness on

the pyrazolyl ligands results in a decrease in percentage yield of the corresponding palladium(II) complexes.

The compounds synthesised were characterised by a number of spectroscopic techniques and elemental analyses. The spectroscopic techniques employed include IR, ^1H NMR, ^{13}C NMR and mass spectrometry. Infra red spectra of all the ligands prepared showed characteristic peaks of the carbonyl functional group within the ranges of 1675 cm^{-1} to 1716 cm^{-1} , Table 2.1. The absence of the N-H stretching band in the pyrazole moiety at 3250 cm^{-1} confirmed the reaction between the carbonyl chloride and N-H functionality.

The IR spectra of the complexes **1–8** showed some differences from their respective ligands especially the carbonyl functionality, with a general shift towards higher frequencies in the complexes as compared to their respective ligands. For example, in **L1** and its corresponding complex **1**, the carbonyl stretching bands were observed at 1702 cm^{-1} and 1723 cm^{-1} respectively, (Table 2.1, entry 1.). Figure 2.1 shows the IR spectrum of complex **2**.

Table 2.1. Selected IR carbonyl frequencies of the ligands and their respective complexes.

Entry	Ligand	$\nu(\text{C=O})\text{ cm}^{-1}$	Complex	$\nu(\text{C=O})\text{ cm}^{-1}$
1	L1	1702	1	1723
2	L6	1686	2	1694

3	L5	1694	3	1702
4	L7	1708	4	1716
5	L2	1697	6	1712
6	L10	1689	8	1694

The compounds synthesised were also characterised by ^1H NMR spectroscopy. All the 3,5-disubstituted pyrazolyl ligands showed two characteristic upfield singlet peaks at about 2.28 ppm and 2.61 ppm for the two methyl groups and 1.33 ppm and 1.44 ppm for the *tert*-butyl groups. A singlet peak at about 6.03 ppm was observed and assigned to the 4-H of the pyrazole. Three doublet of doublets between 6.51 ppm and 7.15 ppm, 7.70 ppm and 8.08 ppm, 7.91 ppm and 8.44 ppm were assigned to the hydrogens of the furan and thiophene units respectively. The splitting pattern observed corresponds to a AMX. Figures 2.2 represents the ^1H NMR spectrum of ligand **L6**.

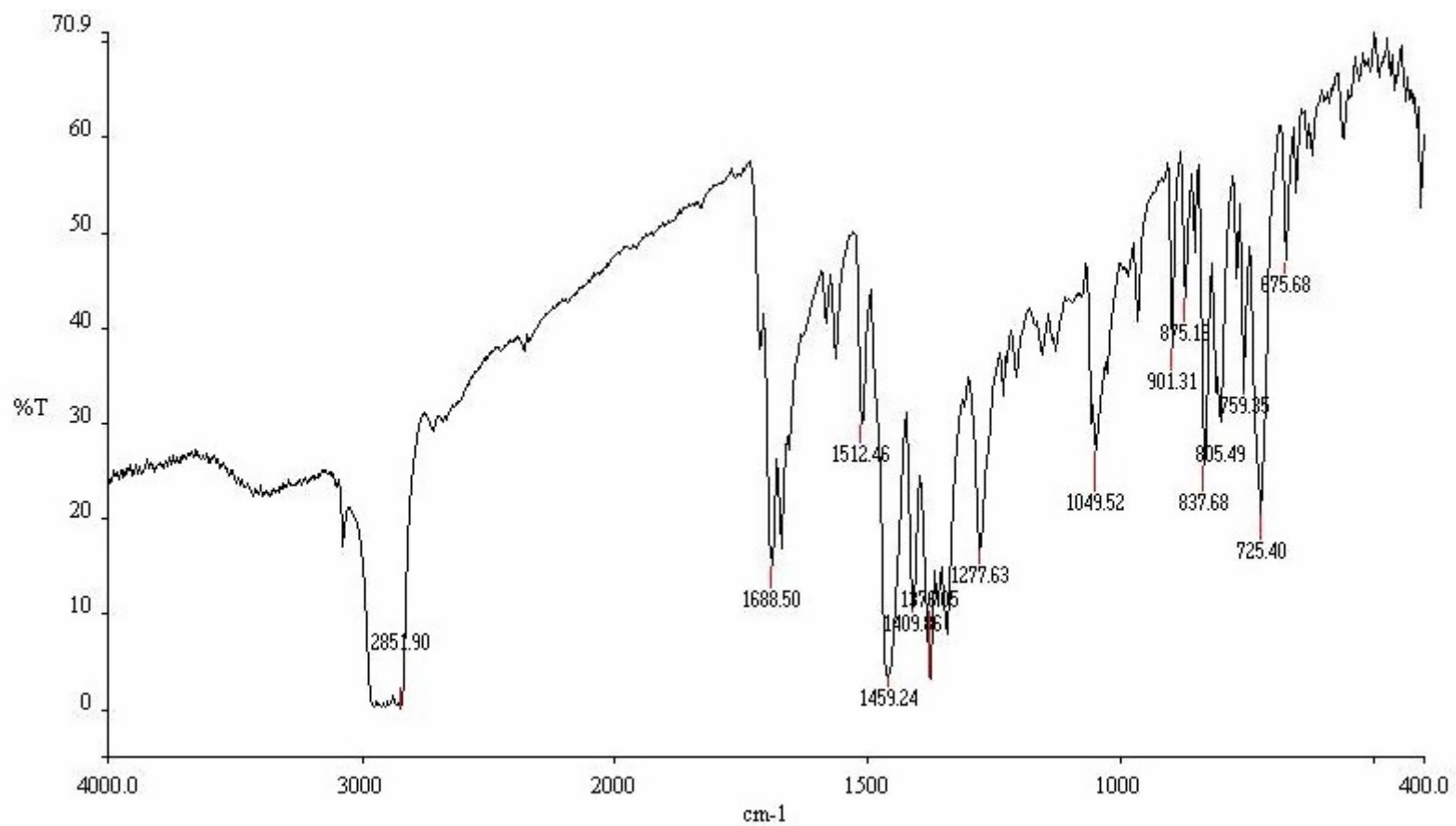


Figure 2.1. Infrared spectrum of complex 2

The observation of doublet of doublets for the three heterocyclic ring hydrogens indicates that there is some interaction between the three protons of the heterocyclic systems in both the furan and thiophene. This was confirmed by the 2-Dimensional Correlation Spectroscopy (COSY) NMR spectrum of ligand **L7**, Figure 2.3. The coupling of the protons with one another (existence of correlation) is indicated by the contour of an off-diagonal peak.

From the ^1H NMR spectral data of compounds **L1–L10**, it is clear that the carbonyl linker has a profound effect on both the thiophene and furan linkers as well as the pyrazole protons. This is evident from the downfield position of the protons adjacent to the carbonyl as compared to the protons at the 4-H position of the furan and thiophene. For **L1**, **L2**, **L5** and **L6**, the protons adjacent to the carbonyl were recorded at 7.71 ppm, 8.08 ppm, 7.72 ppm and 7.74 ppm as compared to the upfield signals of the fourth protons at 6.61 ppm, 6.64 ppm, 6.60 ppm and 7.15 ppm respectively.

^1H NMR spectra of the complexes **1** to **6** showed both upfield and downfield shifts as compared to their corresponding ligands spectra. For example, in complex **2**, the CH_3 and the thiophene protons, were observed at 2.32 ppm and 8.02 ppm compared to 2.62 ppm and 8.33 ppm for the corresponding **L6** respectively. However there was a general downfield shift towards higher frequency of the protons, for example signals at about 6.79 ppm and 7.32 ppm for complexes **1** and **2** as compared to 6.59 ppm and 7.15 ppm of their corresponding ligands **L1** and **L6** respectively were recorded. More interesting was

the appearance of the two CH₃ groups at about the same position (2.30 and 2.32 ppm in complex **2**, Figure 2.4, as opposed to a wider separation in the ligand system at 2.31 and 2.63 ppm as shown in Figure 2.2.

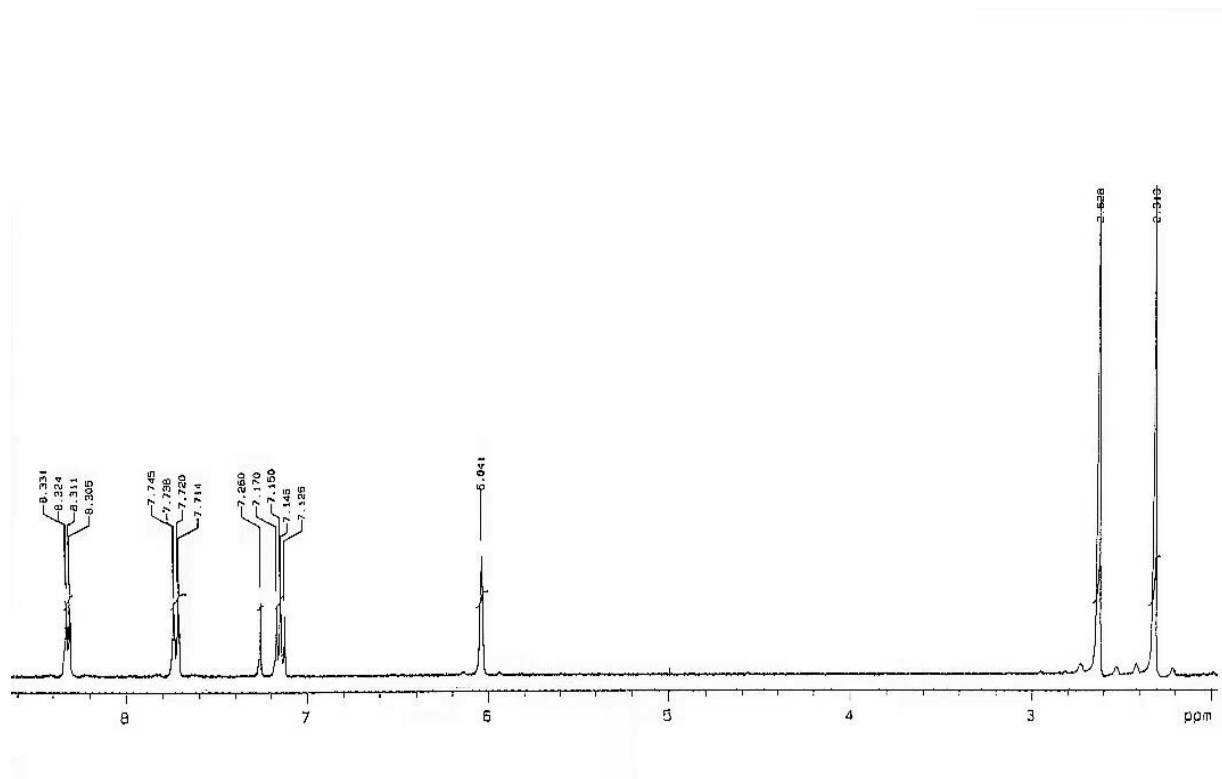


Figure 2.2. ¹H NMR of 2-(3,5-dimethylpyrazolyl-1-carbonyl)thiophene **L6**.

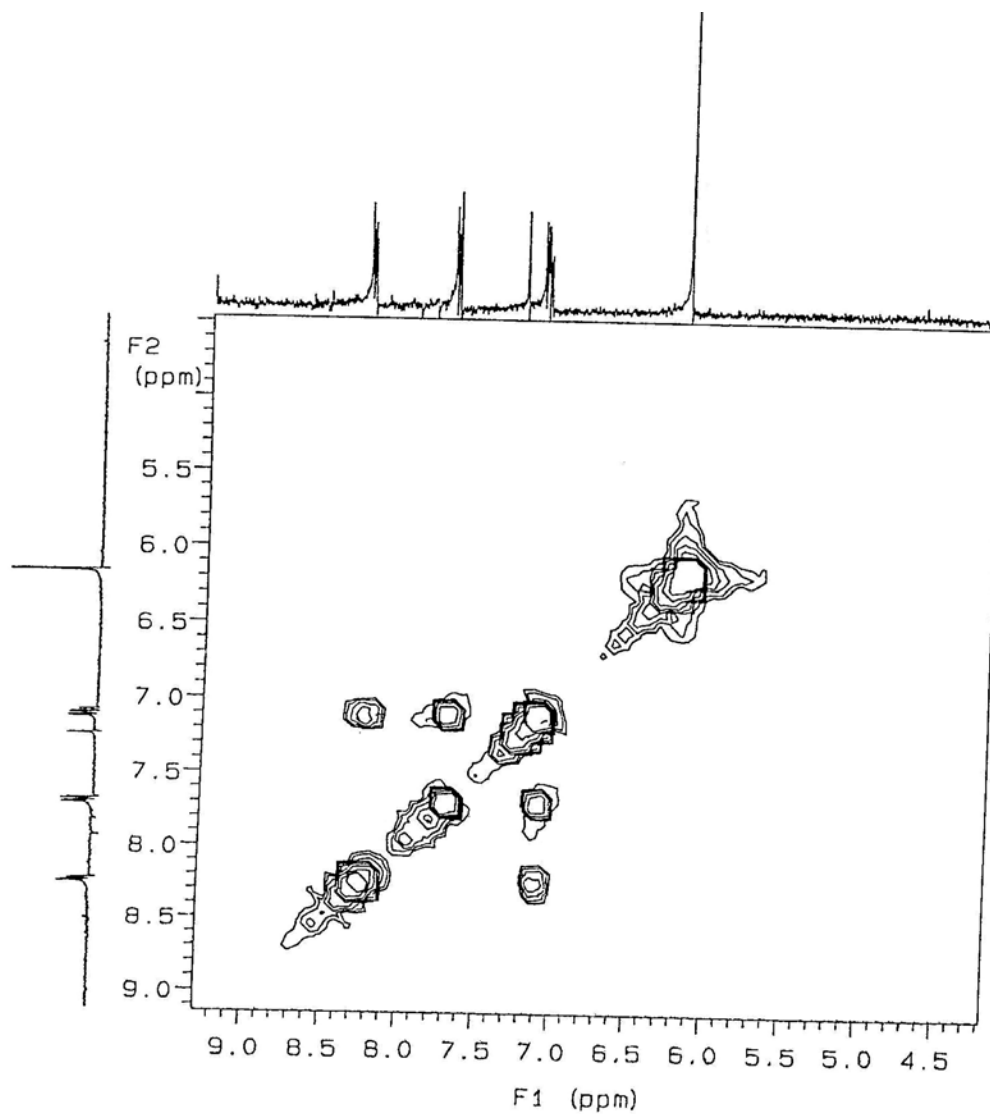


Figure 2.3. Homonuclear proton-proton shift correlation spectrum, COSY for **L7**. A cross-peak establishes correlation with a diagonal peak.

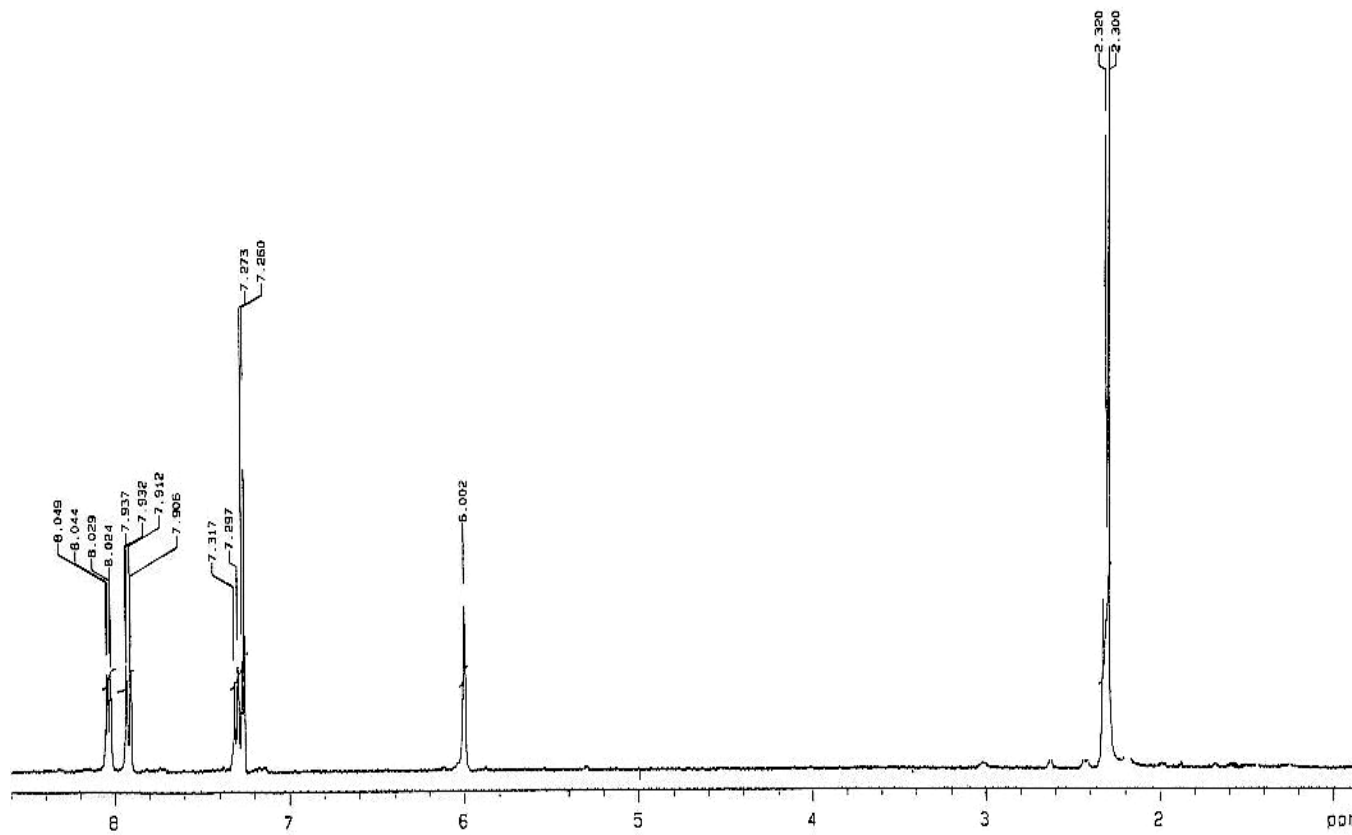


Figure 2.4 ^1H NMR spectrum of dichloro{bis-2-(3,5-dimethylpyrazolyl-1-carbonyl)thiophene}palladium(II) (2)

^{13}C NMR data were also obtained for both the ligands and their corresponding complexes. In the 3,5 substituted ligands, upfield peaks at about 14.4 ppm and 30 ppm for the methyl and tertiary butyl carbons were observed respectively. The signal of the carbonyl carbon in general was observed within the range of 159 to 161 ppm. These values were significantly lower than the average value of 166 ppm reported for similar complexes by Darkwa *et al.*¹⁴ We were unable to observe any peak that corresponds to this frequency in the respective complexes. This could be attributed to the low relaxation frequency of the carbonyl functionality in these compounds. Figure 2.5 shows the ^{13}C NMR spectrum of complex **6**.

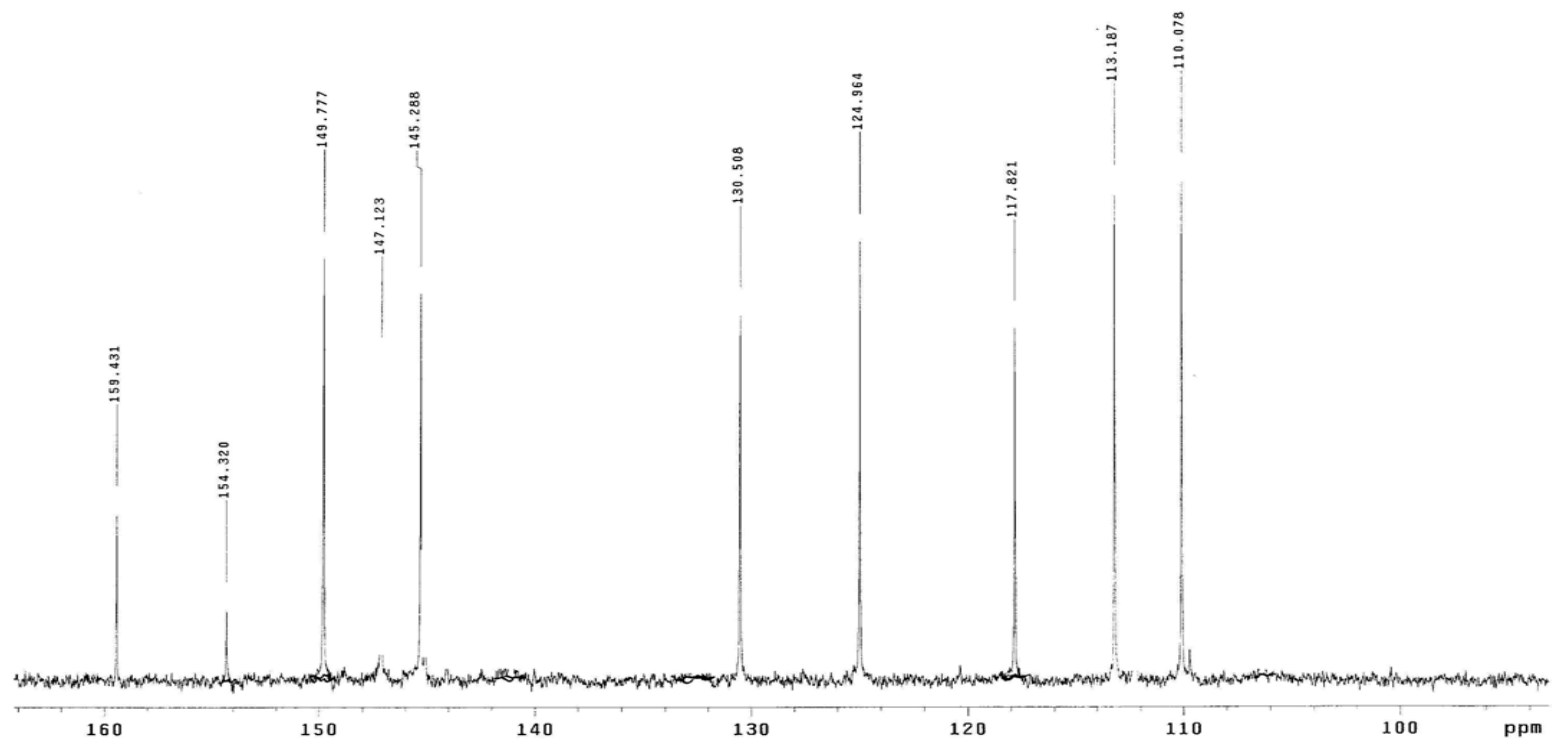
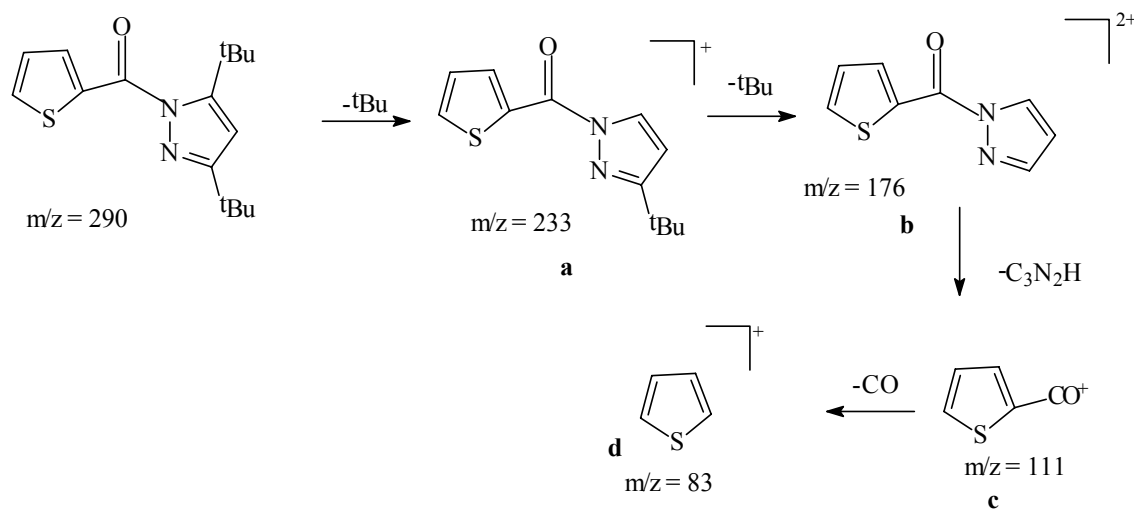


Figure 2.5 ^{13}C NMR spectrum of dichloro{bis-2-(pyrazolyl-1-carbonyl)furan} palladium(II) (**6**)

Electron impact mass spectrometry was used to characterise ligands **L1** to **L10**. All the ligands show similar fragmentation patterns. In the substituted ligands, the substituent groups on the pyrazole structure are lost first, followed by the pyrazole structure, and finally the carbonyl, Scheme 2.3. Table 2.2 shows some of the important molecular ions of the different ligand systems. Ligand **L7** shows molecular ion at m/z 290, Figure 2.6, this is the largest molecular ion and corresponds to the molecular mass of the compound. As shown in Scheme 2.3 compound **L7** fragments by first losing the two tertiary butyl groups to form a fragment ion at m/z 176. This is followed by a loss of the pyrazole system to form Ar-CO, m/z 111 which is the base peak. The loss of CO to form a molecular ion M^+ at 83, which corresponds to the thiophene molecular ion was observed. The same fragmentation pattern was reported for furan analogues e.g. **L1**.



Scheme 2.3. Scheme showing the fragmentation pattern of 2-(3,5-di-*tert*-butylpyrazolyl-carbonyl)thiophene **L7**.

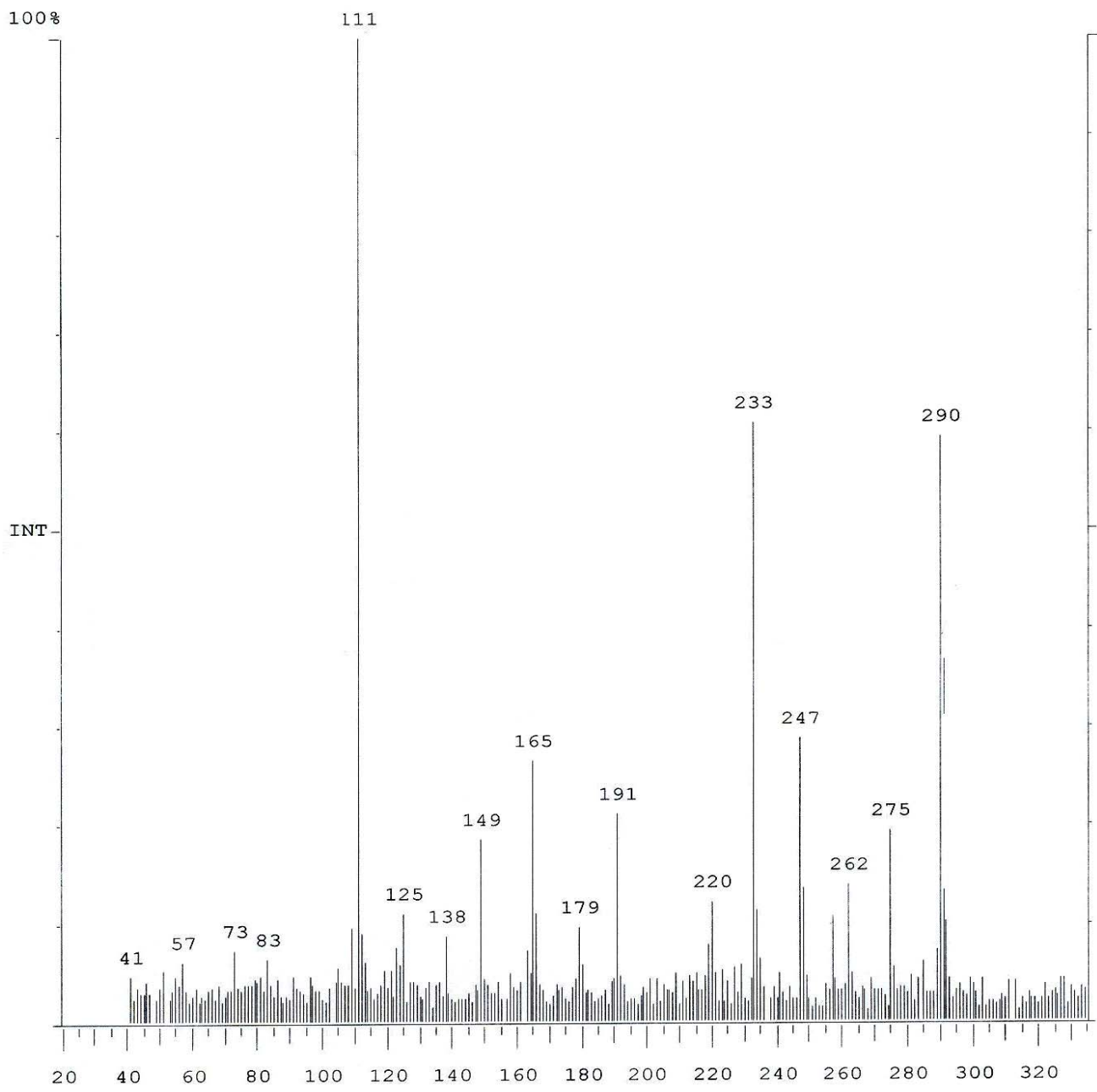


Figure 2.6: Mass spectrum showing the fragmentation pattern of **L7**.

Table 2.2: Correlation of m/z values for the important molecular ions¹ in the mass spectra of ligands **L1–L10**

Compound	Molecular ion	a	b	c	d
L1	190	175	161 ²	95	67
L2	162			95	67
L3	176	161		95	67
L4	178			111	83
L5	274	217	160	95	67
L6	206 ²	190	175	111	83
L7	290	233	176	111 ²	83
L8	192	177	n.d	111	83
L9	314	237	160	95	67
L10	330 ²	n.d	n.d	111	83

¹ Refer to **Scheme 2.3** for assignment of the fragment ions **a**, **b**, **c** and **d**.

²Base peak of the respective compound
n.d not detected

Attempts to synthesise the complexes (**1–6**) using Pd(COD)Cl₂ as the palladium source were unsuccessful, only mixtures of the Pd(COD)Cl₂ and the ligands were recovered. This is an indication that the ligands **L1–L10** are weak electron donors as compared to COD. The same synthetic protocol had been used to obtain the palladium complexes of other substituted pyrazole systems,¹⁵ and this observation clearly depicts the electron withdrawing effect of the carbonyl linker on the pyrazole moiety hence reducing its donor ability. This is expected to result in increased electrophilicity of the metal centre, a factor we hope to exploit by investigating the catalytic ability of these complexes in polymerisation of ethylene. A similar scenario had been reported with the benzenedicarbonyl and benzenetricarbonyl linker pyrazolyl ligands while investigating their palladium complexes for ethylene polymerisation ability.¹⁷

Generally it is the cationic form of the organometallic complexes that is of interest in their various catalytic potential as olefin polymerisation catalysts. It is generally accepted that the reaction between the halo complexes and methylaluminoxane (MAO) in the presence of olefins yield the catalytically active species.¹⁶ This has resulted in the synthesis of discrete cationic α -diimine complexes of Pd(II) and Ni(II).^{17, 18} It has also been reported that complexes containing metal carbon bonds (alkyls) instead of the chloride or bromide yield more active catalysts in ethylene polymerisation.²² This has been attributed to the fact that such complexes do not require methylation/activation by the methylaluminoxane prior to the formation of the active species. On this basis, we made an effort to replace one of the chlorides with a methyl with an aim of producing a relatively more active catalyst precursor using complex **1**.

Since we could not use Pd(COD)MeCl and ligand **L1** directly as discussed earlier, we attempted another synthetic route. In this procedure, complex **1** was directly reacted with tetramethyltin, Sn(Me₄) in a 1:1 ratio. The yellow solution turned black within 15 minutes after the addition of the tetramethyltin. ¹H NMR spectral analysis of the resultant black compound obtained after solvent removal showed a mixture of the original complex **1** and ligand **L1** in equal proportions. This confirms the decomposition of the complex to zerovalent palladium metal and the respective ligand **L1**.

To fully investigate this decomposition, a ¹H NMR experiment was performed and the reaction monitored for a period of 24 h. Figure 2.7 shows the spectral data obtained and

shows complete decomposition of complex **1** to ligand **L1**. This experiment also confirms the weak donor ability of compounds **L1** to **L10** and the resultant instability of their respective complexes **1** to **8**. The first and the second spectra represent the ^1H NMR spectra of ligands **L1** and its corresponding complex **1** respectively. The third spectrum was recorded fifteen minutes after the addition of an equivalent amount of tetramethyl tin into an NMR tube containing complex **1**. The peak at about 0.61 ppm corresponds to the unreacted tetramethyl tin. Four peaks of equal intensity were observed at around the methyl region, 2.29, 2.34, 2.44 and 2.62 ppm. The first and the last (2.29 and 2.62 ppm) correspond to the ligand protons while the middle two (2.34 and 2.44 ppm) are the complex protons. This feature is also visible in the appearance of two downfield furan peaks at 6.58 and 6.76 ppm corresponding to the ligand and complex signals respectively. Interestingly, the other peaks at about 6.03, 7.71 and 7.91 ppm appear at the same signals in both the complex and ligand environments. It is clear from the spectrum recorded after 1 h (spectrum number 4) that the complex is undergoing significant degradation to the original ligand as evidenced in drastic decrease in intensity of the complex peaks. The consumption of $\text{Sn}(\text{Me})_4$ is also witnessed from the disappearance of the peak at 0.61 ppm. After 24 h, we see a complete decomposition of the complex to the ligand as only two ligand peaks were recorded (2.29 and 2.62 ppm).

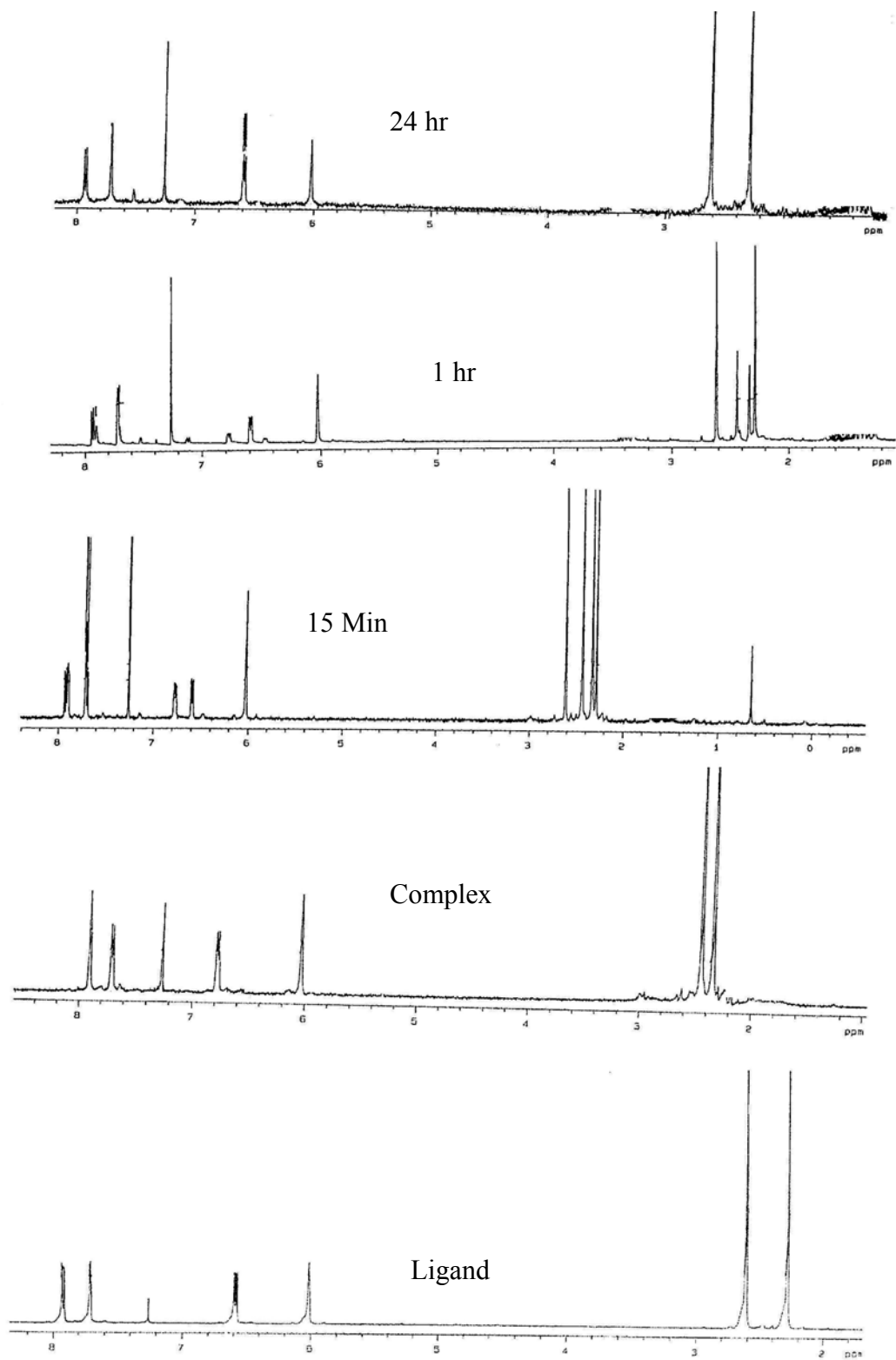
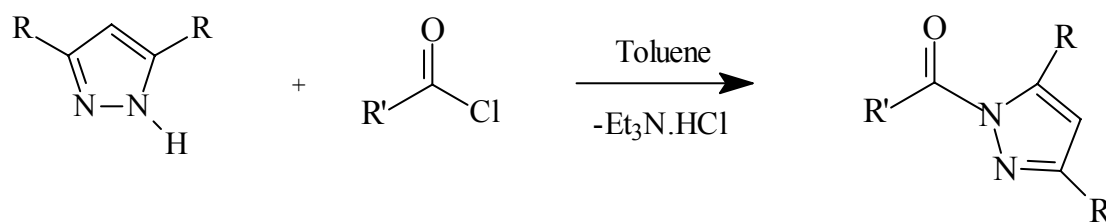


Figure 2.7 ¹H NMR spectra showing the decomposition of complex **1** to **L1** by SnMe₄.

2.5.2 Synthesis and characterisation of alkyl carbonyl pyrazolyl ligands and their palladium(II) complexes

In an attempt to investigate the effect of the heterocycles, furan and thiophene, in the pyrazolyl coordination chemistry and the catalytic activity of their palladium complexes as compared to the alkyl groups, we synthesised three acyl pyrazolyl ligands. In this case, we reacted the acetyl and propionyl chlorides with the appropriate pyrazoles, Scheme 2.4. Analytically pure compounds were isolated as colorless oils in moderate yields upon column chromatography on silica gel using CH₂Cl₂/Hexane as eluent in the ratio 2:1.



Compound	R	R'
L11	Me	Me
L12	^t Bu	Me
L13	^t Bu	Et

Scheme 2.4

Ligands **L11**, **L12** and **L13** were characterised by IR spectroscopy. It is interesting to note the high carbonyl frequency observed (1730, 1745 and 1741 cm⁻¹ respectively) in these compounds relative to the furan and thiophene analogues. For example **L11** (1730 cm⁻¹) compared to **L1** (1702 cm⁻¹) and **L12** (1745 cm⁻¹) compared to **L6** (1686 cm⁻¹). This observation could be ascribed to the mesomeric effect or the delocalization of π electrons between the C=O and the heterocyclic systems, which results in reduced CO

bond order and subsequently lower force constant and leading to the low frequencies observed as compared to the acyl analogues.²⁰ A similar trend has been reported in literature²¹ in which the C=O stretching frequencies of methyl ketone is observed at around 1720 cm⁻¹ as compared to a lower frequencies at 1700 cm⁻¹ for acetophenone bearing the aromatic phenyl substituent.

The ¹H NMR spectroscopy was also used to elucidate the structure of these compounds. In addition to the methyl and tertiary butyl peaks of the pyrazole substituents, **L11** and **L12** spectra exhibited a singlet at about 2.26 ppm and 2.69 ppm respectively assigned to the methyl adjacent to the carbonyl functionality. A triplet at about 1.19 ppm and a quartet at around 3.23 ppm were observed for **L13** and assigned to the methyl and methylene protons respectively of the propionyl groups.

Another interesting feature was observed in the ¹³C NMR spectra of compounds **L11**, **L12** and **L13**. The signals for the carbonyl carbon in all the three compounds were higher than those of the thiophene and furan compounds. Chemical shifts at 170.9, 170.6 and 174.7 ppm were observed for **L11**, **L12** and **L13** respectively. Figure 2.8 represents the ¹³C NMR spectrum of ligand **L13**. This once again confirms the mesomeric effect described earlier in the IR analysis. Significantly, the chemical shifts obtained are lower than those reported for the methyl and propyl ketones of 206.0 ppm²² and 207.6 ppm respectively. This suggests that the pyrazolyl system too has an overall effect of lowering the carbonyl frequency as compared to the alkyl groups.

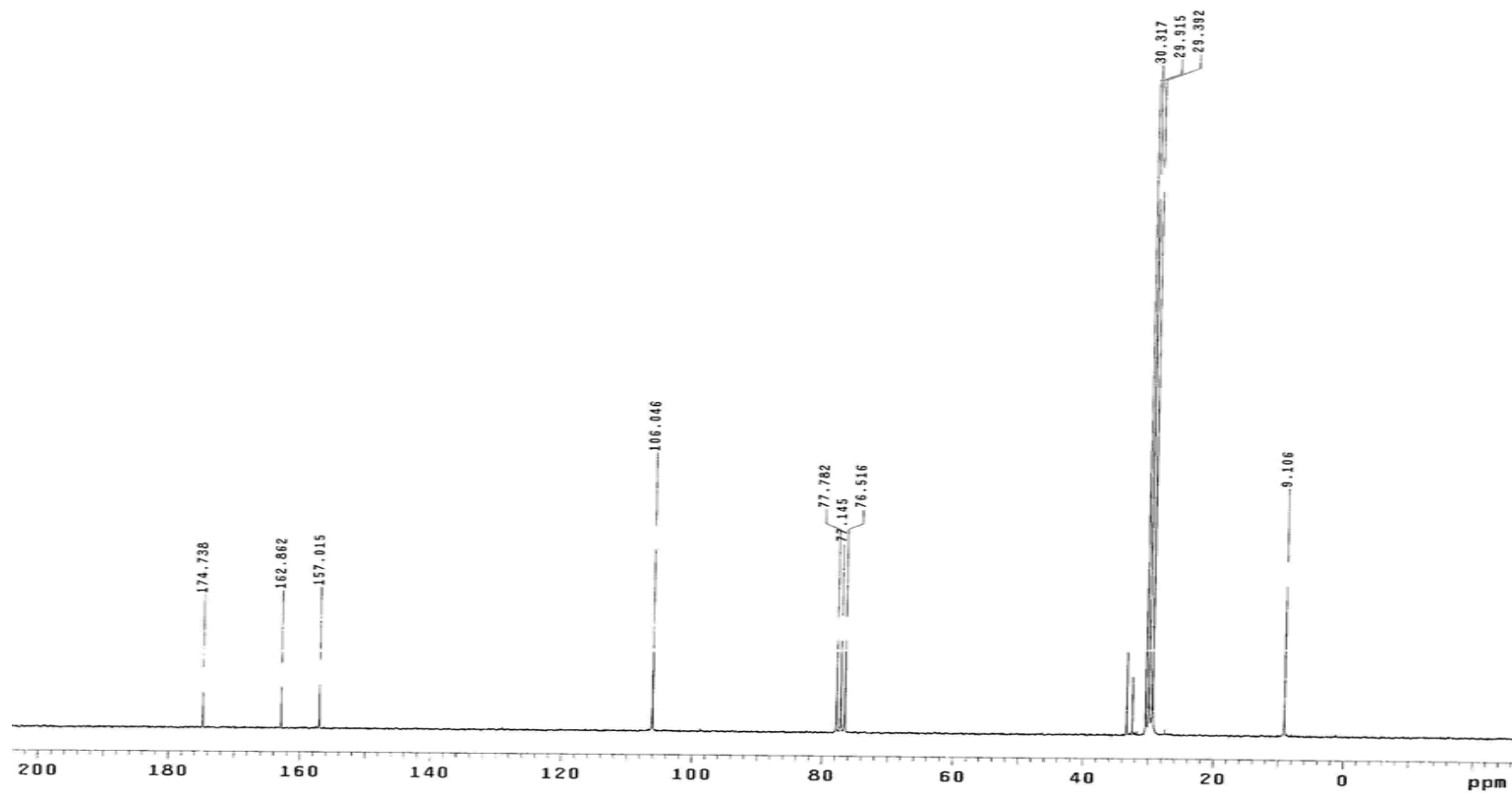
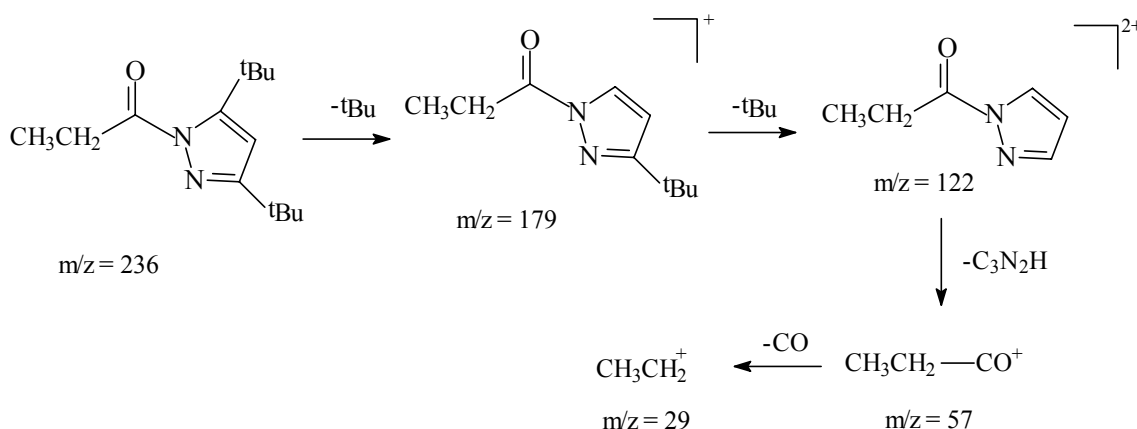


Figure 2.8. ^{13}C NMR spectrum of (3,5-ditertiarybutylpyrazolyl-1-carbonyl)ethane **L13**.

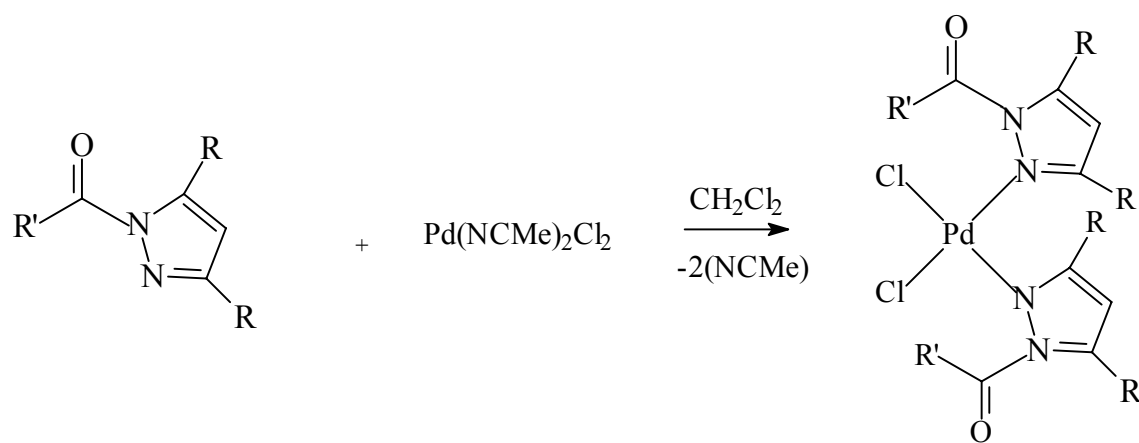
From mass spectrometry data of ligands **L11**, **L12** and **L13**, it is evident that these compounds exhibit similar fragmentation patterns to those of the furan and thiophene analogues, Scheme 2.5. For instance the molecular ion at 236, Figure 2.9, corresponds to the molecular mass of compound **L13**. It follows a similar pattern, which involves the loss of the two ditertiary butyl groups and the pyrazole system to produce a peak at m/z 57 corresponding to $\text{CH}_3\text{CH}_2\text{-CO}$.



Scheme 2.5 Fragmentation pattern of (3,5-ditertiarybutylpyrazolyl-1-carbonyl)ethane **L13**

We attempted to synthesise the palladium complexes using **L11**, **L12** and **L13** according to Scheme 2.6. Interestingly, we were unable to isolate the desired complexes but only a mixture of the starting materials as evident from spectral data. Recrystallization from CH_2Cl_2 /Hexane produced only the ligands as was observed from ^1H NMR spectral analysis. This was an indication that there was no reaction between the ligands and the metal precursor, $\text{Pd}(\text{NCMe})_2\text{Cl}_2$. We can hence deduce that the electron donor ability of

ligands **L11**, **L12** and **L13** is not sufficient enough to stabilize their palladium(II) complexes. The reason behind this observed different electronic behavior as compared to the ligands **L1-L10** is still unclear to us.



Scheme 2.6

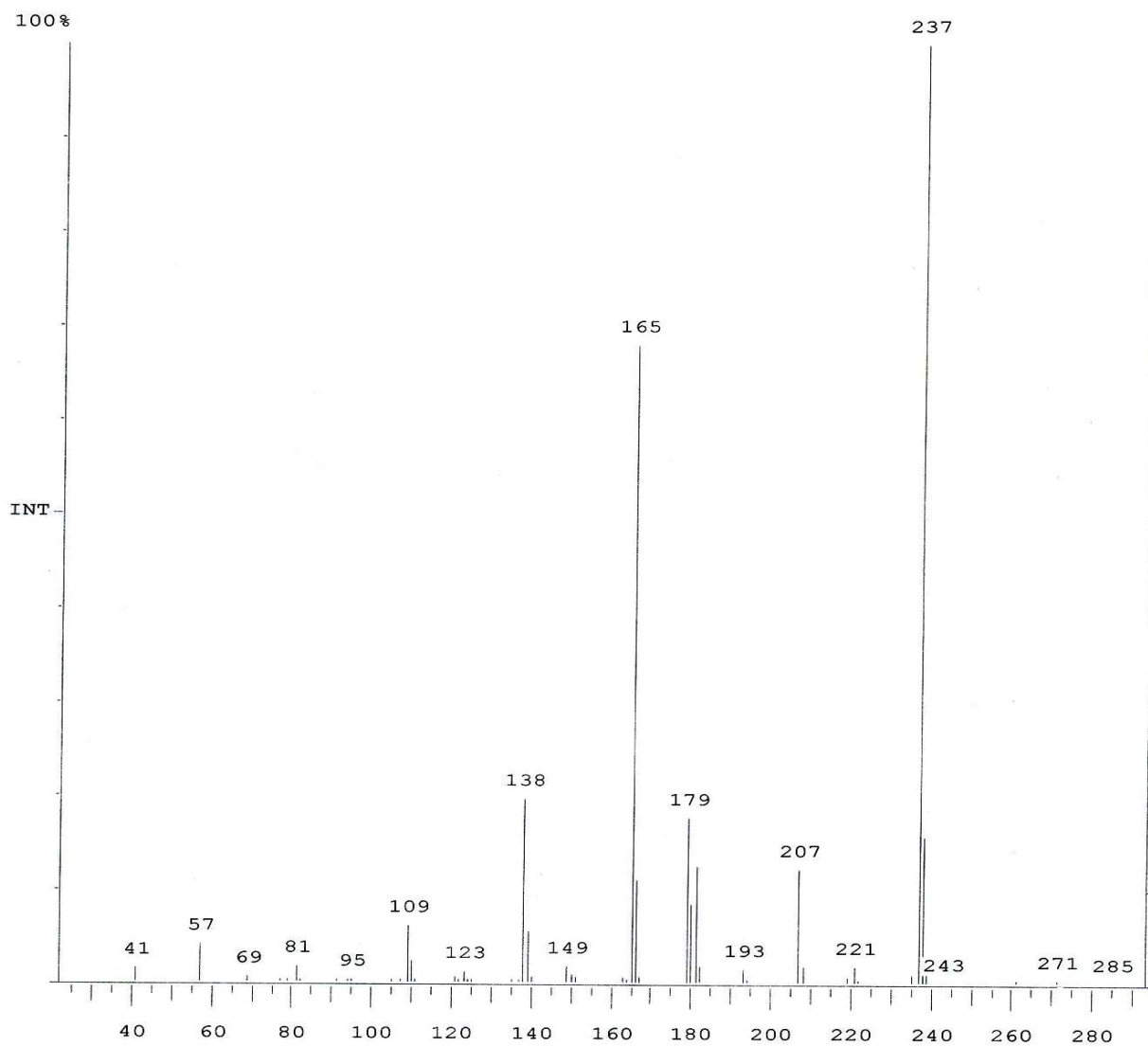


Figure 2.9 Mass spectrum showing the fragmentation pattern of **L13**

2.5.3 Molecular structure determination by single crystal X-ray analysis

Single crystals suitable for X-ray analysis for ligand **L1**, complexes **1** and **2** were grown and used to determine the molecular structures of the respective compounds. The procedure for complex **1** is used to describe the general experimental method adopted in X-ray structural determination of all the compounds.

Data collection

A yellow crystal with approximate dimensions 0.43 x 0.32 x 0.26 mm³ was selected under oil under ambient conditions and attached to the tip of a glass capillary. The crystal was mounted in a stream of cold nitrogen at 100(2) K and centred in the X-ray beam by using a video camera.

The crystal evaluation and data collection were performed on a Bruker CCD-1000 diffractometer with Mo K_α ($\lambda = 0.71073 \text{ \AA}$) radiation and the diffractometer to crystal distance of 4.9 cm. The initial cell constants were obtained from three series of ω scans at different starting angles. Each series consisted of 20 frames collected at intervals of 0.3° in a 6° range about ω with the exposure time of 10 seconds per frame. A total of 92 reflections were obtained. The reflections were successfully indexed by an automated indexing routine built in the SMART program. The final cell constants were calculated from a set of 6434 strong reflections from the actual data collection.

The data were collected by the hemisphere data collection routine. The reciprocal space was surveyed to the extent of a full sphere to a resolution of 0.80 Å. A total of 8891 data

were harvested by collecting three sets of frames with 0.3° scans in ω with an exposure time 20 sec per frame. These highly redundant datasets were corrected for Lorentz and polarization effects. The absorption correction was based on fitting a function to the empirical transmission surface as sampled by multiple equivalent measurements.²³

Structure Solution and Refinement

The systematic absences in the diffraction data were consistent for the space groups $P\bar{1}$ and $P1$. The E -statistics strongly suggested the centro symmetric space group $P\bar{1}$ that yielded chemically reasonable and computationally stable results of refinement.²⁴ A successful solution by the direct methods provided most non-hydrogen atoms from the E -map. The remaining non-hydrogen atoms were located in an alternating series of least-squares cycles and difference Fourier maps. All non-hydrogen atoms were refined with anisotropic displacement coefficients. All hydrogen atoms were included in the structure factor calculation at idealized positions and were allowed to ride on the neighbouring atoms with relative isotropic displacement coefficients. There are two half molecules of the complex in the asymmetric unit. The Pd atoms occupy crystallographic inversion centres.

The final least-squares refinement of 287 parameters against 4401 data resulted in residuals R (based on F^2 for $I \geq 2\sigma$) and wR (based on F^2 for all data) of 0.0271 and 0.0750, respectively. The final difference Fourier map was featureless. The ORTEP diagrams are drawn with 50% probability ellipsoids.

2.5.4 Molecular structure of ligand L1

Single crystals of compound **L1** suitable for X-ray analysis were grown by slow diffusion of hexane into dichloromethane at -4°C . Tables 2.3 and 2.4 show some of the selected bond lengths and angles and structure refinement data for **L1** respectively. Figure 2.10 represents an Ortep diagram of a single structure of the ligand.

Table 2.3 Selected bond lengths [\AA] and angles [$^{\circ}$] for **L1**

Bond length		Angles	
O(1)-C(6)	1.209(2)	C(10)-O(2)-C(7)	105.82(18)
O(2)-C(10)	1.355(3)	N(1)-N(2)-C(4)	111.88(16)
O(2)-C(7)	1.377(2)	N(1)-N(2)-C(6)	120.58(16)
N(1)-C(2)	1.311(3)	O(2)-C(7)-C(6)	112.40(17)
N(1)-N(2)	1.379(2)	O(1)-C(6)-C(7)	122.49(18)
N(2)-C(6)	1.405(2)	N(2)-C(6)-C(7)	117.53(17)

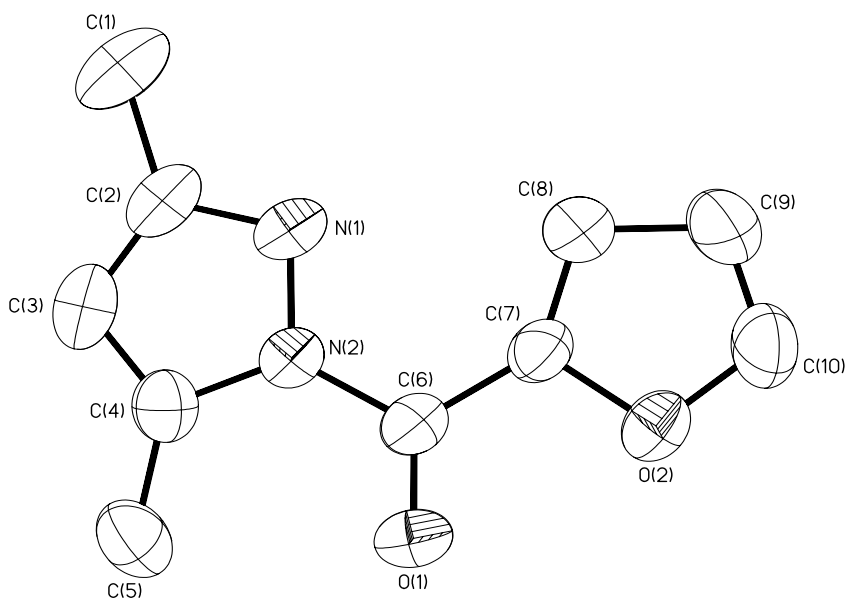


Figure 2.10: ORTEP diagram of single moiety of ligand **L1**. Atoms are shown with 50% thermal probability ellipsoid

2.5.5 Molecular structures of complexes **1** and **2**

Single crystals suitable for X-ray analysis for complexes **1** and **2** were grown by slow diffusion of hexane into dichloromethane at $-4\text{ }^{\circ}\text{C}$. Tables 2.5 and 2.6 show crystal data refinement and some of the selected bond lengths and angles respectively of **1**. Figure 2.19. represents an ellipsoid diagram of a single structure of **1** drawn in 30% probability, hydrogen atoms are omitted for clarity. Tables 2.7 and 2.8 show the crystal data refinement and selected bond lengths and angles respectively of **2**. Figure 2.11 represents the crystal structure of **2**.

Table 2.4 Crystal data and structure refinement parameters for L1.

Empirical formula	C ₁₀ H ₁₀ N ₂ O ₂	
Formula weight	190.20	
Temperature	294(2) K	
Wavelength	0.71073 Å	
Crystal system	Monoclinic	
Space group	P2 ₁ /n	
Unit cell dimensions	a = 8.0057(10) Å	α = 90°.
	b = 17.761(2) Å	β = 97.148(2)°.
	c = 13.8083(15) Å	γ = 90°.
Volume	1948.2(4) Å ³	
Z	8	
Density (calculated)	1.297 Mg/m ³	
Absorption coefficient	0.093 mm ⁻¹	
F(000)	800	
Crystal size	0.40 x 0.20 x 0.10 mm ³	
Theta range for data collection	1.88 to 26.38°.	
Index ranges	-10 ≤ h ≤ 9, -22 ≤ k ≤ 20, -16 ≤ l ≤ 7	
Reflections collected	9077	
Independent reflections	3753 [R(int) = 0.0296]	
Completeness to theta = 26.38°	94.2 %	
Absorption correction	Empirical with SADABS	
Max. and min. transmission	0.9908 and 0.9639	
Refinement method	Full-matrix least-squares on F ²	
Data / restraints / parameters	3753 / 0 / 313	
Goodness-of-fit on F ²	1.025	
Final R indices [I > 2σ(I)]	R1 = 0.0513, wR2 = 0.1264	
R indices (all data)	R1 = 0.0948, wR2 = 0.1457	
Largest diff. peak and hole	0.174 and -0.245 e.Å ⁻³	

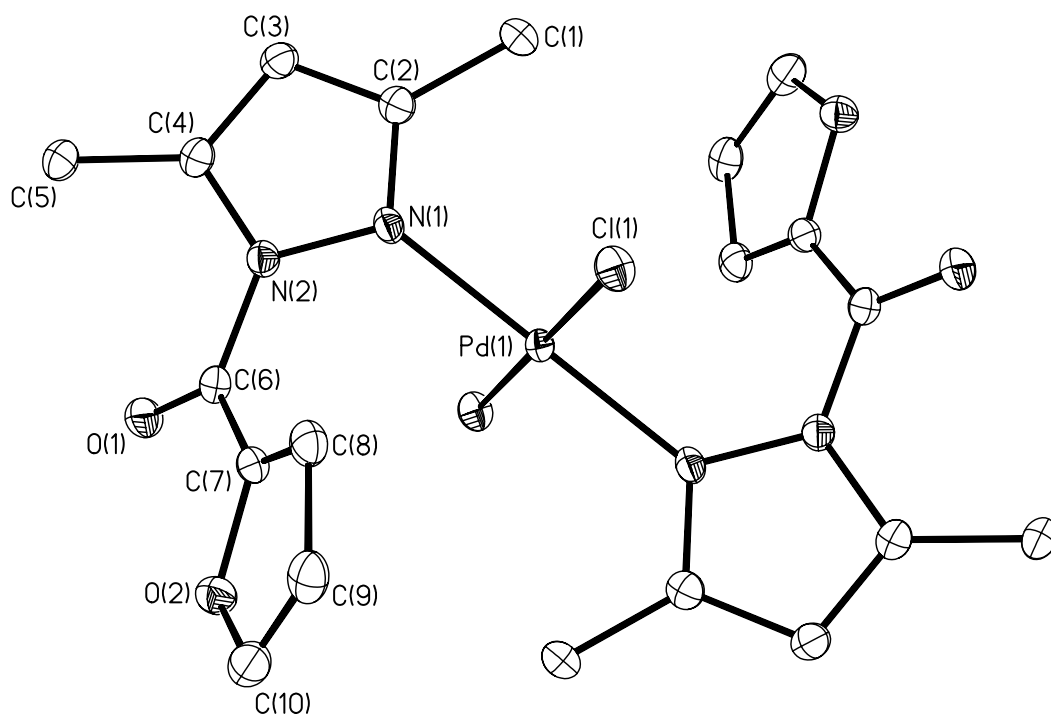


Figure 2.11: Molecular drawing of complex 1 shown with 30% probability ellipsoids.

The hydrogen atoms are omitted for clarity.

Table 2.5. Crystal data and structure refinement parameters for 1

Empirical formula	C ₂₀ H ₂₀ Cl ₂ N ₄ O ₄ Pd	
Formula weight	557.70	
Temperature	273(2) K	
Wavelength	0.71073 Å	
Crystal system	Triclinic	
Space group	$\bar{P}1$	
Unit cell dimensions	a = 7.4422(8) Å	$\alpha = 88.898(2)^\circ$.
	b = 9.2097(10) Å	$\beta = 88.049(2)^\circ$.
	c = 15.7422(17) Å	$\gamma = 86.608(2)^\circ$.
Volume	1076.3(2) Å ³	
Z	2	
Density (calculated)	1.721 Mg/m ³	
Absorption coefficient	1.146 mm ⁻¹	
F(000)	560	
Crystal size	0.43 x 0.32 x 0.26 mm ³	
Theta range for data collection	2.22 to 26.39°.	
Index ranges	-9 ≤ h ≤ 9, -11 ≤ k ≤ 11, -19 ≤ l ≤ 19	
Reflections collected	8891	
Independent reflections	4401 [R(int) = 0.0207]	
Completeness to theta = 26.39°	99.1 %	
Absorption correction	Empirical with SADABS	
Max. and min. transmission	0.7549 and 0.6386	
Refinement method	Full-matrix least-squares on F ²	
Data / restraints / parameters	4401 / 0 / 287	
Goodness-of-fit on F ²	1.063	
Final R indices [I > 2σ(I)]	R1 = 0.0271, wR2 = 0.0737	
R indices (all data)	R1 = 0.0288, wR2 = 0.0750	
Largest diff. peak and hole	1.011 and -0.529 e.Å ⁻³	

The two palladium complexes **1** and **2** have the same geometry. The palladium centre in each case is in a slightly distorted square planar environment with the pyrazolyl ligands trans to each other. The monodentate nature of these ligands as evidenced from the X-ray structures confirms that the heteroatoms sulfur and oxygen are non-coordinating. This observation has also been made by Steel *et al.* while studying the palladium complexes of 1-thenylpyrazole²⁵. The angles about the central palladium centres range between 88.16(5) to 91.84(5)^o for complex **1** and 88.47(17) to 91.29(17)^o for complex **2**. It is significant to point out that the angles around the N-Pd-N and Cl-Pd-Cl in **1** is linear and are exactly 180.00(8)^o. This has also been reported in literature for the palladium complex of 1-benzyl-3,5-dipropyl-4-ethylpyrazole,²⁶ but these angles are greater than those reported for the complex *trans*-[Pd(dmpz)₂Cl₂] (dmpz = 3,5-dimethylpyrazole) which were reported as 171.91(9)^o and 178.60(3)^o.¹⁵ This signifies greater distortion in the later, which has been attributed to hydrogen bonding due to the N-H in the complex. In comparison, the N-Pd-N and Cl-Pd-Cl angles of complex **2** were found to be 178.7(3) and 178.78(9)^o showing the different electronic effects of the thiophene and furan moieties.

Table 2.6 Selected bond lengths [\AA] and angles [$^\circ$] for complex 1

Bond lengths		Bond angles	
Pd(1)-N(1)	2.0332(15)	N(1)-Pd(1)-N(1)	180.00(8)
Pd(1)-Cl(1)	2.2993(5)	N(1)-Pd(1)-Cl(1)	91.84(5)
Pd(2)-N(3)	2.0300(17)	N(1)-Pd(1)-Cl(1)	88.16(5)
Pd(2)-Cl(2)	2.3125(5)	N(1)-Pd(1)-Cl(1)	91.84
N(1)-C(2)	1.327(2)	N(3)-Pd(2)-Cl(2)	88.84(5)
N(1)-N(2)	1.388(2)	N(3)-Pd(2)-Cl(2)	91.16(5)
O(1)-C(6)	1.203(2)	N(2)-C(6)-C(7)	116.36(16)

The average Pd-N bond lengths of 2.033(15) and 2.031(6) \AA for complexes **1** and **2** respectively are similar and lie within the normal range of the Pd-N interactions.²⁷ This average bond length of 2.032(6) \AA correlates to those of the benzenedicarbonyl and benzenetricarbonyl palladium complexes [2.0332(5) \AA]¹⁴ previously reported but is slightly shorter than the average value of 59 Pd-N (2.1 \AA) (pyrazole) bond lengths reported in the Cambridge Structural Database²⁸ (CDS), though the variation is statistically insignificant.

Table 2.7 Crystal data and structure refinement parameters for 2.

Empirical formula	C ₂₁ H ₂₂ C ₁₄ N ₄ O ₂ Pd S ₂	
Formula weight	674.75	
Temperature	100(2) K	
Wavelength	0.71073 Å	
Crystal system	Monoclinic	
Space group	P21	
Unit cell dimensions	a = 10.696(2) Å	α = 90°.
	b = 13.332(3) Å	β = 96.345(4)°.
	c = 18.015(4) Å	γ = 90°.
Volume	2553.1(9) Å ³	
Z	4	
Density (calculated)	1.755 Mg/m ³	
Absorption coefficient	1.337 mm ⁻¹	
F(000)	1352	
Crystal size	0.30 x 0.20 x 0.20 mm ³	
Theta range for data collection	1.90 to 28.31°.	
Index ranges	-14<=h<=12, -16<=k<=17, -23<=l<=20	
Reflections collected	16039	
Independent reflections	10829 [R(int) = 0.0508]	
Completeness to theta = 28.31°	92.8 %	
Max. and min. transmission	0.7758 and 0.6898	
Refinement method	Full-matrix least-squares on F ²	
Data / restraints / parameters	10829 / 409 / 622	
Goodness-of-fit on F ²	1.045	
Final R indices [I>2sigma(I)]	R1 = 0.0616, wR2 = 0.1404	
R indices (all data)	R1 = 0.0700, wR2 = 0.1486	
Absolute structure parameter	0.00	
Extinction coefficient	0.0000(2)	
Largest diff. peak and hole	3.060 and -0.849 e.Å ⁻³	

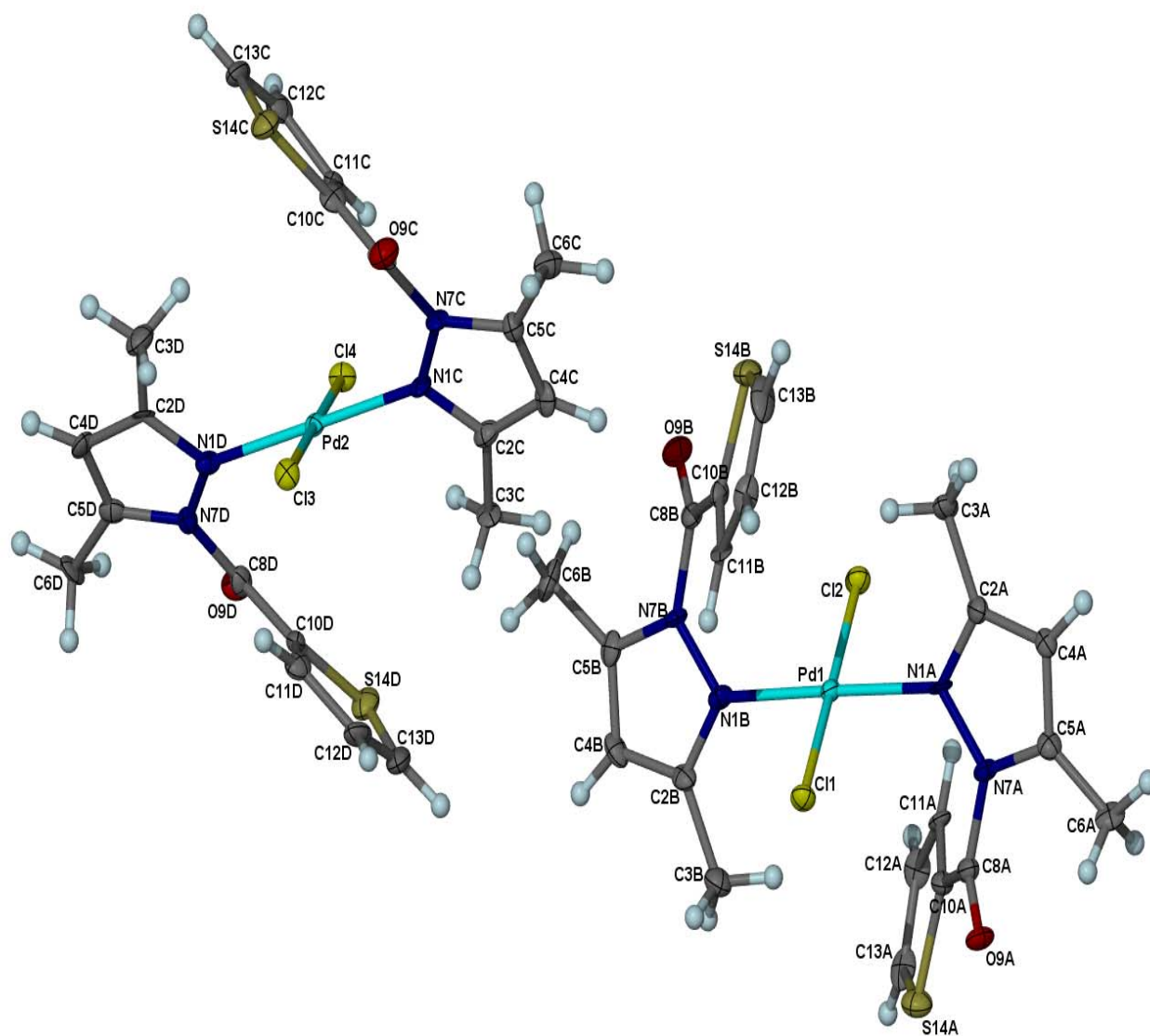


Figure 2.12: Molecular structure of complex 2 showing the two unique parts in a single crystal structure.

Table 2.8 Selected bond lengths [Å] and angles [°] for 2

Bond lengths		Bond angles	
Pd(1)-N(1A)	2.026(6)	N(1A)-Pd(1)-N-(1B)	178.7(3)
Pd(1)-Cl(1)	2.3029(19)	N(1A)-Pd(1)-Cl(1)	88.47(5)
Pd(2)-N(1B)	2.035(6)	N(1B)-Pd(1)-Cl(1)	90.93(5)
Pd(1)-Cl(2)	2.3101(19)	N(1A)-Pd(1)-Cl(2)	91.29(17)
S(14A)-C(13A)	1.694(8)	N(1C)-Pd(2)-N(1D)	179.5(3)
O(9A)-C(8A)	1.202(8)	O(9A)-C(8A)-N(7A)	119.5(7)
N(1A)-C(2A)	1.363(8)	O(9A)-C(8A)-C(10A)	123.4(7)

The distance between the Pd and Cl atoms are reported as 2.299(5) Å for complex **1** and is equal in both the Pd-Cl bonds in the complex. This could be due to the absence of any *trans* influence in the structures. In comparison, the Pd-Cl bond lengths in complex **2** range between 2.303(19) to 2.310(19) Å. This is slightly higher than the bond length in **1** by 0.01 Å but in both cases lie within the usual ranges for the Pd-N interactions.²⁹ It is also noteworthy to point out that there is no significant difference between the CO bond lengths in both complexes. The bond lengths were reported as [1.203(2) Å] for complex **1** and [1.202(2) Å] for **2** indicating similar donor ability of both ligands **L1** and **L6**. There was a slight decrease in the CO bond length of complex **1** [1.203(2) Å] relative to its respective ligand **L1** [1.209(2) Å] showing decreased electron density in the carbonyl functionality in the complex system. This suggests flow of electrons from the ligand³⁰ system to the palladium metal centre as already observed in the IR and ¹H NMR studies.

2.6 Conclusion

A series of heterocyclic carbonyl pyrazolyl ligands have been successfully synthesised and obtained in moderate to high yields. The reaction of these ligands with $\text{Pd}(\text{NCMe})_2\text{Cl}_2$ gave the respective palladium(II) complexes in good yields. The compounds synthesised have been characterised by a combination of ^1H NMR, ^{13}C NMR and IR spectroscopic techniques including mass spectrometry and X-ray analysis. Microanalysis was used to confirm the molecular formulae and purity of the ligands synthesised. X-ray analysis of complexes **1** and **2** confirms that the ligands are monodentate with the heteroatoms oxygen and sulfur in the furan and thiophene moieties being non-coordinating. A general formulae for all the complexes can thus be deduced as $\text{Pd}(\text{L})_2\text{Cl}_2$ with the trans geometry being preferred.

The weak donor ability of these ligands is attested by their inability to displace COD when $\text{Pd}(\text{COD})\text{Cl}_2$ is used as the metal precursor. This is also confirmed by the ^1H NMR experiment carried out which shows the complete dissociation of the ligands from the palladium metal centre upon reaction with $\text{Sn}(\text{Me})_4$.

The acyl pyrazolyl ligands have been successfully synthesised and were in good yields and high purity. These ligands have also been fully characterised by a combination of ^1H NMR, ^{13}C NMR and IR spectroscopic techniques. However, attempts to isolate their Pd(II) complexes were unsuccessful.

2.7 References

1. Y. Sun, X. Chen, P. Cheng, S. Yan, D. Zheng Liao and P. Wen Shen, *J. Mol. Struct.* **613** (2002) 167.
2. Y. Sun, X. Chen, P. Cheng, S. Yan, D. Zheng Liao and P. Wen Shen, *J. Mol. Struct.* **597** (2001) 191.
3. S. Trofimenko, *Prog. Inorg. Chem.* **34** (1986) 115. (b) S. Trofimenko, *Chem. Rev.* **93** (1993) 943.
4. R. Mukherjee, *Coord. Chem. Rev.* **203** (2000) 166.
5. A. Boixassa, J. Pons, A. Virgili, X. Solans, M. Bardia and J. Ros, *Inorg. Chim. Acta* **340** (2002) 49.
6. D. House, P. Steel, and A. Watson, *Aust. J. Chem.* **39** (1986) 1525.
7. P. Gamez, R. Steensma, W. Driessen and J. Reedijk, *Inorg. Chim. Acta.* **333** (2002) 51.
8. A. Downward, G. Honey, P. Steel, *Inorg. Chem.* **30** (1991) 3733.
9. J. Elguero, in *Comprehensive Heterocyclic Chemistry, Vol. 5* (Eds. A. R. Katritzky, C. W. Rees), Pergamon Press, Oxford, **1984**, p. 167. (b) J. Elguero, C. FocesFoces, D. Sanz, R. M. Claramunt, in *Advances in Nitrogen Heterocycles, Vol. 4* (Ed. C. J. Moody), Jai Press Inc, 100 Prospect Street, Stamford, CT 06901-1640, USA, **2000**, pp. 295.
10. D. Curtis, B. Shiu and M. Burtler, *J. Am. Chem. Soc.* **108** (1986) 1550.
11. R. Alsfasser, S. Trofimenko, A. Looney, G. Parkin, H. Vahrenkamp, *Inorg. Chem.* **30** (1991) 4098.
12. T. Lal, J. Richardson, R. Buchanan, R. Mukherjee, *Polyhedron* **16** (1997) 4331.
13. R. Warthen, J. Carrono, *J. Inorg. Biochem.* **94** (2003) 198.

14. I. A. Guzei, K. Li, G. Bikzhanova, J. Darkwa, S. F. Mapolie, *Dalton Trans.* (2003) 715.
15. K. Li, J. Darkwa, I. A. Guzei, S. Mapolie, *J. Organomet. Chem.* **660** (2002) 108.
16. L. Johnson, C. Killian, M. Brookhart, *J. Am. Chem. Soc.* **117** (1995) 6414.
17. J. Paul, Y. Kaiyuan, E. Richard, *Organometallics* **18** (1999) 2747.
18. L. Johnson, S. Mecking, M. Brookhart, *J. Am. Chem. Soc.* **118** (1996) 267.
19. S. Ittel, L. Johnson, *Chem. Rev.* **100** (2000) 1169.
20. L. S. Hegedus, L. G. Wade, *Compendium of organic synthetic methods*, Volume III, John Wiley and Sons (1977) 123.
21. W. Kemp, *Organic Spectroscopy*, Third edition, Macmillan Education Ltd. (1991) 36.
22. L. F. Johnson, W. C. Jankowski, *Carbon-13 NMR Spectra*, John Wiley and Sons, New York (1972) 28.
23. R. H. Blessing, *Acta Cryst.* **A51** (1995) 33.
24. All software and sources of the scattering factors are contained in the SHELXTL (version 5.1) program library (G. Sheldrick, Bruker Analytical X-Ray Systems, Madison, WI).
25. P. J. Steel and A.A. Watson, *Aust. J. Chem.* **39** (1986) 1525.
26. D. Combs, and S. Van, *Inorg. Chem.* **39** (2000) 2080.
27. G. Palenik and M. Steffen, *Inorg. Chem.* **15** (1976) 2432.
28. F. H. Allen, and O. Kennard, *Chem. Des. Autom. News* **8** (1993) 31.
29. J. Pons, A. Virgili and X. Solans, *Inorg. Chim. Acta.* **340** (2002) 49.
30. G. Minghetti, M. Cinellu, A. B. G. Banditelli, F. Demartin, *J. Organomet. Chem.* **15** (1986) 387.

CHAPTER 3

Ethylene oligomerisation and polymerisation catalyzed by furan and thiophene carbonyl pyrazolyl palladium(II) complexes

3.1 Introduction

Research in single-site metal catalyzed olefin oligomerisation and polymerisation has witnessed intense growth over the past three decades both in the academic and industrial arenas.¹ As a result, various highly active catalyst systems containing well-defined active centres and catalyst structures have been discovered. This has resulted in proper control of polymer properties by fine-tuning the catalyst precursor itself.² Some of these new catalysts, particularly Group 4 metallocenes have already been commercialized alongside the well established Ziegler-Natta catalysts in the plastics industry.³

Oligomerisation catalysts are known to exhibit extremely high reactivity towards ethylene and with remarkable specificity towards α -alkenes.⁴ The two most important factors influencing the oligomerisation process are the metal-ligand design and the nature of the co-catalysts.⁵ Olefin dimerisation and oligomerisation reactions are typically carried out using late transition metal catalysts, particularly nickel.⁶ A wide variety of ligands have been employed with these systems, and careful tuning of ligands and choice of appropriate co-catalyst can be used to vary product composition from lower oligomers to polymer.⁷

The oxophilic nature of early transition metal catalysts e.g. titanium, zirconium, or chromium towards oxygen leads to their poisoning by most functionalized olefins like

methyl acrylates.⁸ In contrast, the lower oxophilicity and greater functional-group tolerance of the late transition metals make them potential targets for the development of single-site catalysts for the oligomerisation and polymerisation of ethylene.⁹ However, late transition metal catalysts have traditionally been considered poor polymerisation catalysts for simple alkenes¹⁰ such as ethylene and propylene leading to short chain products. This is mainly due to the highly competitive chain-termination step as opposed to chain propagation.¹¹

In 1995 the group of Brookhart,¹² however, was able to produce high molecular weight polyethylene with Ni(II) and Pd(II) α -diimine based catalysts. The major discovery here was the use of sterically hindered 1,4-diazabutadiene ligands, which effectively block the axial coordination sites hence impeding chain termination.¹³ They found that when the bulkiness of the aryl groups attached to the imino nitrogens is reduced, the product composition can be shifted to lower oligomers.¹⁴

Consequently considerable effort is being expended to identify Ni(II) and Pd(II) complexes containing other nitrogen based donor ligands which expand the scope of utility of such catalysts.¹⁵ An important goal is to identify catalysts with increased activity, lifetime and thermal stability while maintaining chain propagation giving rise to high molecular weight polymers. The ease with which the electronic and steric properties of pyrazole ligands can be varied has resulted in increased interest in their late transition metal complexes as catalysts for the transformation of saturated hydrocarbons. Such complexes are electrophilic and it is expected that the introduction of a carbonyl containing functionality would create even greater electrophilic metal centres and hence leading to increased

catalytic activity. A report by Jordan *et al.*¹⁶ on the polymerisation of ethylene by $\{R_2C(3\text{-}^t\text{Bu}_2\text{pz})_2\}\text{PdCl}_2$ (R = Me, Ph and pz = pyrazole), represents an example that involves the use of pyrazolyl ligands in late-transition metal olefin catalysis. The catalytic potential in ethylene polymerisation of the simple pyrazole systems with Ni(II) and Pd(II) transition metals have already been investigated by Darkwa and co-workers.¹⁷

In an attempt to enhance the electrophilicity of the metal centre, we are currently involved in the use of carbonyl linkers to impart some electron withdrawing effect in the pyrazole moiety. Benzenedicarbonyl and benzenetricarbonyl linker pyrazolyl palladium(II) complexes have already been tested by Darkwa *et al.*¹⁸ The activities of these systems were significantly higher than their analogous simple isolated systems. For example, turn-over numbers of 2590 kg per mol of Pd per h as compared to 1005.7 kg per mol of Pd per h of $\{(3,5\text{-}^t\text{Bu}_2\text{pz})_2\}\text{PdCl}_2$ were obtained. It is on this basis that we undertook to study the ability of the furan and thiophene carbonyl pyrazolyl Pd(II) complexes as catalysts for ethylene oligomerisation and polymerisation. The focus here is also to establish the effect of the presence of the donor atoms as compared to the benzene systems previously investigated.

In this Chapter, we report the preliminary results of ethylene oligomerisation and polymerisation using some of the complexes synthesised in Chapter 2, $(3,5\text{-Me}_2\text{pz-CO-furan})_2\text{PdCl}_2$, (**1**), $(3,5\text{-Me}_2\text{pz-CO-thiophene})_2\text{PdCl}_2$, (**2**), $(3,5\text{-}^t\text{Bu}_2\text{pz-CO-furan})_2\text{PdCl}_2$, (**3**), $(3,5\text{-}^t\text{Bu}_2\text{pz-CO-thiophene})_2\text{PdCl}_2$, (**4**), and $(3,5\text{-Ph}_2\text{pz-CO-thiophene})_2\text{PdCl}_2$, (**8**). The ethylene polymerisation results of complexes **1** to **4** when activated with methylaluminoxane, MAO, are discussed. We also report ethylene oligomerisation based

on complexes **1-4** and **8** using ethylaluminium dichloride, EtAlCl₂, as the co-catalyst. The effect of the Lewis acid, B(C₆F₅)₃, on these catalysts and the trends in the catalytic behaviour of complexes **1-4** and **8** as oligomerisation and polymerisation conditions are varied is also discussed.

3.2 Materials and methods

3.2.1 Ethylene polymerisation procedure

Ethylene polymerisation was performed in a 300 mL stainless steel autoclave loaded with the respective catalyst and excess amount of co-catalyst methylaluminoxane, MAO. This was carried out in a nitrogen-purged glove box. The general procedure involved charging of the autoclave with the palladium complex and MAO (10% in toluene) in 100 mL dry toluene. The Al:Pd ratio used was between 1000-6000. The autoclave was sealed, removed from the glove box and loaded into the reactor chamber. The autoclave was flushed three times with ethylene and heated to the set temperature. The desired ethylene pressure was set and a constant flow maintained throughout the reaction time. At the end of the polymerisation, the ethylene supply was closed, and the autoclave vented. The reaction was quenched by addition of ethanol. The polymer was filtered, suspended in 2M HCl for several days to remove excess Al or Pd, and filtered again. The polymer was dried in an oven at 60 °C overnight to afford a constant mass. The polymers produced were characterised by high temperature ¹³C NMR in 1,2,3-trichlorobenzene/benzene-d⁶ on a Varian 2000 Gemini instrument (50.3 MHz) and high temperature gel permeation chromatography (GPC).

3.2.2 Oligomerisation of ethylene procedure

Ethylene oligomerisation reactions were performed as described in the polymerisation section. EtAlCl₂ was used as the co-catalyst. At the end of the reaction, an aliquot of the reaction mixture was taken for the GC analysis. The remaining products in the reactor were hydrolyzed by addition of ethanol after which the solvent was removed in *vacuo* and the mass of the total non-volatiles products determined. Analysis of the oligomers was performed by GC-MS using a Finnigan-Matt GCQ gas chromatograph equipped with electron impact ionization detector at 70 eV, a 30 m HP PONA capillary column with a stationary phase based on 5% poly(methylphenylsiloxane). The oven temperature program adopted was as follows: 40°C for 2 min, then the temperature was increased by 10°C/min heating until 260°C was reached. This temperature was maintained for another 6 min. Under this condition, it was possible to separate the olefins in the C₄ to C₂₀ range. The retention times of the individual components were determined using authentic samples. Quantitative analysis was done by internal standard reference method using pentadecane as the internal reference.

3.3 Results and discussion

3.3.1 Evaluation of complexes 1 to 4 as catalyst precursors for ethylene polymerisation

Four catalyst precursors (**1** to **4**) were investigated for ethylene polymerisation activity. All the complexes showed considerable catalytic activity upon activation with MAO as shown in Figure 3.1. From Table 3.1 it is evident that the activities of the catalysts decrease with increase in the bulkiness of the substituent groups. For example complex **2**, the thiophene analogue, containing methyl groups on the pyrazole moiety gave a turn-over number of 462

kg per mol of Pd per h compared to 125 kg per mol of Pd per h obtained from catalyst **4** bearing the *tert*-butyl substituents. This suggests that the bulkier *tert*-butyl groups inhibit ethylene monomer insertion into the metal-alkyl bonds. This trend could also be ascribed to the hindrance of the formation of the *cis*-isomer of the catalysts necessary for the formation of the active species. This observation contrasts with that observed by Darkwa *et al.*¹⁷ during the study of simple pyrazole Pd(II) systems. In this case, there is an increase in activity with increase in bulky substituent groups. This was ascribed to enhanced solubility of the complexes with increase in bulkiness of the substituents on the pyrazole moiety. However, a similar trend has been reported by Laine *et al.*¹⁹ in the pyridylimine based Ni(II) and Pd(II) complexes where the methyl groups in the pyridyl ring decrease activity as compared to the unsubstituted structures.¹⁹ Interestingly, no activity was observed with these catalysts at temperatures below 50 °C. This is in sharp contrast with α -diimine Pd(II) complexes which are known to be active even at room temperatures.⁹

Table 3.1: Ethylene polymerisation data^a for complexes **1**, **2**, **3**, and **4**.

Entry	Catalyst	$M_w \times 10^5$	$M_n \times 10^5$	M_w/M_n^b	TON ^c
1	1	8.41	4.05	2.08	301
2	2	8.01	3.98	2.01	426
3	3	5.74	2.88	1.99	176
4	4	6.17	3.25	1.90	125

^aConditions Al:Pd 4000:1, temperature, 50 °C, pressure, 5 atm, time, 2 h.

^bPolydispersity index determined by GPC based on polystyrene standards.

^cThe turn-over number in kg of polymer per mol of Pd per h determined by the total mass of polymer produced.

The dependence of the polymer molecular weights on the nature of the substituent groups is clearly visible (Table 3.1 entries 1 and 2). Replacing the methyl groups in complex **1** with *tert*-butyl groups, **3**, results in a significant decrease of polymer molecular weight from 8.41×10^5 to 5.74×10^5 . This is in sharp contrast to the theoretical calculations that bulky groups inhibit β -hydride elimination hence leading to higher molecular weights.²⁰ However, few literature reports exist in which increase in steric bulk of the ligand backbone results in reduction of polymer molecular weight. One such example is the findings of Brookhart *et al.*²¹ in the ethylene polymerisation using cationic Pd(II) catalysts containing imine-phosphine ligands. They found that an increase of steric bulk at the phosphorus from phenyl to *o*-toluene resulted in a drastic decrease of polymer molecular weight from 133 000 to 75 000. It is interesting to note that despite the variation of molecular weights, the polydispersity indices remain roughly constant (Table 3.1).

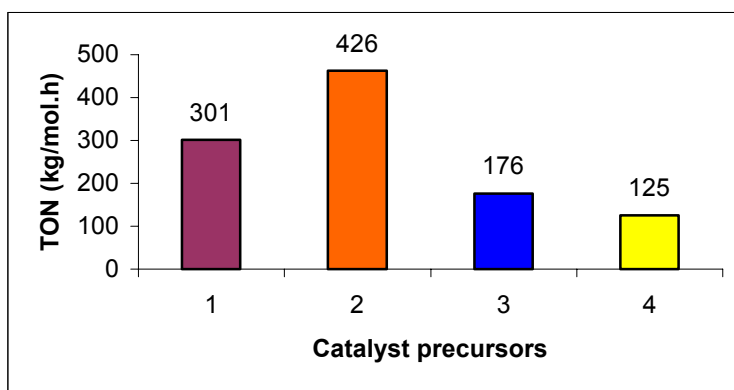


Figure 3.1: The turn-over numbers for catalysts **1-4** in the polymerisation of ethylene run at Al:Pd ratio of 1:4000 at 5 atm, 50 °C for 2 h

3.3.2 Effect of co-catalyst concentration on ethylene polymerisation

The co-catalyst, methylaluminoxane, to palladium ratio was varied in order to establish the optimum conditions for ethylene polymerisation using catalyst **2**. From Figure 3.2, the optimum activation was found to be at 5000:1. This value is significantly high compared to those frequently reported in literature of 1000:1.⁹ The optimum ratio reported by Darkwa *et al.*¹⁸ when investigating the benzenedicarbonyl pyrazolyl systems was 3000:1. The higher values reported here could be attributed to the coordination of the free heteroatoms, oxygen and sulfur in the furan and thiophene moieties to the aluminium centres of the co-catalyst. This could result in higher MAO ratios required to initiate the formation of the active species.

Table 3.2 The dependence of ethylene polymerisation^a on the Al:Pd ratio

Entry	Al:Pd Ratio	$M_w \times 10^5$	$M_n \times 10^5$	M_w/M_n^b	TON ^c
1	500:1	3.30	1.71	1.93	24
2	1000:1	5.53	2.85	1.94	62
3	2000:1	5.83	2.89	2.01	104
4	3000:1	7.15	3.45	2.07	126
5	4000:1	8.01	3.98	2.01	426
6	5000:1	4.89	2.05	2.38	471
7	6000:1	5.38	1.85	2.90	141

^aPolymerisation conditions: Al:Pd 4000:1, temperature, 50 °C, pressure, 5 atm, time, 2 h.

^bPolydispersity index determined by GPC based on polystyrene standards.

^cThe turn-over number in kg of polymer per mol of Pd per h determined by the total mass of polymer produced.

It is also noteworthy to point out the dependence of the molecular weights on the Al:Pd ratios of the polyethylene produced. For instance, from Table 3.2 (entries 1 and 5) an increase of the Al:Pd ratio from 500 to 4000 results in an increase of polymer molecular weight from 3.30×10^5 to 8.01×10^5 . Beyond this ratio the trend becomes erratic giving higher polydispersity indices.

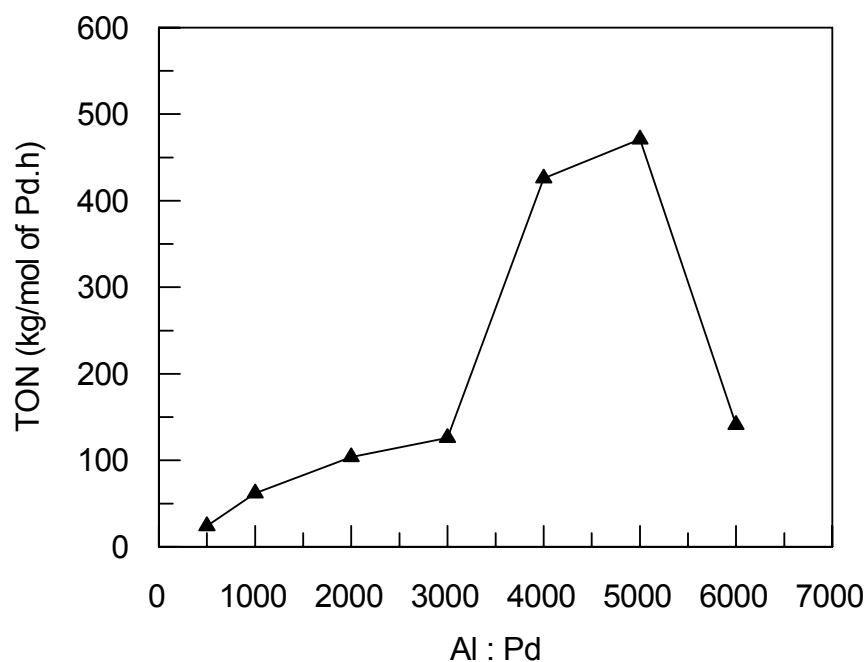


Fig 3.2. The effect of Al:Pd ratio on polymerisation activity of catalyst **2** run at 50°C, 5 atm for 2 h

This trend has also been reported by Chen *et al.*²² in the behaviour of halogenated iminopyridyl iron complexes. They however, noted a decrease in molecular weight with increase in the co-catalyst concentration. An increase of Al:Fe ratio from 250 to 5000 resulted in a significant decrease in polymer molecular weight from 184 000 to 19 400 respectively. They ascribed this trend to the transfer of matured polymer chains to the

aluminium complexes during polymerisation. The increase of molecular weights with increase in the Al:Pd ratio in this study therefore depicts a decrease in the chain transfer to the aluminium adducts. From this data we can predict that the polyethylene produced contain saturated end groups. This, however, could not be confirmed from the NMR spectra due to the high molecular weights of the polymers produced.

3.3.3 The effect of tris(pentafluorophenyl)borane on the catalytic activity of catalyst 2

The Lewis acidity of boron compounds has been exploited recently by Bazan *et al.*²³ to modify the electrophilicity of Ni(II) complexes in ethylene oligomerisation and polymerisation. They recently reported that the catalyst $[(C_6H_5)_2PC_6H_4C-(OB(C_6F_5)_3O-\kappa^2P,O)Ni(\eta^3-CH_2CMeCH_2)]$ displays an activity towards ethylene polymerisation orders of magnitude greater than the precursor $[(C_6H_5)_2PC_6H_4C-(O)O-\kappa^2P,O]Ni(\eta^3-CH_2CMeCH_2)$. They attributed this to decreased electron density at the metal centre owing to the Lewis acidity of $B(C_6F_5)_3$. In this contribution, preliminary investigations indicate that the addition of $B(C_6F_5)_3$ to the catalyst precursor **2** and MAO enhances the activity of this catalyst system. Table 3.3 (entries 3 and 4) shows an eight fold increase in activity of catalyst **2** upon incorporation of $B(C_6F_5)_3$, 62 kg/mol·h and 462 kg/mol·h respectively.

From Table 3.4, it is also evident that the addition of $B(C_6F_5)_3$ to the catalyst precursor **2** results in decreased molecular weight, entries 3 and 4. This indicates increased chain transfer to the aluminium adducts due to the bulkier phenyl groups consistent with the trend already observed in catalysts **1**, **2**, **3** and **4**.

Table 3.3 The effect of $B(C_6F_5)_3$ on ethylene polymerisation using complex **2**^a

Entry	Catalyst	Al:Pd	$M_w \times 10^5$	$M_n \times 10^5$	M_w/M_n^c	TON ^d
1	2	500:1	3.30	1.71	1.93	24
2	2 ^b	500:1	2.73	1.34	1.94	48
3	2 ^b	1000:1	5.83	2.89	2.01	62
4	2	1000:1	4.19	2.06	2.07	462

^aPolymerisation conditions: temperature, 50 °C, pressure, 5 atm, time 2 h.

^bComplex **2** plus 2 eq. of $B(C_6F_5)_3$.

^cPolydispersity index determined by GPC based on polystyrene standards.

^dThe turn-over number in kg/mol of catalyst per h determined by the total mass of polymer produced.

The polymers obtained in all cases showed one peak at around 30.02 ppm in the ^{13}C NMR spectra, Figure 3.3, indicating the production of High Density Linear Polyethylene (HDLPE). This confirms the absence of chain walking during polymerisation process.⁹ The molecular weight average M_w of the polymers produced were in the range of 2.73 to 8.41×10^5 , characteristic of high molecular weight polyethylene.

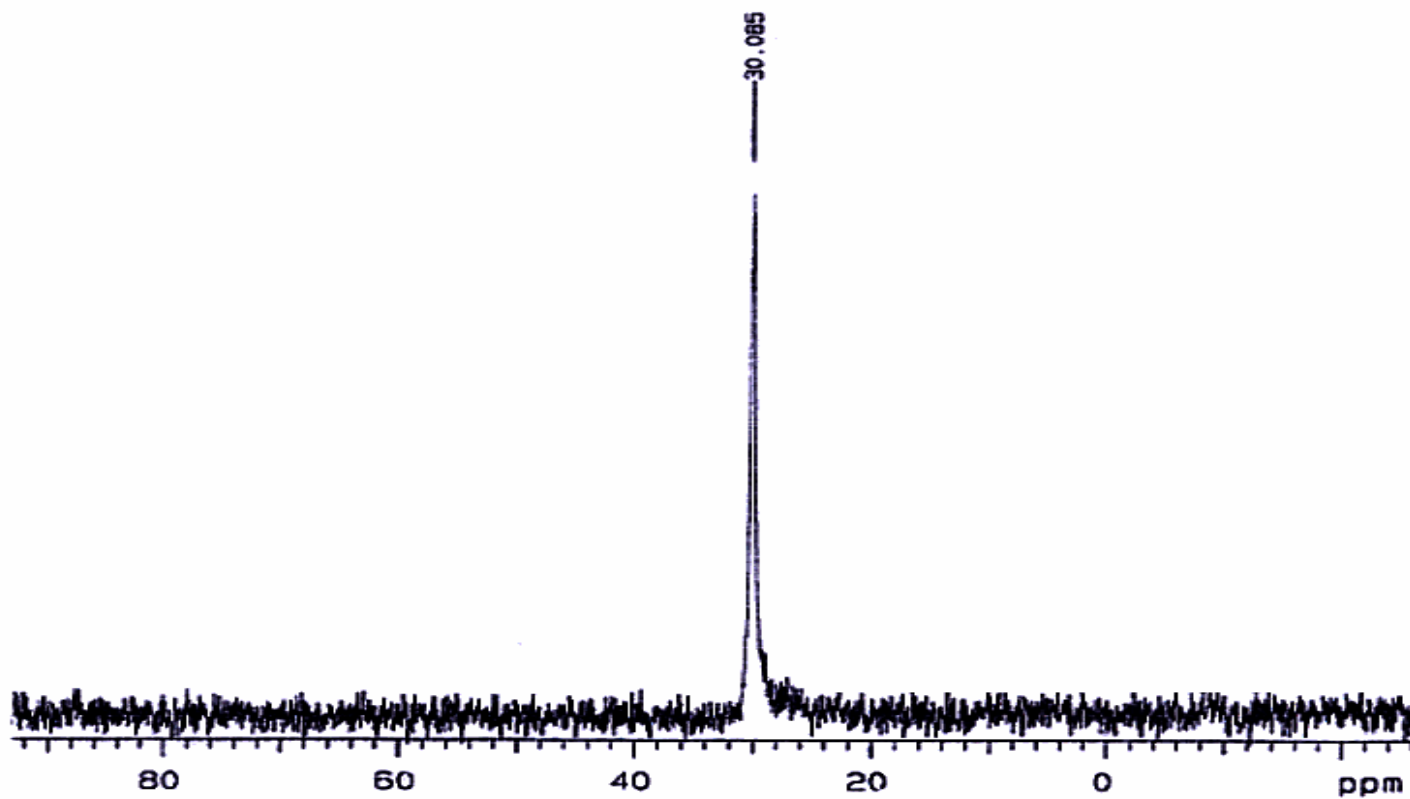


Figure 3.3: ^{13}C NMR spectrum of polyethylene produced at Al:Pd of 4000:1, 5 atm, 50 °C for 2 h.

3.3.4 Evaluation of complexes 1 to 5 as catalysts for ethylene oligomerisation

To investigate the role played by various aluminium compounds as catalytic activators, we also used ethylaluminium dichloride to form the active catalysts from complexes **1-4** and **8**. Interestingly only oligomers were obtained as opposed to the polymers when MAO is used. Table 3.4 shows the oligomerisation data obtained using complexes **1-4** and **8**. We found that the ligand structure influences both the catalyst activity and the product distributions. Complex **1** (furan analogue) with the methyl groups is less active (TON = 60 kg per mol Pd per h) than complex **3** with the *tert*-butyl substituents (TON = 70 kg per mol Pd per h). A similar trend is observed for the thiophene analogues, Table 3.4 entries 2 and 5. Catalyst **8**, bearing the phenyl substituent was found to be the most active.

Table 3.4 Effect of catalyst system on ethylene oligomerisation^a

Entry	Catalyst	Oligomers (%) ^d			Yield (g) ^b	TON ^c
		C ₁₀	C ₁₂	C ₁₄₊		
1	1	38	59	3	1.15	62
2	2	66	30	4	1.00	54
3	3	45	52	3	1.29	70
4	4	54	41	5	1.05	56
5	8	34	61	5	1.36	73
6	8^e	30	64	6	2.97	124

^aReaction conditions: solvent, toluene (50 mL); pressure 5 atm; temperature, 25 °C; time 2 h; amount of catalyst 9.00 µm Al: Pd, 500; ^bYield of products determined by total mass of oligomers produced after solvent evaporation.

^cTurn over number expressed as kg of total product produced per mole of catalyst per hour.

^dProduct distribution determined by gas chromatography-mass spectrometry (GC-MS).

^eAl: Pd, 1000:1.

A similar observation has been reported by Guan *et al.*²⁴ when investigating the catalytic behaviour of the Pd(II) complexes based on phosphine-imine ligands. The phenyl

analogue gave a turn-over number of 17 200 kg per mol.of catalyst per hour as compared to 960 and 1 670 kg per mol of catalyst per hour for the methyl and *tert*-butyl analogues respectively, a trend attributed to the difference in electronic structure of the complexes. The *tert*-butyl group has a stronger donor ability than the phenyl group leading to higher electron density on the metal centre. This postulate could explain the low activity observed in complex **4** as compared to complex **8** with the phenyl substituents in this work.²⁵

The nature of the linker in the ligand systems appears to have some effect on the oligomer distribution. For example, the catalysts with furoyl linkers gave higher percentages of the C₁₂ than C₁₀ oligomers (Table 3.4 entries 1 and 3) whereas the thiophene carbonyl analogues gave higher percentage of C₁₀ than C₁₂ (Table 3.4 entries 2 and 4). There was however, no clear trend in oligomer distribution as the steric bulk of the ligands in the catalysts changed.

3.3.5 Effect of co-catalyst (EtAlCl₂) concentration on ethylene oligomerisation

EtAlCl₂ to palladium ratio was varied to establish the optimum ratio of Al:Pd for ethylene oligomerisation using catalyst **2**. No activity was observed for Al:Pd ratio below 20. This indicates that no activation process occurs at below this ratio. Increase in Al:Pd from 20 to 1000 resulted in a general increase in oligomer yield, Figure 3.5. The optimum value of 1000 was obtained. Beyond this ratio, the yield was observed to decrease (Table 3.5 entry 6). Catalyst **1**, the furan analogue shows the same trend (Table 3.4, entries 7 and 8). A similar trend has been reported by Speiser *et al.*²⁶ in ethylene oligomerisation using

phosphinitooxazoline and pyridine Ni(II) complexes where an increase in EtAlCl₂:Ni ratio from 1.3 to 6 resulted in a significant increase in turn-over frequency from 11 600 to 49 000 mol C₂H₄ per mol of Ni per hour.

Table 3.5. Effect of co-catalyst (EtAlCl₂) concentration on ethylene oligomerisation^a

Entry	Al : Pd	Oligomers (%) ^d			Yield (g) ^b	TON ^c
		C ₁₀	C ₁₂	C ₁₄₊		
1	20	-	-	-	trace	-
2	50	49	45	6	0.21	10
3	100	57	38	5	0.41	21
4	500	66	30	4	1.00	54
5	1000	65	30	5	1.66	94
6	2000	66	29	5	1.19	64
7	500 ^e	38	59	3	1.15	62
8	1000 ^e	50	45	5	2.10	110

^aReaction conditions: solvent, toluene (50 mL); pressure 5 atm; temperature, 25 °C; time 2 h; amount of catalyst 9.00 μm, catalyst **2**.

^bYield of products determined by total mass of oligomers produced after solvent evaporation

^cTurn over number expressed as kg of total product produced per mole of catalyst per h.

^dProduct distribution determined by gas chromatography-mass spectrometry (GC-MS). ^eCatalyst

1.

In this study, we also observed that higher Al:Pd ratio resulted in an increase in the percentage of lower oligomers (C₁₀) as compared to higher oligomers (C₁₂), Table 3.5. For instance at Al:Pd of 50, 49% of C₁₀ and 45% of C₁₂ were produced. While at Al:Pd of 1000, 66% of C₁₀ and 30% of C₁₂ were produced. It is unclear to us why the changes in co-catalyst to catalyst ratio affect product distribution.

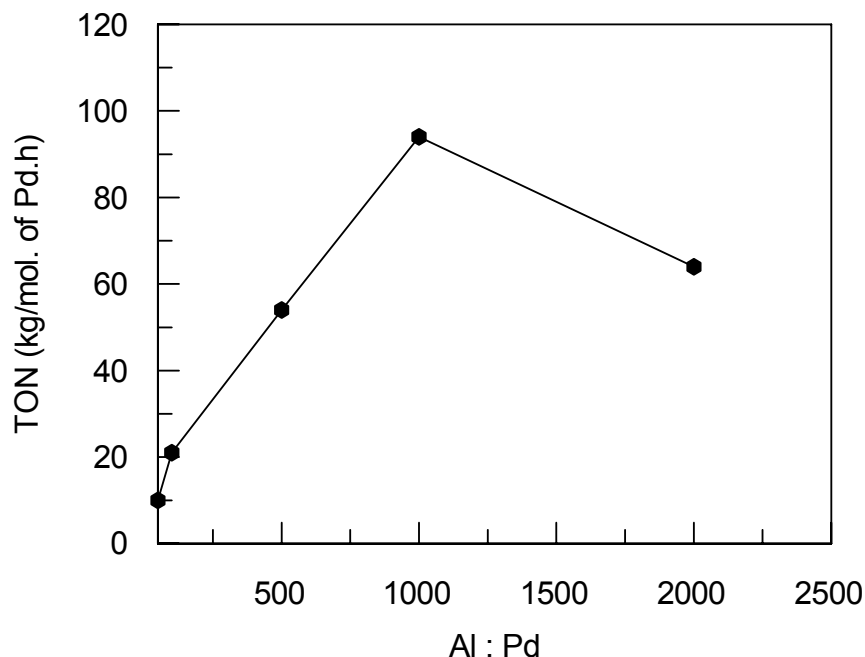


Figure 3.4: The effect of Al:Pd on monomer conversion run at 25 °C, 5 atm for 2 h using catalyst 2.

3.3.6 Effect of reaction time on ethylene oligomerisation

Reaction time is known to have a profound effect on catalyst activity. This is due to the stability of the active catalyst species in solution. In this work, we investigated the effect of time in ethylene oligomerisation activity using catalyst **1** at 25 °C, 5 atm and Al:Pd ratio of 500. Longer reaction times resulted in a significant decrease in turnover number, Figure 3.6, an indication of catalyst decomposition even at room temperature. The maximum turnover number (177 kg per mol. of Pd per h) was obtained after 30 min, (Table 3.6 entry 2). After 15 min, it is evident that the initiation process to produce the active species is still incomplete resulting in lower yields, (120 kg per mol Pd per h). The yields reported for 1 h and 2 h runs (1.27 and 1.30 g respectively) are almost comparable signifying a near complete catalyst decomposition of the active species after 1 h. A similar trend was obtained for catalyst **8** (Table 3.6, entries 5 and 6). Brookhart *et al.*²⁷

observed the same phenomena in ethylene oligomerisation using cationic Ni(II) and Pd(II) complexes containing bidentate phenacyldiarylphosphine ligands where after 15 min, only 10 mg of oligomer (TOF = $1.2 \times 10^3 \text{ h}^{-1}$) was obtained. However, at 30, 45 min and 1 h, oligomer yields increased to 170 mg (TOF = $8.2 \times 10^3 \text{ h}^{-1}$), 720 mg (TOF = $2.3 \times 10^4 \text{ h}^{-1}$) and 2170 mg (TOF = $5.3 \times 10^4 \text{ h}^{-1}$) respectively. These results show an increase in the number of active sites with time. After 3 h run, the activity dropped to $3.3 \times 10^4 \text{ h}^{-1}$ indicating catalyst decomposition.

Table 3.6 Effect of reaction time on ethylene oligomerisation.^a

Entry	Time (min)	Oligomers (%) ^d			Yield (g) ^b	TON ^c
		C ₁₀	C ₁₂	C ₁₄₊		
1	15	77	20	3	0.28	120
2	30	71	25	4	0.82	177
3	60	58	38	4	1.27	137
4	120	38	59	3	1.30	70
5	30 ^e	70	24	6	0.93	200
6	60 ^e	54	41	5	1.40	151

^aReaction conditions: solvent, toluene (50 mL); pressure 5 atm; temperature, 25 °C; amount of catalyst 9.00 μm Al/Pd 500, catalyst **1**.

^bYield of products determined by total mass of oligomers produced after solvent evaporation.

^cTurn-over number expressed as kg of total product produced per mole of catalyst per hour.

^dProduct distribution determined by gas chromatography-mass spectrometry (GC-MS).

^eCatalyst **8**.

Reaction time was also found to have a profound effect on the nature of the oligomers formed. A high percentage of lower olefins i.e C₁₀ (77%) was obtained for the 15 min run as compared to 38% for the 2 h run (Table 3.6, entries 1 and 4). This indicates increasing oligomer molecular weight with time. This could be due to co-oligomerisation of the released matured oligomers with time hence production of higher oligomers. Daugalis *et al.*²⁵ however, reported an opposite trend with phosphinidine Pd(II) complexes. In their

work, an increase in reaction time from 3 h to 15 h resulted in reduced oligomer molecular weight from 215 to 180.

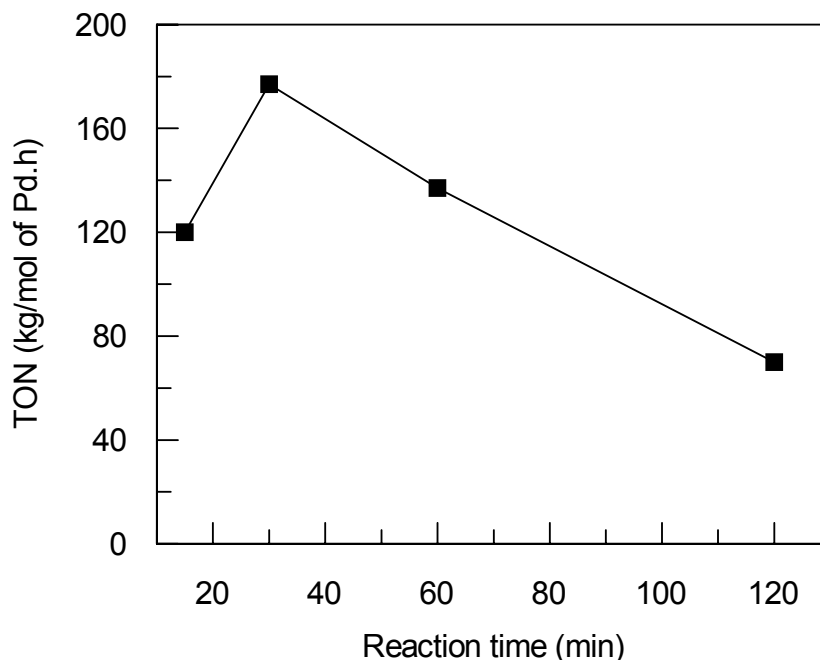


Fig. 3.5 The effect of reaction time on monomer conversion run at 25 °C, 5 atm, Al:Pd, 500 using catalyst **1**.

3.3.7 Effect of temperature on ethylene oligomerisation

The temperature dependence of ethylene oligomerisation was investigated using catalyst **1**. The productivity of this catalyst increases initially with temperature and reaches a maximum at around 60 °C, Figure 3.6. This could be due to increased monomer insertion with increase in temperature. Beyond 60 °C, the activity drops (Table 3.7 entries 4 and 5), indicating catalyst deactivation at higher temperatures. This is consistent with Pd(II) α -diimine catalysts which are known to decompose rapidly at about 50 °C.^{6,9,12} Guan *et al.*²⁸ observed a similar trend with bis-azaferrocene Pd(II) complexes and obtained a maximum activity at 80 °C. Contrary to the Pd(II) α -diimine catalysts, they found that

these catalysts remain active even at 120 °C to oligomerise ethylene for several hours. There was, however, no significant effect of temperature on the identity of the oligomers produced (Table 3.7, entries 3 and 4).

Table 3.7 Effect of reaction temperature on ethylene oligomerisation^a on catalyst 1.

Entry	Temp (°C)	<u>Oligomers (%)</u> ^d			Yield (g) ^b	TON ^c
		C ₁₀	C ₁₂	C ₁₄₊		
1	25	71	25	4	0.82	177
2	40	36	61	3	1.60	345
3	50	34	64	2	2.95	635
4	60	32	64	4	4.86	1050
5	70	33	62	5	3.15	680

^aReaction conditions: solvent, toluene (50 mL); pressure 5 atm; time, 30 min; amount of catalyst 9.00 µm Al:Pd 500.

^bYield of products determined by total mass of oligomers produced after solvent evaporation

^cTurn-over number expressed as kg of total product produced per mole of catalyst per hour.

^dProduct distribution determined by gas chromatography-mass spectrometry (GC-MS).

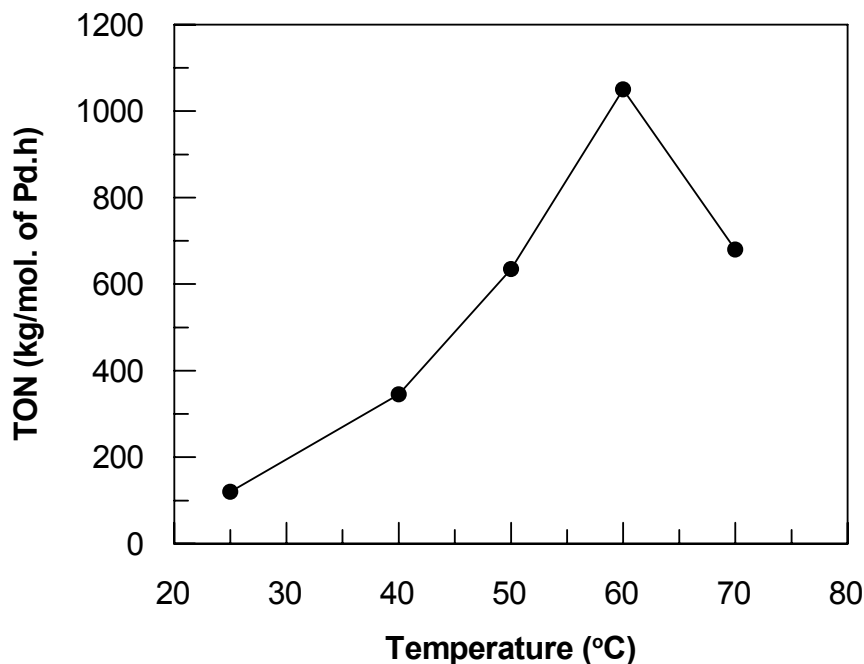


Figure 3.6: Effect of temperature on the activity of catalyst **1** run at 5 atm for 30 min, Al:Pd, 500

3.3.8 Effect of ethylene pressure on oligomerisation

The influence of pressure on ethylene oligomerisation is well established, especially on catalytic activity.^{6, 9} Here, we investigated the effect of ethylene concentration on oligomerisation using catalyst **1** by varying the ethylene pressure from 5 to 35 atm (Table 3.8). An increase in ethylene concentration resulted in a significant increase in oligomer yield, Figure 3.7. This could be ascribed to increased local concentration of ethylene hence enhanced monomer insertion.

Table 3.8 Effect of monomer concentration on ethylene oligomerisation.^a

Entry	Pressure (atm)	Oligomers (%) ^d			Yield (g) ^b	TON ^c
		C ₁₀	C ₁₂	C ₁₄₊		
1	5	71	23	3	0.28	175
2	10	61	36	3	1.00	216
3	20	51	44	5	1.28	276
4	30	52	45	4	2.03	438
5	35	48	41	11	2.56	542

^aReaction conditions: solvent, toluene (50 mL); temp 25 °C; time, 30 min; amount of catalyst 9.00 μm Al: Pd 500, catalyst **1**.

^bYield of products determined by total mass of oligomers produced after solvent evaporation

^cTurn-over number expressed as kg of total product produced per mole of catalyst per hour.

^dProduct distribution determined by gas chromatography-mass spectrometry (GC-MS).

We also observed selectivity towards higher oligomers with increase in pressure, (Table 3.8). For instance, at 5 atm, 71% of C₁₀ and 23% of C₁₂ were produced respectively, while at 35 atm, 48% of C₁₀ and 41% of C₁₂ were obtained. Under high pressures it has been postulated that ethylene co-oligomerises with the pre-formed olefins resulting in significant increase in molecular weight.⁶ Carlini *et al.*²⁹ observed a similar trend with bis(salicylaldiminate)nickel complexes in ethylene oligomerisation. An increase in

ethylene pressure from 1 to 20 atm resulted in a significant increase of the percentage of higher oligomers (C_6 – C_{12}) from 23 to 70%. While on the hand, there was a drastic drop in the percent composition of butenes from 76 to 30%.

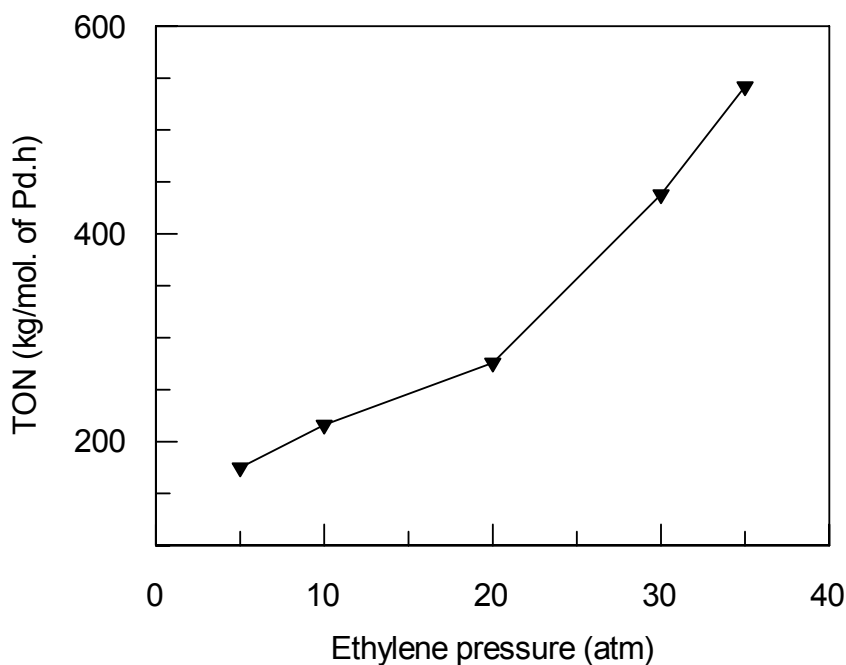


Figure 3.7: The effect of ethylene pressure on turn over number of catalyst **1** run at 25°C, Al:Pd 500 for 30 min.

3.4 Conclusion

Five carbonyl containing pyrazolyl palladium(II) complexes bearing furan and thiophene moieties have been investigated for ethylene oligomerisation and polymerisation catalysis. The complexes give active catalysts for ethylene polymerisation upon activation with MAO, producing high-density linear polyethylene (HDLPE). Activation by the alkyl aluminium compound, $EtAlCl_2$, results in active catalysts for ethylene oligomerisation. The major oligomers produced are C_{10} and C_{12} . No lower oligomers in the C_4 – C_8 range are obtained. This shows that the catalysts favour chain propagation

relative to chain termination consistent with Pd(II) α -diimine complexes abound in literature.

Generally the activities of these heterocyclic carbonyl catalysts are lower compared to the simple pyrazole systems previously investigated and were only active at elevated temperatures. This behaviour is due to the existence of non-coordinating donor atoms, sulfur and oxygen, which might to cause catalyst deactivation by forming adducts with the aluminium co-catalyst. The thermal instability of these catalysts could also contribute to their observed low catalytic activity. It is clear that the activity of these catalysts depend on the nature of the substituents in the ligand system as well as the reaction conditions. It can also be concluded that the dominating factor in controlling the molecular weight, besides reaction conditions is the steric bulk of the ligands. The blocking of the axial coordination site in the metal centre, which according to theoretical calculations is essential for obtaining higher molecular weights is still insufficient since lower molecular weight polymers were obtained with the bulkier substituent groups.

3.5 References

1. (a) S. Mecking, *Coord. Chem. Rev.* **203** (2000) 325. (b) W. Kaminsky, H. Sinn (eds) *Transition metals and organometallics as catalysts for olefin polymerisation*, Springer, Berlin (1998).
2. (a) A. M. Thayer, *Chem Eng. News*, **73** (1995) 15. (b) J. D. Scollard, N. C. Payne J. Vittal, *Macromolecules* **29** (1996) 5241.
3. E. Albizzati, M. Galimberti, *Catal. Today* **41** (1998) 159.
4. (a) B. L. Small, M. Brookhart, *J. Am. Chem. Soc.* **120** (1998) 7143. (b) B. Y. Lee, G. C Bazan, J. Vela, Z. J. A. Komon, X. Bu, *J. Am. Chem. Soc.* **123** (2001) 5352.
5. E.Y. Chen, T. J. Marks, *Chem. Rev.* **100** (2000) 1391.
6. J. Skupinska, *Chem Rev.* **91** (1991) 613.
7. (a) W. Keim, *J. Mol. Cat.* **52** (1989) 19. (b) S. Y. Desjardins, K. J. Cavell, H. Jin, B. W. Skelton, A. H. White, *J. Organomet. Chem.* **515** (1996) 233.
8. W. Keim, *Angew. Chem. Int. Ed. Engl.* **17** (1979) 466.
9. S. D. Ittel, M. Brookhart, L. K. Johnson, *Chem. Rev.* **100** (2000) 1169-1203.
10. A. M. al-Jarallah, J. A. Anabtawi, M. B. Siddiqui, A. M. Aitani, *Catal. Today* **14** (1992) 42.
11. B. L. Small, M. Brookhart, *J. Am. Chem. Soc.* **120** (1998) 7129.
12. L. K. Johnson, C. M. Killian, M. Brookhart, *J. Am. Chem. Soc.* **117** (1995) 6414.
13. L. Deng, T. K. Woo, L. Cavallo, P. M. Margl, T. Ziegler, *J. Am. Chem. Soc.* **119** (1997) 6177.
14. L. K. Johnson, C. M. Killian, M. Brookhart, *Organometallics* **16** (1997) 2005.

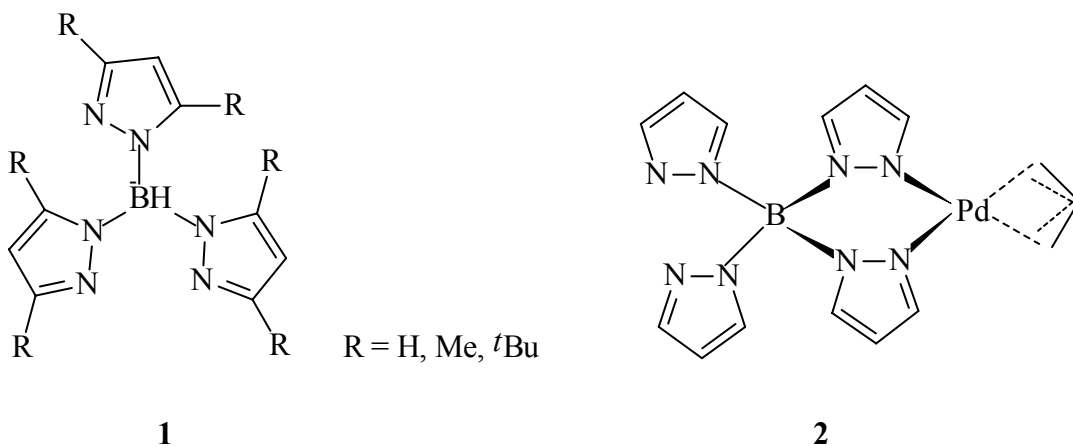
15. G. J. P. Britovsek, S. P. D. Baugh, V. C. Gibson, D. F. Wass, *Angew. Chem. Int. Ed. Engl.* **38** (1999) 428.
16. (a) S. Tsuji, T. R. Younkin, D. C. Swenson, R. F. Jordan, *Organometallics* **18** (1998) 4758. (b) S. Trofimenko, *Chem. Soc.* **72** (1972) 497.
17. (a) K. Li, J. Darkwa, I. A. Guzei, S. F. Mapolie, *J. Organomet. Chem.* **660** (2002) 108. (b) S. M. Nelana, J. Darkwa, I. A. Guzei, S. F. Mapolie, *J. Organomet. Chem.* **689** (2004). 1835.
18. I. A. Guzei, K. Li, G. A. Bikzhanova, J. Darkwa, S. F. Mapolie, *Dalton Trans.* (2003) 715.
19. T. V. Laine, U. Piironen, K. Lappalainen, M. Klinga, E. Aitola, M. Leskela, *J. Organomet. Chem.* **606** (2000) 112.
20. Y. Lee, Y. Dong, H. Yun, *Organometallics* **22** (2003) 4272.
21. O. Daugulis, M. Brookhart, *Organometallics* **21** (2002) 5926.
22. Y. Chen, R. Chen, C. Qian, X. Dong, J. Sun, *Organometallics* **22** (2003) 4312.
23. (a) Z. J. A. Komon, X. Bu, G. C. Bazan, *J. Am. Chem. Soc.* **122** (2000) 12379. (b) Z. J. A. Komon, X. Bu, G. C. Bazan, *J. Am. Chem. Soc.* **122** (2000) 1830.
24. Z. Guan, W. J. Marshall, *Organometallics* **21** (2002) 3580.
25. O. Daugulis, M. Brookhart, P. S. White, *Organometallics* **21** (2002) 5935.
26. F. Speiser, P. Braunstein, L. Saussine, R. Welter, *Inorg. Chem.* **43** (2004) 1649.
27. J. M. Malinoski, M. Brookhart, *Organometallics* **22** (2003) 5324.
28. Z. Guan, E. V. Salo, *Organometallics* **22** (2003) 5033.
29. C. Carlini, M. Isola, V. Liuzzo, A. M. R. Galletti, G. Sbrana, *App. Catal. A. Gen.* **231** (2002) 307.

CHAPTER 4

Synthesis and characterisation of bis(pyrazolyl)acetic acid ligands and their palladium(II) complexes

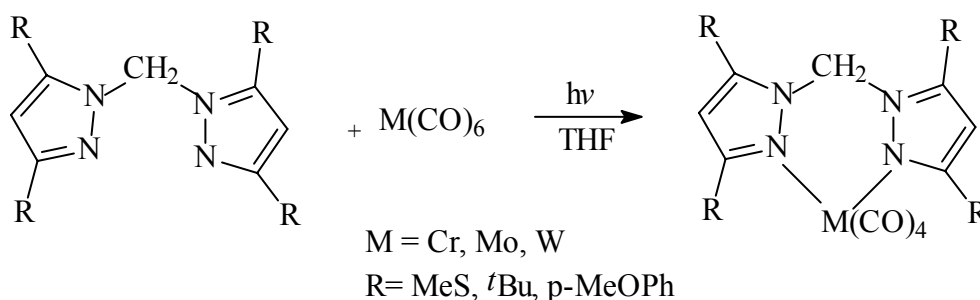
4.1 Introduction

Since the discovery of poly(pyrazolyl)borates or “scorpionate” ligands by Trofimenko in the 1960s, a vast number of the metal complexes of these ligands have been reported.¹ The tris(pyrazol-1-yl)borate compound, **1**, represents such ligands that are now widely used in the metal carbonyl chemistry.² Some of the current studies involving these ligands are focused on the electron donating ability of the tris(pyrazolyl)borates. Recently, a review article has appeared on the organometallic chemistry of palladium and platinum with poly(pyrazolyl)alkanes.³ Reedjik⁴ in his article, *Heterocyclic Nitrogen Donor Ligands*, provided a survey of the coordination chemistry of various kinds of nitrogen heterocyclic ligand systems.



The coordination chemistry of these ligands, poly(pyrazolyl)borates, with Group 8 metals have also been reported.⁴ Examples of bidentate, and bis-bidentate coordination in Pd(II)

complexes were obtained by the reaction of K[tris(pyrazolyl)borate] with $[\eta^3\text{-allyl}]\text{PdCl}_2$ giving compound **2**.⁵ Following the first report on poly(pyrazol-1-yl)alkanes in 1970s⁷ and improved synthetic methods by Elguero *et al.*⁸, the coordination chemistry of these ligands has received significant attention.⁹ Recently, numerous main group¹⁰ and transition metal¹¹ complexes containing poly(pyrazol-1-yl)alkanes have been synthesised. Tang and co-workers¹² recently reported the synthesis of Group 6 metal carbonyl complexes containing S-rich bis(pyrazol-1-yl)methane ligands, Scheme 4.1. Carrano *et al.*¹³ have also reported the synthesis and crystal structure of Cu(II) acetate complex of the heteroscorpionate ligand, 2-(hydroxy-3-*t*-butyl-methylphenyl)bis(3,5-dimethylpyrazol-1-yl)methane.

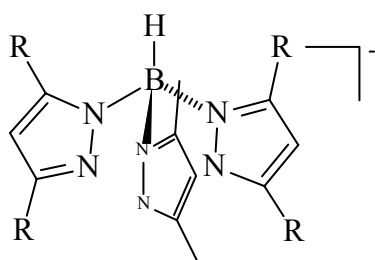


Scheme 4.1

These main group and transition metal complexes containing poly(pyrazol-1-yl)alkanes have good physical and chemical properties and their development involving improved synthetic methods is continuously being explored. Their wide applications in transition metal chemistry, bioinorganic and organometallic are of great interest today.^{14, 15}

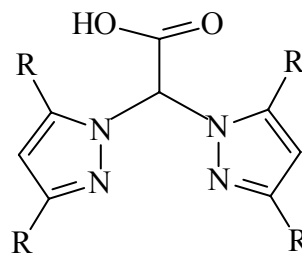
The potential of poly(pyrazolyl)borate complexes as catalysts for olefin polymerization has been explored.¹⁶ Like all olefin polymerization catalysts, the Groups 3 and 4 catalysts

are less suited for functionalized monomers like methyl acrylates than their group 5 analogues.¹⁷ A report by Etienne *et al.*¹⁸ on the Nb complexes based on ligand hydrotris(pyrazolyl)borate, **3**, shows that when these complexes are activated with $B(C_6F_5)_3$, they catalyze ethylene polymerization with catalytic activities of 20 to 100 kg per mol per h.



3

R = H, Me



4

The ease of synthesis of different substituted pyrazole and pyrazolyl ligands is the most fundamental feature in the incorporation of pyrazole groups in the design of new ligands. This property is instrumental in their ligand design since it offers the opportunity to control both the steric and electronic properties of the metal complexes. Recently, Otero *et al.*¹⁹ reported the synthesis of bis(pyrazolyl)acetate ligand, **4**. This ligand system offers less steric hindrance as compared to compound **1** hence could possess considerable coordinative flexibility. We developed an interest in this ligand due to the presence of carboxylate group, which could impart some water solubility significant in biological activity. Despite extensive reports on these ligands with the metal carbonyls of Group 5 transition metals,^{1,2} their palladium(II) complexes have never been reported.

In this chapter we report the synthesis of some bis(pyrazolyl)acetic acid ligands and their respective Pd(II) complexes. The dependent of the acidity of these compounds on the pyrazolyl substituents is also reported. Finally we investigate the ability of these ligands to undergo the classical esterification reactions.

4.2 Materials and methods

All experimental and analytical manipulations were carried out as earlier described in Chapter 2, section 2.2. All the chemicals, dibromoacetic acid, pyrazoles, KOH, NaOH, K₂CO₃, HCl and benzyltriethylammonium chloride were of analytical grade and used as received. THF was dried and distilled under inert atmosphere using sodium and benzophenone. Diethyl ether, acetone and acetonitrile were obtained from Merck and used as received.

4.3 Synthesis of pyrazolyl acetic acid ligands and their palladium(II) complexes

4.3.1. Synthesis of bis(pyrazol-1-yl)acetic acid (L14)

To a basic solution containing KOH (8.00 g, 142.85 mmol) and K₂CO₃ (19.70 g, 142.50 mmol) in THF (100 mL), pyrazole (2.50 g, 36.76 mmol), dibromoacetic acid (4.00 g, 18.43 mmol) and benzyltriethylammonium chloride (1.00 g), as a phase transfer catalyst, were added. The solution was refluxed for 15 h after which the solvent was removed in *vacuo* to obtain a yellowish powder. The residue was dissolved in deionised water (50 mL) and acidified to a pH of 2 with 5M HCl. The product was extracted with diethyl ether (6 × 50 mL) and the solvent evaporated in *vacuo* to obtain an analytically pure compound. Yield = 2.92 g (82 %). ¹H NMR (DMSO-d₆): δ 6.32 (t, 2H, pz, ³J_{HH} = 2.2 Hz); 7.55 (s, 2H, pz, 1H, CH); 7.95 (d, 2H, pz, ³J_{HH} = 2.2 Hz). ¹³C{¹H} NMR

(DMSO-d₆): δ 73.9; 106.5; 131.0; 140.1; 166.2; IR (nujol cm⁻¹): $\nu_{(C=O)}$ = 1727; $\nu_{(O-H)}$ = 3439.

4.3.2 Synthesis of bis(3,5-dimethylpyrazol-1-yl)acetic acid (L15)

This ligand, **L15**, was synthesised using the same procedure as described above for **L14**. KOH (8.01 g, 140.12 mmol), K₂CO₃ (19.98 g, 141.00 mmol), THF (150 mL), 3,5-dimethylpyrazole (3.57 g, 37.20 mmol), dibromoacetic acid (4.01 g, 18.60 mmol), and benzyltriethylammonium chloride (1.00 g). Yield = 1.40 g (40 %). ¹H NMR (CDCl₃): δ 2.23 (s, 12H, CH₃, pz); 5.89 (s, 1H, pz); 6.75 (s, 1H, CH); 7.30 (br, 1H, OH). ¹³C{¹H} NMR (DMSO-d₆): δ 11.0; 13.4; 71.7; 106.6; 140.8; 147.0; 166.1. IR (Nujol cm⁻¹): $\nu_{(C=O)}$ = 1741, $\nu_{(O-H)}$ = 3402.

4.3.3 Synthesis of bis(3,5-di-tertiarybutylpyrazol-1-yl)acetic acid (L16)

This compound was prepared in the same way as **L14**, but using 3,5-ditertiarybutylpyrazole (3.50 g, 19.44 mmol), dibromoacetic acid (2.00 g, 9.60 mmol) KOH (8.20 g, 142.65 mmol) and K₂CO₃ (19.10 g, 141.50 mmol) and benzyltriethylammonium chloride (1.00 g). Yield = 1.94 g (48%). ¹H NMR (CDCl₃): δ 1.21 (s, 18H, ^tBu, pz); 1.26 (s, 18H, ^tBu, pz); 5.91 (s, 1H, pz); 6.52 (s, 1H, CH). ¹³C{¹H} NMR (CDCl₃): δ 29.3; 29.9; 31.4; 66.0; 101.3; 152.5; 158.6 IR (Nujol cm⁻¹): $\nu_{(C=O)}$ = 1712, $\nu_{(O-H)}$ = 3424. EIMS (70 eV, 260 °C). m/z (%) = 415 (18) [M⁺]; 359 (15) [M⁺-C₄H₉]; 299 (100) [M⁺-C₈H₁₈]; 281 (50) [M⁺-C₈H₁₁ OH].

4.3.4. Synthesis of bis(pyrazol-1-yl)ethyl acetate (L17)

Esterification reaction between **L14** and ethanol produced the above compound, **L17**. This was carried out by reacting **L14** (0.50 g, 2.6 mmol) and excess ethanol (40 mL) under acidic conditions (HCl, 5 mL). The mixture was refluxed for 18 h. After cooling the mixture to room temperature, 50 mL of deionised water was added and the pH adjusted to alkaline by using sodium hydrogen carbonate. The organic phase was extracted using dichloromethane (50 mL). The solvent was then removed in *vacuo* to afford an analytically pure white crystalline material. Yield = 0.33 g (58 %). ^1H NMR (CDCl_3): δ 1.26 (t, 3H, Et, $^2J_{\text{HH}} = 7.4$ Hz); 4.34 (q 2H, Et, $^2J_{\text{HH}} = 7.4$ Hz); 6.33 (t 2H, pz $^2J_{\text{HH}} = 1.8$ Hz); 7.10 (s, CH, 1H, pz,); 7.59 (t, 2H, pz, $^2J_{\text{HH}} = 1.6$ Hz,) 7.74 (d, 2H, pz, $^2J_{\text{HH}} = 2.2$ Hz). $^{13}\text{C}\{^1\text{H}\}$ NMR (CDCl_3): δ 13.4; 62.7; 74.1; 106.8; 129.6; 140.4; 163.8; . EIMS (70 eV, 260°C). m/z (%) = 221 (2) [M^+]; 147 (100) [$\text{M}^+ - \text{C}_2\text{O}_2\text{H}_5$]; IR (Nujol cm^{-1}): $\nu_{(\text{C}=\text{O})} = 1750$.

4.3.5 Dichloro{bis(pyrazol-1-yl)acetic acid }palladium(II) (9)

This compound was prepared by dissolving **L14** (0.10 g, 0.52 mmol) in THF (20 mL), to which $\text{Pd}(\text{NCMe})_2\text{Cl}_2$ (0.13 g, 0.50 mmol) was added. A yellow precipitate was observed immediately. The mixture was stirred for 6 h, filtered and the solid residue dried to afford an analytically pure complex. Yield = 0.15 g; (75%). ^1H NMR (DMSO-d_6) δ 6.63 (t 2H, pz $^2J_{\text{HH}} = 2.6$ Hz); 8.02 (d, 2H, pz $^2J_{\text{HH}} = 1.8$ Hz); 8.14 (s, 1H, CH,) 8.29 (t, 2H, pz, $^2J_{\text{HH}} = 2.6$ Hz). $^{13}\text{C}\{^1\text{H}\}$ NMR (DMSO-d_6): δ 67.0; 107.4; 136.3; 143.9; 164.4; IR (Nujol cm^{-1}): $\nu_{(\text{C}=\text{O})} = 1738$, $\nu_{(\text{O}-\text{H})} = 3441$.

4.3.6 *Dichloro{bis(3,5-dimethylpyrazol-1-yl)acetic acid}palladium(II) (10)*

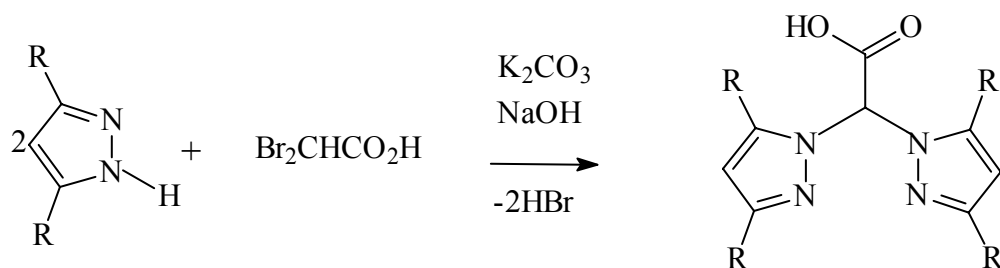
This complex, **10**, was synthesised in a similar way as **9** but using **L15** (0.13 g, 0.60 mmol) in dichloromethane (20 mL) and PdCl₂(NCMe)₂ (0.15 g, 0.58 mmol). Yield = 0.10 g; (45%). ¹H NMR (DMSO-d₆): δ 2.31 (s, 6H, CH₃, pz); 2.42 (s, 6H, CH₃, pz); 5.61 (s, H, CH); 6.04 (s, 2H, pz). IR (Nujol cm⁻¹) ν_(C=O) = 1756; ν_(O-H) = 3410. Anal. Calc. C₁₂H₁₆N₄O₂PdCl₂·0.5CH₂Cl₂; C, 32.25; H, 3.23; N, 12.04 %. Found. C, 32.27; H, 3.41; N, 12.25 %.

4.3.7 *Dichloro{bis(3,5-ditertiarybutylpyrazol-1-yl acetic acid}palladium(II) (11)*

This complex was prepared by dissolving **L16** (0.31 g, 0.72 mmol) and PdCl₂(NCMe)₂ (0.19 g, 0.72 mmol) in dichloromethane (20 mL). The mixture was stirred for 6 h. After the reaction period, the solution was concentrated and recrystallization from CH₂Cl₂-hexane produced an analytically pure compound. Yield = 0.21 g (50%). ¹H NMR (CDCl₃): δ 1.48 (s, 18H, pz); 1.68 (s, 18H, pz); 6.08 (s, 2H, pz); 6.85 (d, H, CH, ²J_{HH} = 14.2 Hz); 8.54 (d, 1H, OH, ²J_{HH} = 14.2 Hz). ¹³C{¹H} NMR (CDCl₃): δ 30.5; 30.8; 32.1; 32.6; 63.0; 105.5; 155.4; 166.2 IR (Nujol cm⁻¹) ν_(C=O) = 1701; ν_(O-H) = 3451. Anal. Calc. C₂₄H₄₀N₄O₂PdCl₂·2NCMe; C, 49.85; H, 6.82; N, 12.33 %. Found. C, 50.01; H, 7.01; N, 9.92 %.

4.4 Results and discussion

The bis(pyrazolyl)acetic acid ligands, **L14-L16**, were synthesised according to literature methods¹⁹ by phase transfer catalyzed reaction of an appropriate pyrazole and dibromoacetic acid in moderate yields. This one step synthetic route was developed by Burzlaff and co-workers,²⁰ Scheme 4.2, as an alternative procedure to the multi step method reported by Otero *et al.*²¹ which could not be used to synthesise the non-substituted pyrazole. Longer reactions periods, 15 h as opposed to 6 h in the literature, were employed and the yields obtained were slightly higher (82%) for **L14** to those already reported (64 %).²⁰ Maximum extraction of the product from the aqueous phase was obtained after three steps compared to the six steps reported by Burzlaff and the group.²⁰



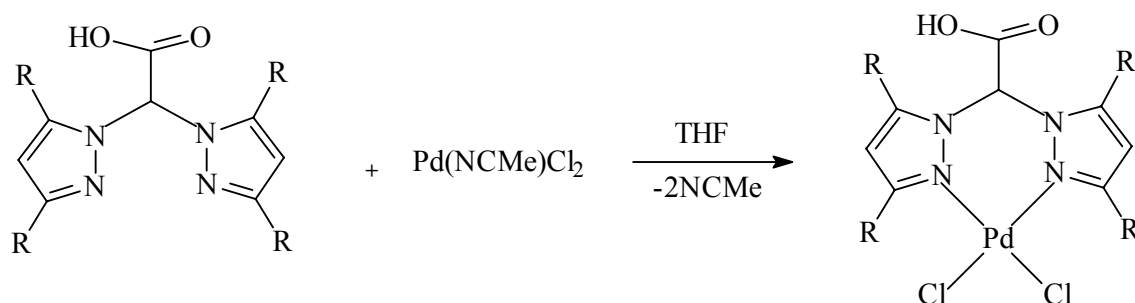
Compound	R
L14	H
L15	Me
L16	^t Bu

Scheme 4.2

The methyl and di-*tert*-butyl analogues, **L15** and **L16**, were obtained in relatively low yields (40% and 48%) respectively but are comparable to those reported in literature (45%).²⁰ **L16** was relatively less soluble in water and highly soluble in organic solvents,

both chlorinated and non-chlorinated, and maximum extraction from the aqueous phase was achieved in one step as compared to three for ligand **L14** and **L15**.

To investigate the ability of these ligands to stabilize palladium complexes, they were reacted with $\text{Pd}(\text{NCMe})_2\text{Cl}_2$ as the metal precursor. Complexes **9**, **10** and **11** were synthesised by reacting **L14** and **L15** with $\text{PdCl}_2(\text{NCMe})_2$ in a 1:1 ratio in THF (20 mL), Scheme 4.3. A yellow precipitate formed immediately in the case of complexes **9** and **10** indicating the insolubility of these complexes in THF. The mixtures were stirred for 6 h after which the precipitates formed were isolated by filtration and dried to afford analytically pure compounds **9** and **10** in good yields (75% and 45% respectively). Analytically pure compound, **11**, was obtained upon recrystallization from $\text{CH}_2\text{Cl}_2/\text{Hexane}$ in moderate yield (50%). The solubility of this complex in polar organic solvents like dichloromethane is attributed to the bulkier tertiary butyl groups on the pyrazolyl moiety.



Complex	R
9	H
10	Me
11	^t Bu

Scheme 4.3

The compounds synthesised were characterised by a combination of ^1H , ^{13}C NMR and infrared spectroscopic techniques. The IR spectra of ligands **L14**, **L15** and **L16** showed characteristic carbonyl stretching frequencies at around 1727, 1741 and 1712 cm^{-1} respectively. O-H stretching frequencies were observed at 3439, 3402 and 3424 cm^{-1} respectively. The absence of N-H stretching frequency at 3300 cm^{-1} confirmed the formation of the products through the N-H functional group. IR spectra of complexes **9**, **10** and **11** showed significant shifts to higher frequencies as compared to their respective ligands **L14**, **L15** and **L16**. For example, carbonyl stretching frequencies of complexes **9** and **10** were recorded at 1738 and 1756 cm^{-1} compared to 1727 and 1740 cm^{-1} of their corresponding ligands **L14** and **L15**. This confirms the flow of electrons to the metal center hence increased double bond character of the carbonyl group. The same trend was observed for the O-H stretching frequencies, for instance, complex **11** (3451 cm^{-1}) compared to its corresponding ligand, **L16** (3424 cm^{-1}). Figure 4.1 shows the IR spectrum of ligand **L14**.

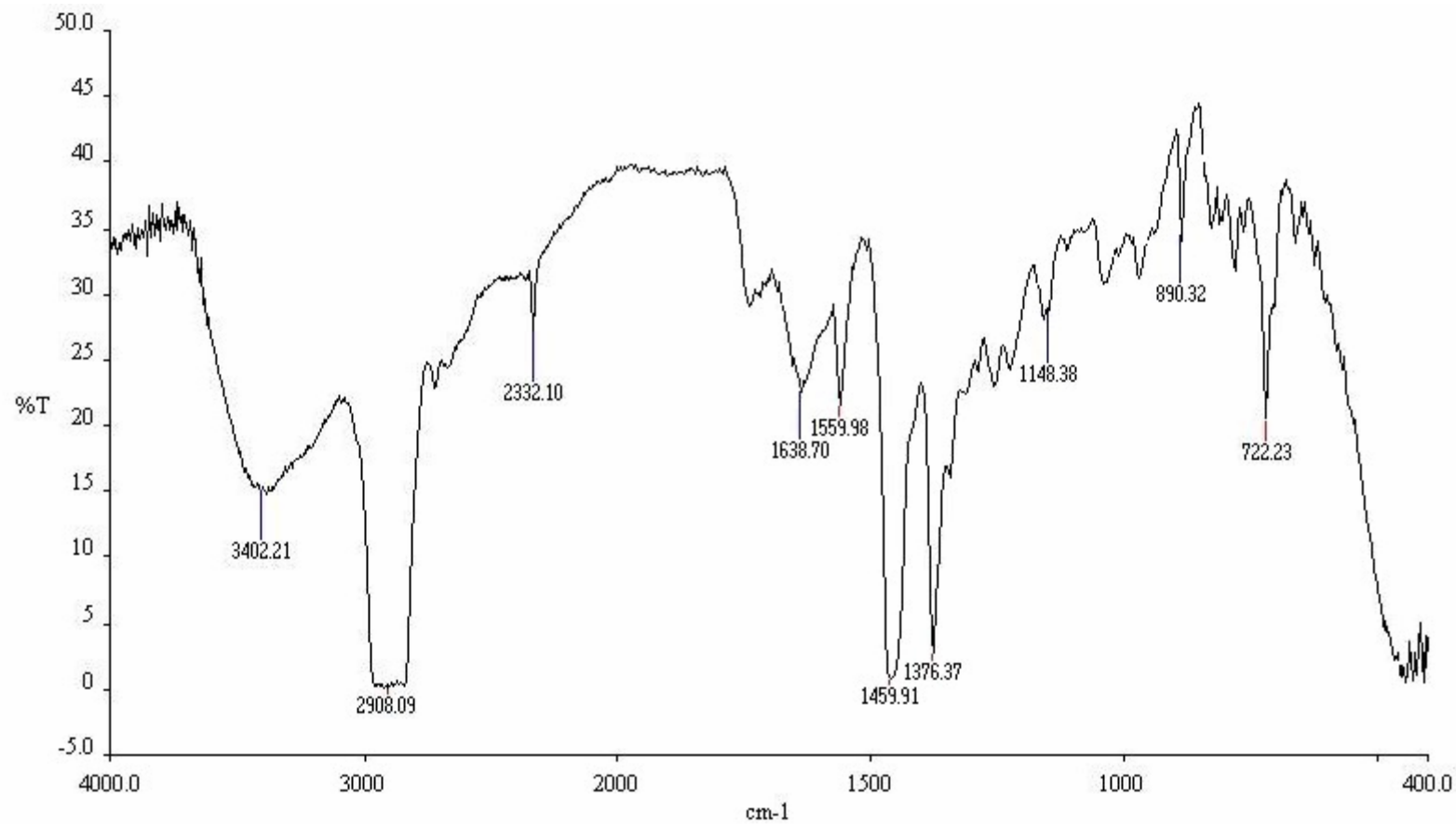


Figure 4.1 Infrared spectrum of bis(pyrazolyl)acetic acid L14.

^1H NMR spectroscopy was also used to characterise all the compounds prepared. The ^1H NMR spectrum of **L14** shows three doublet between 6.31 and 7.95 ppm. The peak at about 6.31 ppm is assigned to the fourth pyrazole protons, while those at 7.54 and 7.94 ppm were assigned to the 3,5 protons respectively. It is interesting to note that the CH proton was observed at the same position as the two 3-pyrazole protons (7.54 ppm). This is in contrast to the earlier reports by Burzlaf *et al*²⁰ who recorded four peaks, one at 7.27 ppm (CH). The deceptive simplicity²² may suggest the effect of the different instrument operating frequencies (200 MHz and 250 MHz). A similar observation is reported in literature for the compound 2,5-dichloronitrobenzene.

^1H NMR spectrum of **L15** and **L16** show characteristic upfield peaks at about 2.23 and 1.24 ppm respectively corresponding to the methyl and ditertiarybutyl groups of the pyrazole system. Two singlets at about 5.90 and 6.86 ppm for **L15** and 5.91 and 6.52 ppm for **L16** were recorded and assigned to the pyrazole and methylene linker protons respectively. It is noteworthy to mention the significant decrease in the chemical shift of the CH protons from 7.54 ppm in **L14** to 6.52 ppm in **L16**. This clearly shows the greater electron donor ability of the tertiary butyl groups relative to the hydrogen atoms.

The ^1H NMR spectral data of complexes **9**, **10** and **11** exhibit significant differences from those of their corresponding ligands **L14**, **L15** and **L15**. Shifts to higher frequencies for all the protons were found in complex **9** (6.63, 8.02 and 8.30 ppm) as compared to the respective ligand **L14** peaks (6.32, 7.55 and 7.95 ppm). The downfield signals observed in the complexes indicate reduced electron density around the protons due to the electron

flow towards the palladium center consistent with those observed in the infrared data. A similar trend is evident in complexes **8** and **9**. Figures 4.2 and 4.3 show the ^1H NMR spectra of **L14** and the corresponding complex **9**.

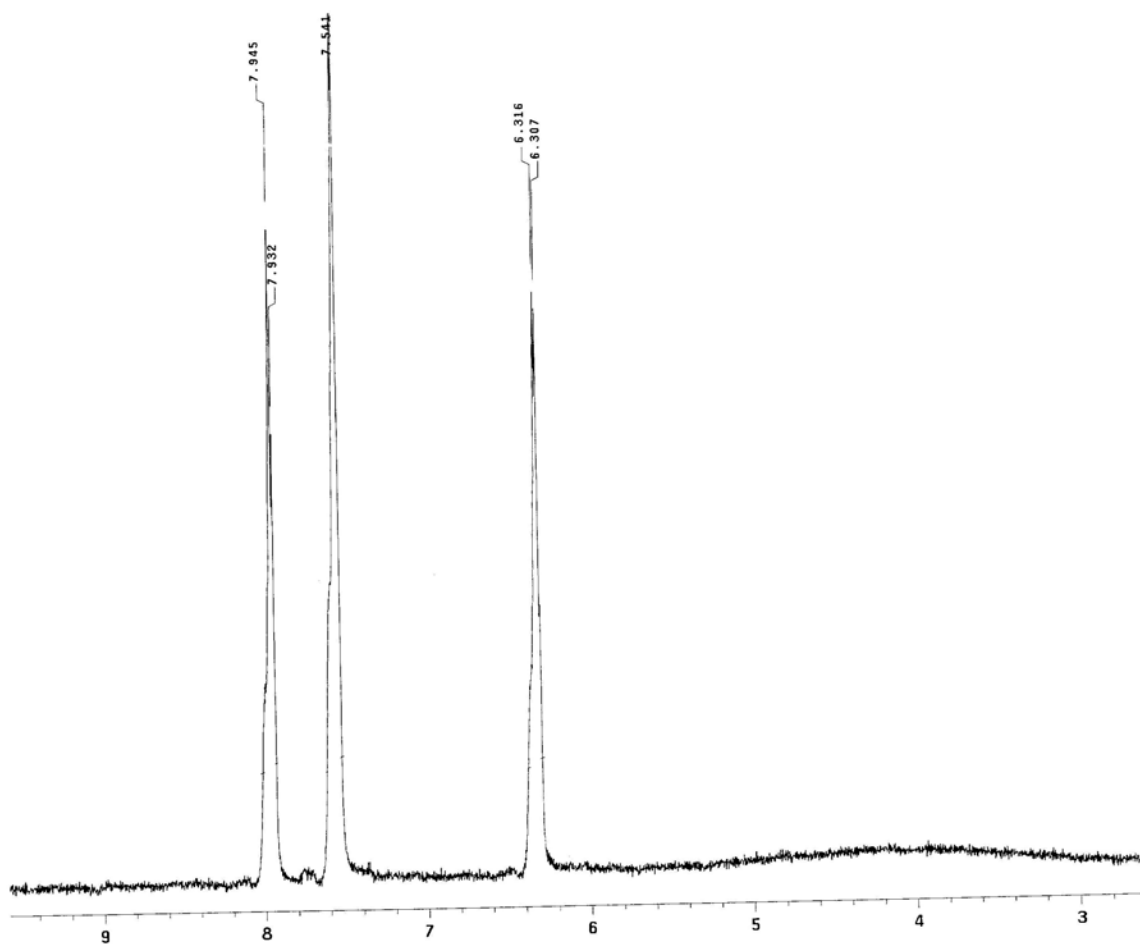


Figure 4.2 ^1H NMR spectrum of bis(pyrazolyl)acetic acid **L14**.

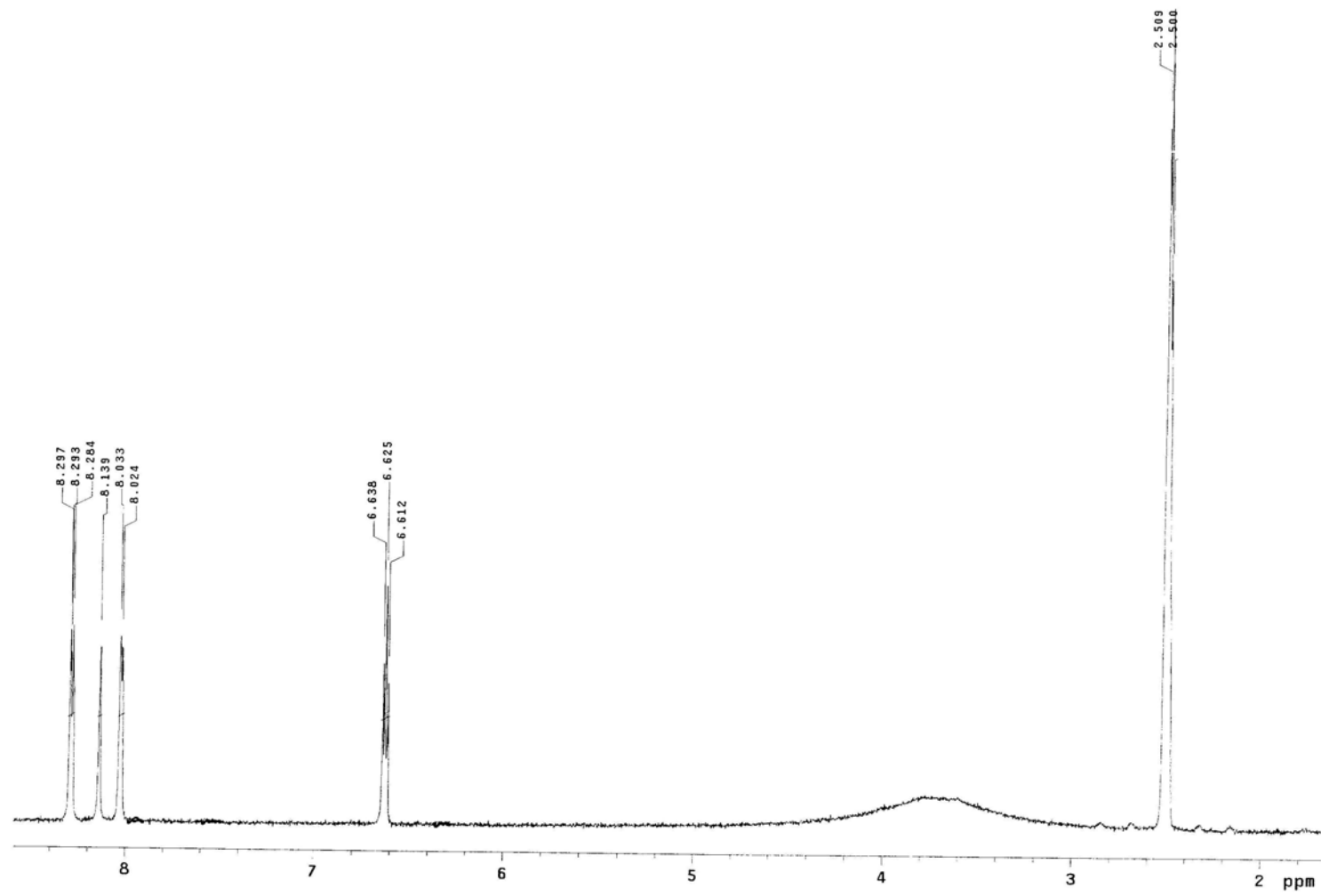


Figure 4.3 ^1H NMR spectrum of bis{(pyrazolyl)acetic acid}palladium dichloride **9**.

^{13}C NMR spectroscopy was also used to characterise the compounds synthesised. The characteristic carbonyl signals were recorded within the range of 166.2 ppm (**L14**), 166.1 ppm (**L15**) and 158.6 ppm (**L16**). This trend depicts a general decrease in the chemical shift with increase in the steric bulk of the pyrazole substituents. This feature is also prominent in the chemical shift of CH carbon, **L14** (73.9 ppm), **L15** (71.7 ppm) and **L16** (66.0 ppm). Figure 4.4 represent the ^{13}C NMR spectrum of ligand **L15**.

The respective complexes of the ligands show similar ^{13}C NMR spectra. We observed slight decrease in the chemical shift of the carbonyl functionalities in complexes **9** (164.4 ppm) and **10** (165.5 ppm) as compared to their respective ligands, **L14** (166.2 ppm) and **L15** (166.1 ppm). Similar trend is recorded for the CH linker carbon, for instance complex **9** (70.0 ppm) and **10** (67.5 ppm) as compared to their respective ligands **L14** (73.9 ppm) and **L15** (71.7 ppm). This observation contradicts the ones earlier made in the IR and ^1H NMR data in which there occur shifts to higher frequencies in the complexes as expected. However, we observed significant shifts to higher frequencies in the pyrazolyl carbons in the complexes as compared to the ligands. For example, complex **9** (136.3, 107.4 and 143.9 ppm) and **10** (144.4, 108.0 and 153.3 ppm) as compared to their corresponding ligands **L14** (131.0, 106.5 and 140.1 ppm) and **L15** (140.8, 106.6 and 147.0 ppm) for the 3, 5, 4 pyrazolyl carbons respectively.

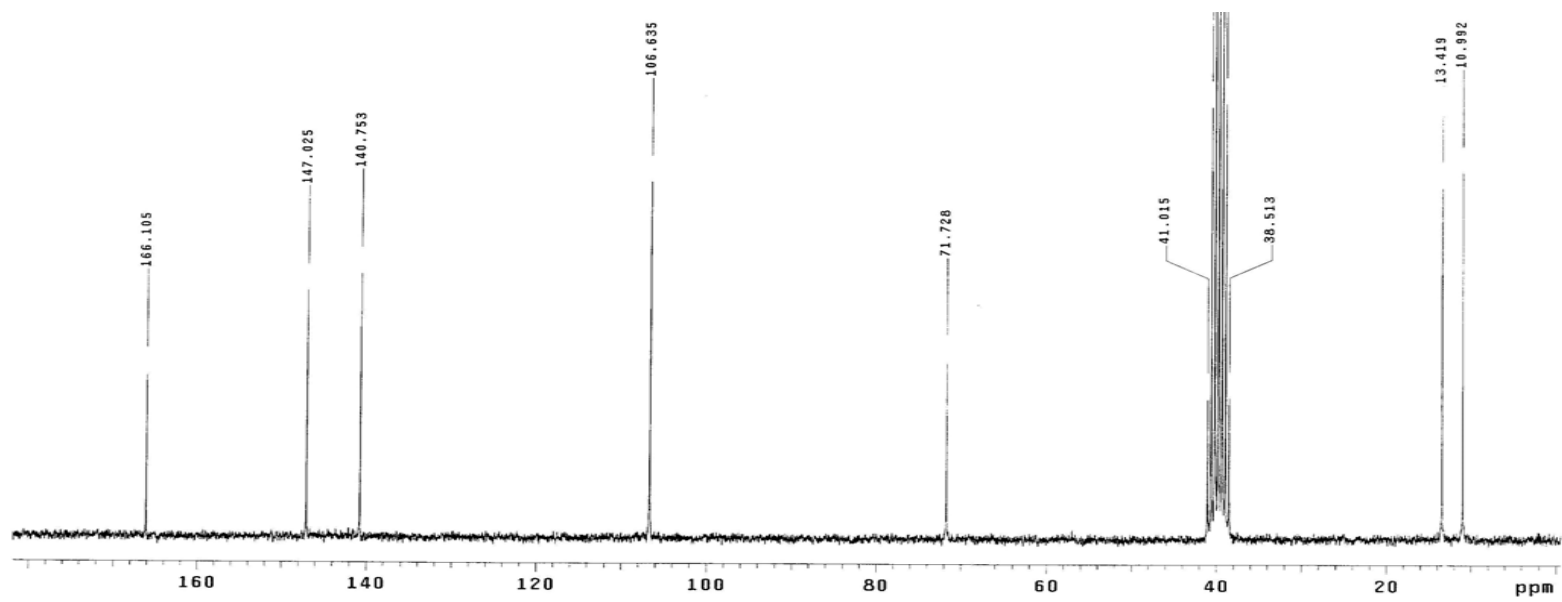


Figure 4.4 ^{13}C NMR spectrum of bis(3,5-dimethylprazolyl)acetic acid **L15**.

The compound bis(3,5-ditertiarybutyl-pyrazol-1-yl)acetic acid, **L16** was also characterised by mass spectrometry. The spectrum exhibits a molecular ion at $m/z = 415$, which corresponds to the relative molecular mass of the compound (416), Figure 4.5. Fragmentation occurs by a loss of one tertiary butyl (M-57) substituent to produce an ion at $m/z = 359$. This is followed by a loss of a second ditertiary butyl group to produce a signal at $m/z = 299$, which is the most, stable fragment ion. The loss of 18 atomic mass units to produce a peak at $m/z = 281$ could be attributed to the loss of the hydroxyl group ($M^+ - OH$). The spectrum produced thereafter appears complicated for identification of the respective fragment ions formed.

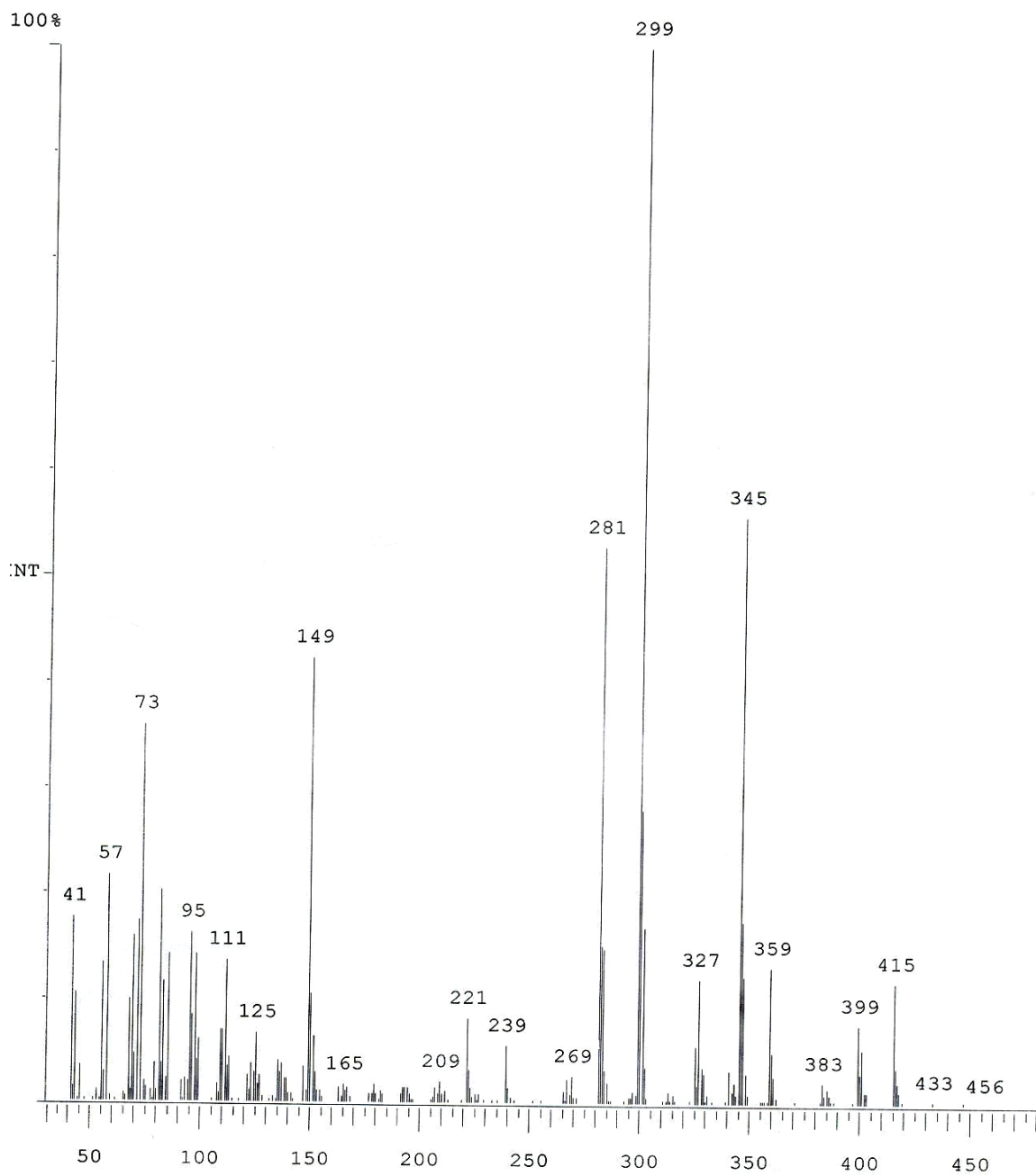
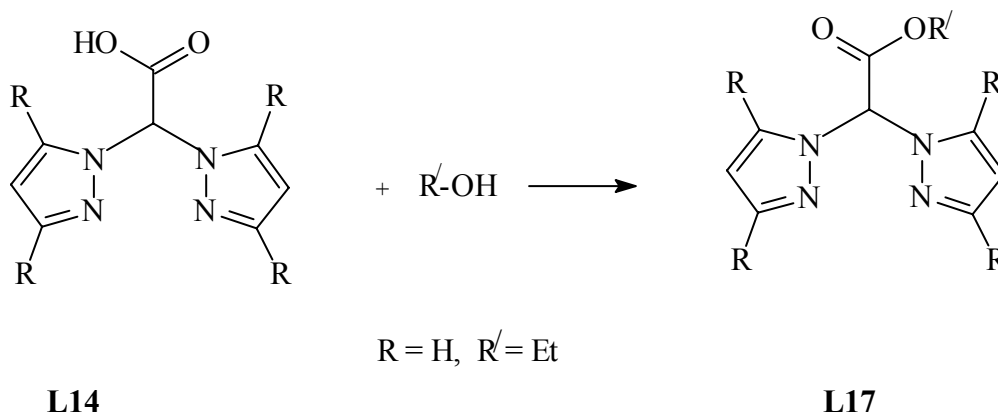


Figure 4.5 Mass spectrum showing the fragmentation pattern of bis(3,5-di-tert-butylpyrazolyl)acetic acid **L16**.

4.5 Esterification reactions of bis(pyrazol-1-yl)acetic acid, L14 with ethanol

The interaction between a carboxylic acid and an alcohol is a reversible process and is known to proceed very slowly with equilibrium only attained after refluxing for several days.²³ To increase the rate of reaction and favour the formation of the ester, the reaction can be catalyzed by use of either concentrated sulfuric or hydrochloric acid and an excess of either an acid or alcohol. In this section, we investigated the ability of the bis(pyrazolyl)acetate ligands to undergo the classical esterification reactions. This was carried by reacting **L14** with excess ethanol under acidic media (concentrated hydrochloric acid) to obtain compound **L17**, Scheme 4.4.



Scheme 4.4

The reaction was refluxed for 15 h after which the pH of the solution was increased to about 11 using sodium hydrogen carbonate. The ester was isolated by extraction using dichloromethane. Upon removal of the solvent, an analytically pure compound was obtained in good yields (58%). However, this is significantly lower than that reported in literature for butyl acetate (69%)²⁴ but higher than that of benzyl acetate (37%)²⁴ indicating the effect of the steric bulk in the percent yield. The compound was characterised by ¹H NMR, ¹³C NMR and IR spectroscopy and mass spectrometry. The ¹H

NMR spectrum, Figure 4.6 shows an additional triplet (1.26 ppm) and quartet (4.34 ppm) characteristic of the methylene and methyl protons of the alcohol (ethanol) respectively. There is no significant effect on the pyrazolyl protons. The ^{13}C NMR spectrum as expected exhibits an additional up field signals at 13.4 and 62.7 ppm corresponding to the CH_3 and CH_2 of the ethoxy moiety. The mass spectrum obtained also confirms the formation of this compound. The molecular ion at 221 corresponds to the molecular mass of the ligand (220). The fragmentation ion m/z 147 is formed after the loss of 74 amu, which corresponds to the ester group (CO-OEt).

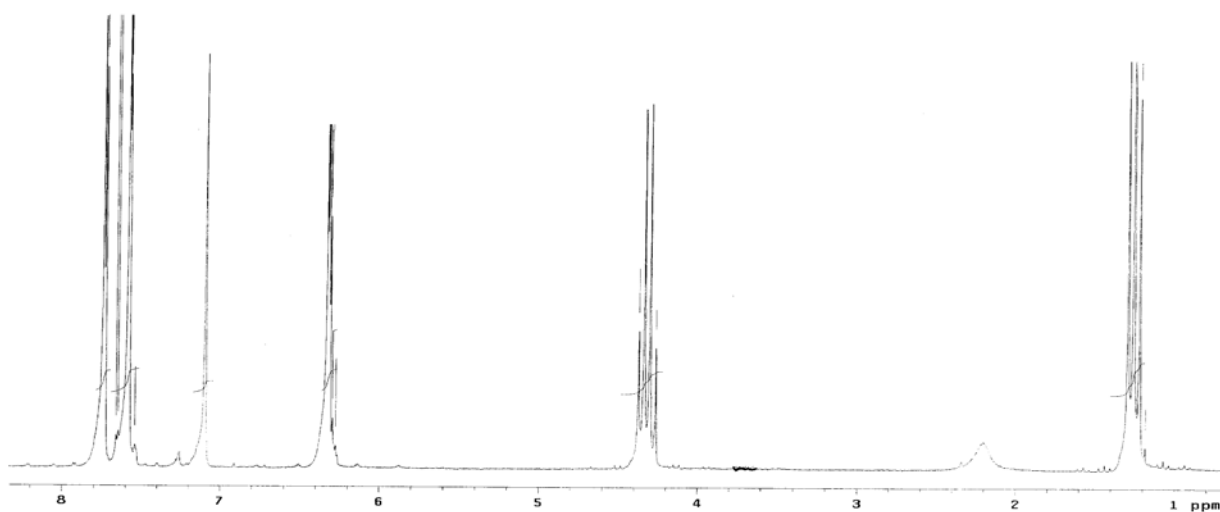
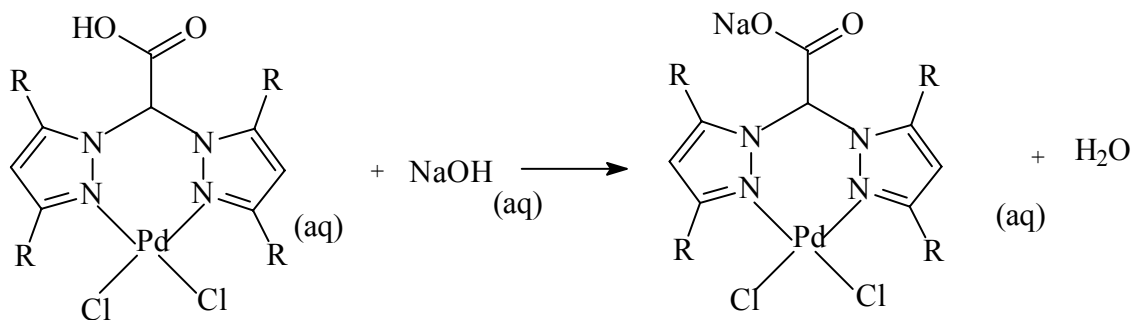
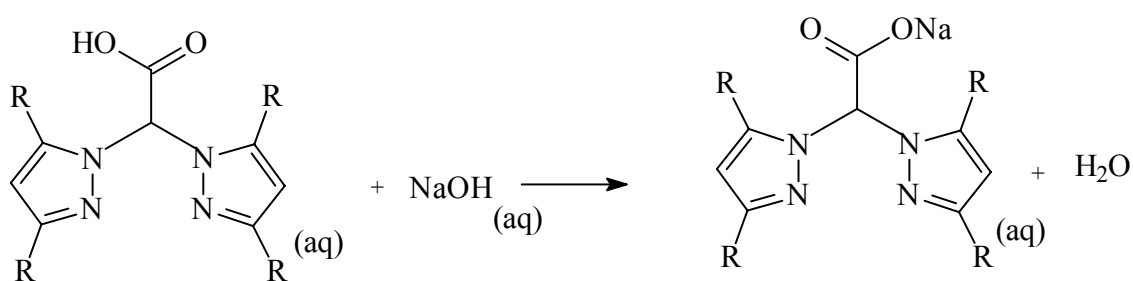


Figure 4.6 ^1H NMR spectrum for bis(pyrazol-1-yl)ethyl acetate **L7**.

4.6 Evaluation of the acid dissociation constants of bis(pyrazolyl)acetic acid ligands and their palladium(II) complexes.

In an attempt to explore the acidity of the synthesised water soluble ligands **L14** and **L15** and the effect of the metal centre on this acidity, a pH titration curve of the ligands **L14** and **L15** and their corresponding complexes **9** and **10** were constructed using dilute sodium hydroxide. Equations 4.1 and 4.2 represent the reactions between the ligand and complex with sodium hydroxide respectively.



The acid dissociation constant, K_a of **L15** (methyl analogue) was found to be 2.0×10^{-4} ($pK_a = 3.70$). This value is comparable to that of acetic acid,²⁵ $K_a = 1.8 \times 10^{-4}$ ($pK_a = 3.74$).

However, it is significantly lower compared to the K_a of the corresponding complex, **10** of 1.30×10^{-2} ($pK_a = 2.0$). This clearly demonstrates that there is electron flow from the ligand to the metal center hence reduced basicity²⁵ or increased acidity of the carboxylic functionality in the complex system. Figure 4.7 represents the pH titration graph of Ligand **L15** and its complex **10**. The pH titration curves resemble that of acetic acid with dilute NaOH.²⁵ Figure 4.8 represents the pH titration curve of ligand **L14**.

Interestingly the K_a of ligand **L14**, which is non-substituted, was found to be 9×10^{-3} ($pK_a = 2.04$). This is slightly higher than the K_a of **L15**, bearing the methyl substituents ($K_a = 2.0 \times 10^{-4}$). This suggests that the methyl substituents significantly reduce the acidity of the ligand. This factor could be ascribed to greater σ -donor ability of methyl substituents relative to the hydrogen atoms. A similar trend was observed for the respective complexes, with complex **9** being more acidic ($K_a = 1.75 \times 10^{-2}$) than **10** ($K_a = 1.30 \times 10^{-2}$).

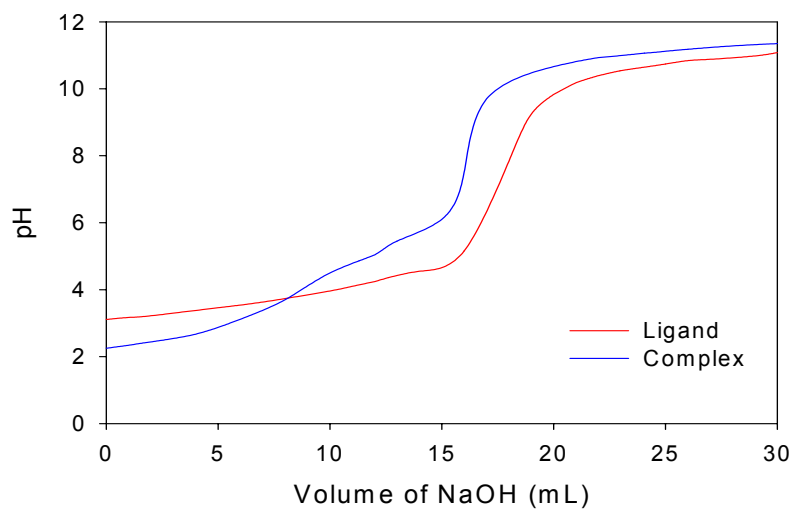


Fig 4.7 pH titration curves of ligand **L15** and complex **10** with 0.01M NaOH

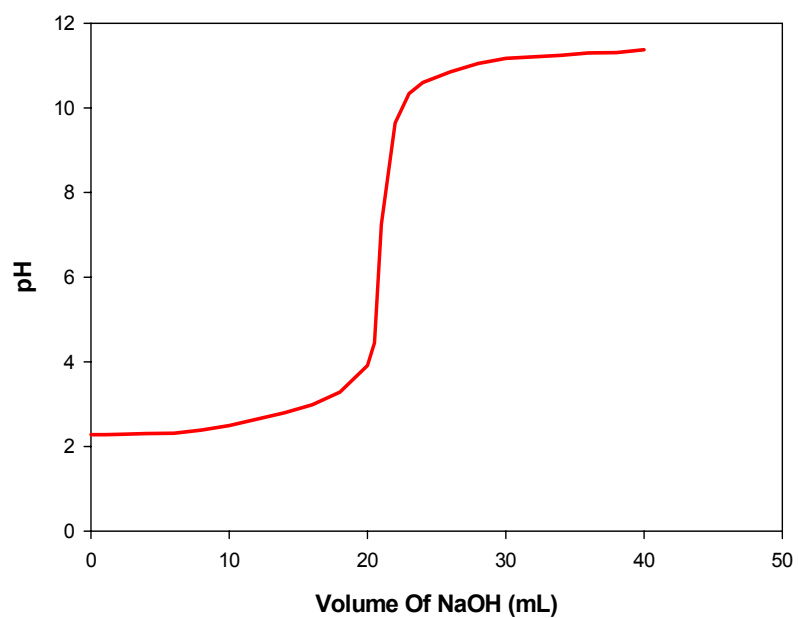


Figure 4.8. pH titration curve of bis(pyrazolyl)acetic acid, **L14** with NaOH.

4.7 Conclusion

Three bis(pyrazolyl)acetate ligands have been synthesised by one step phase transfer catalyst using dibromoacetic acid and an equivalent amount of the appropriate pyrazole. The ligands were obtained in moderate to high yields. ^1H NMR, ^{13}C NMR and IR spectroscopic techniques have been used to fully characterise these compounds. Substituent effect on solubility of these ligands is prominent with the non-substituted system having high solubility in water while the bulkier di-*tert*-analogue showing high solubility in organic solvents. The reactions of these ligands with $\text{Pd}(\text{NCMe})_2\text{Cl}_2$ afforded their respective palladium(II) complexes in good yields. From microanalyses data available, a general empirical structure of the form $\text{Pd}(\text{L})\text{Cl}_2$ can be proposed for all the complexes synthesised.

It has been successfully shown that these bis(pyrazolyl)acetate ligands undergo classical esterification with primary alcohols reactions to give the resulted esters in good yields. We have also established that the acidity of both the ligands and their palladium(II) complexes depend on the nature of the pyrazolyl substituent on the ligand system. In general, the acidity of the compounds decreases with increase in the donor ability of the substituent groups. The palladium(II) complexes also exhibit higher acidity than their corresponding ligands.

4.8 References

1. S. Trofimenko, *Chem Rev.* **93** (1993) 943. S. Trofimenko, *J. Am. Chem. Soc.* **89** (1967) 3170. S. Trofimenko, *Scorpionates. The Coordination Chemistry of Poly(pyrazolyl)borate Ligands*, Imperial College Press, London (1999).
2. S. Trofimenko, *Chem. Rev.* **72** (1971) 17.
3. D. M. Tellers, S. J. Skoog, R. G. Bergman, T.B.Gunnoe, W. D. Harman, *Organometallics*, **19** (2000) 2428.
4. J. Reedjik, G. Wilkinson, R. D. Gillard, J. A. McCleverty (Eds), *Comprehensive Coordination Chemistry*, vol 2, Pergamon, Oxford, (1987) 73.
5. M. K. Das, K. Niedenzu, *Inorg. Chim. Acta.* **150** (1998) 47.
6. A. J. Canty, *Acc. Chem. Res.* **25** (1992) 83.
7. S. Trofimenko, *J. Am. Chem. Soc.* **70** (1970) 5118.
8. S. Julia, J. M. Del Mazo, J. Elguero, *Org. Prep. Proc. Int.* **16** (1984) 299.
9. P. K. Byers, A. J. Canty, R. T. Honeyman, *Adv. Organomet. Chem.* **34** (1992) 1.
10. L. F. Hang, W. L. Jia, Y. M. Xu, J. T. Wang, *Polyhedron*, **19** (2000) 381.
11. (a) S. Tsuji, D. C. Swenson, R. F. Jordan, *Organometallics*, **18** (1999) 4758. (b) D. L. Reger, J. E. Collins, A. L. Rheingold, L. M. Liable-Sand, *Inorg. Chem.* **38** (1999) 3235.
12. L-F. Tang, W. L. Jia, Z. H. Wang, J. T. Wang, H. G. Wang, *J. Organomet. Chem.* **649** (2002) 152.
13. C. R. Warthen, C. J. Carrano, *J. Inorg. Biochem.* **94** (2003) 197.
14. D. L. Reger, T. C. Grattan, K. J. Brown, C. A. Little, J. J. S. Lamba, A. R. Reingold, R. D. Sommer, *J. Organomet. Chem.* **607** (2000) 120.

15. (a) B. S. Hammes, C. J. Carrano, *Inorg. Chem.* **38** (1999) 3562. (b) A Beck, B. Weibert, N. Burzlaff, *Eur. J. Inorg. Chem.* (2001) 521.
16. M. Bochman, *J. Chem. Soc. Dalton Trans.* (1996) 255.
17. D. M. Antolleni, A. Leins, J. F. Stryker, *Organometallics*, **16** (1997).
18. J. Jaffart, C. Neyral, R. Choukroun, R. Mathieu, M. Etienne, *Eur. J. Inorg. Chem.* (1998) 425.
19. A. Otero, J. Fernandez-Beza, J. Tejada, A. Antinolo, *J. Chem. Soc. Dalton Trans.*, (1999) 3537.
20. N. Burzlaff, I. Hegelmann, B. Weibert, *J. Organomet. Chem.* **626** (2001) 16.
21. A. Otero, J. Fernandez-Beza, J. Tejada, A. Antinolo, *J. Chem. Soc. Dalton Trans.*, (2000) 2367.
22. W. Kemp, *Organic Spectroscopy*, 3rd ed. MacMillan eds. Ltd, Hongkong, (1991) 149.
23. R. T. Morrison and R. N. Boyd, *Organic Chemistry*, 5th ed, Allyn and Bacon, Inc. Boston (1987) 567.
24. B. S. Furniss, A. J. Hannaford, P. W. G. Smith, A. R. Tatchell *Vogel's Book Of Practical Organic Chemistry*, 5th ed. Longman Scientific and Technical, New York (1991) 692. W. L. Masterton, E. J. Slowinski, C. L. Stanitski, *Chemical Principles*, 6th ed Holt-Saunders International Editions, New York, (1985) 622.

CHAPTER 5

5.1 Summary

A series of heterocyclic carbonyl pyrazolyl ligands have been successfully synthesised and obtained in good yields. The reaction of these ligands with $\text{Pd}(\text{NCMe})_2\text{Cl}_2$ gave the respective palladium(II) complexes, in moderate to high yields. The compounds synthesised have been characterised by a combination of ^1H NMR, ^{13}C NMR and IR spectroscopic techniques as well as mass spectrometry and single crystal X-ray analysis. Microanalysis was used to confirm the empirical formulae and purity of the compounds synthesised. Single crystal X-ray crystallography of complexes **1** and **2** confirms the monodentate binding mode of the ligands with the heteroatoms oxygen and sulfur in the furan and thiophene moieties being non-coordinating. A general formulae for all the complexes can thus be deduced as $\text{Pd}(\text{L})_2\text{Cl}_2$ with the *trans* geometry being preferred. From the two molecular structures and crystal parameters, it is evident that both the oxygen and sulfur heteroatoms in the furan and thiophene moieties display similar electron donor abilities.

The weak donor ability of these ligands is attested by their inability to displace COD when $\text{Pd}(\text{COD})\text{Cl}_2$ is used as the metal precursor. This is also confirmed by the ^1H NMR experiment carried out which shows the complete dissociation of the ligands from the palladium metal centre upon reaction with $\text{Sn}(\text{Me})_4$. Acyl pyrazolyl ligands have also been synthesised and fully characterised. However, attempts to isolate their palladium(II) complexes were not successful.

Five carbonyl containing pyrazolyl palladium(II) complexes, (3,5-Me₂pz-CO-furan)₂PdCl₂, **(1)** (3,5-Me₂pz-CO-thiophene)₂PdCl₂, **(2)** (3,5-^tBu₂pz-CO-furan)₂PdCl₂, **(3)** (3,5-^tBu₂pz-CO-thiophene)₂PdCl₂ **(4)** and (3,5-Ph₂pz-CO-thiophene)₂PdCl₂ **(8)** have been investigated for ethylene oligomerisation and polymerisation catalysis. They have been found to give active catalysts for ethylene polymerisation upon activation with MAO, producing high-density linear polyethylene (HDLPE). Activities of these heterocyclic carbonyl catalysts are lower compared to the simple pyrazole systems already investigated and were only active at elevated temperatures. This behaviour could be ascribed to the existence of non-coordinating donor atoms, sulfur and oxygen which might cause catalyst deactivation by forming adducts with the aluminium co-catalyst. Thermal instability of these catalysts could also contribute to their observed low catalytic activity. The weak donor ability of these pyrazolyl ligands, as indicated above could lead to ligand dissociation from the metal centre resulting to catalyst deactivation. It has been shown that the activity of these pyrazolyl palladium complexes could be enhanced by incorporation of electron deficient compounds.

It is clear that the activity of these catalysts depend on the nature of the substituents in the ligand system as well as the reaction conditions. It can also be concluded that the dominating factor in controlling the molecular weight, besides reaction conditions is the steric bulk of the ligands. The blocking of the axial coordination site in the metal centre, which according to theoretical calculations is essential for obtaining higher molecular weights is still insufficient since lower molecular weight polymers were obtained with the bulkier substituent groups.

The activation of these complexes by alkyl aluminium compound, EtAlCl₂, resulted in active catalysts for ethylene oligomerisation. This is due to the low Lewis acidity of EtAlCl₂ as compared to MAO. The major oligomers produced were C₁₀ and C₁₂. No lower oligomers in the C₄-C₈ range were obtained. This shows that the catalysts favour chain propagation relative to chain termination consistent with Pd(II) α -diimine complexes abound in literature.

Three bis(pyrazolyl)acetic acid ligands have been synthesised by one step phase transfer catalyst using dibromoacetic acid and an equivalent amount of the appropriate pyrazole. The ligands were obtained in moderate to high yields. ¹H NMR, ¹³C NMR and IR spectroscopic techniques have used to fully characterise these compounds. Substituent effect on solubility of these ligands is prominent with the un-substituted system having high solubility in water while the bulkier di-*tert*-butyl analogue is highly soluble in organic solvents. The reactions of these ligands with Pd(NCMe)₂Cl₂ afforded their corresponding palladium(II) complexes in good yields. From microanalysis data available, a general molecular structure of the form Pd(L)Cl₂ can be proposed.

It has been successfully shown that these bis(pyrazolyl)acetic acid ligands undergo classical esterification reactions with primary alcohols to give the resultant esters in good yields. We have also established that the acidity of both the ligands and their palladium(II) complexes depend on the nature of the pyrazolyl substituent on the ligand system. In general, it was found that the acidity decreases with increase in the electron donor ability of the pyrazolyl substituents. The palladium(II) complexes also exhibit

higher acidity than their respective ligands. This confirms decreased electron density in the ligand system as electrons flow to the metal centre.

5.2 Future directions

Future prospects of this work include investigation of the catalytic behaviour of these heterocyclic carbonyl palladium(II) complexes when activated with other aluminium compounds such as Et_2AlCl as co-catalysts. Probing the effect of other reaction conditions such as temperature and pressure on ethylene polymerisation using these catalyst systems is recommended. Mechanistic studies involving the interactions of these pyrazolyl complexes with the α -olefins also require considerable attention. This would lead to a better understanding of the observed activity trends from kinetics and thermodynamics point of view. The catalytic potential of the bis(pyrazolyl)acetic acid palladium(II) complexes synthesised is another area that require some future attention.